



TECHNISCHE
UNIVERSITÄT
WIEN
Vienna | Austria

Dissertation

Hydrogels in 3D Bioprinting and Tissue Engineering

carried out for the purpose of obtaining the degree of

Doctor technicae (Dr. techn.),

under supervision of

Univ. Prof. Dipl.-Ing. Dr. techn. Heinz Redl

E166

Institute of Chemical, Environmental and Bioscience Engineering

submitted at TU Wien,

Faculty of Technical Chemistry

by

Katja HÖLZL

Mat.Nr.: 1429166

Vienna, on the _____

Signature

This work was supported by the European Research Council within the framework of the project *Laser-engineered Biomimetic Matrices with Embedded Cells* (ERC Starting Grant-307701, AO).

I confirm that going to press of this thesis needs the confirmation of the examination committee.

Affidavit

I declare in lieu of oath, that I wrote this thesis and performed the associated research myself using only literature cited in this volume. If text passages from sources are used literally, they are marked as such. I confirm that this work is original and has not been submitted elsewhere for any examination, nor is it currently under consideration for a thesis elsewhere.

Vienna, March 2022

Signature

KURZFASSUNG

Tissue Engineering beschreibt die Herstellung von funktionsfähigem biologischem Gewebe *in vitro* mit dem Ziel beschädigtes Gewebe wieder zu regenerieren. Um dies zu ermöglichen, muss das künstlich hergestellte Gewebe dem Original in Struktur, Funktion und Eigenschaften so gut wie möglich gleichen: Zellen werden mit einer Gerüststruktur - sogenannten Scaffolds in die gewünschte 3-dimensionale Form gebracht und mit bioaktiven Substanzen versetzt, um Zellwachstum und Differenzierung zu ermöglichen. Die Anforderungen an Scaffold-Materialien sind vom herzustellenden Zielgewebe und ihrer Fertigungsmethode abhängig. Im Rahmen dieser Arbeit, nutzen wir die Eigenschaften von Hydrogelen, um dem Ziel der künstlichen Herstellung von biomimetischem Gewebe näher zu kommen.

Hydrogele sind vielversprechende Materialien, die sich vor allem für die direkte Verkapselung von Zellen eignen. Viele sind biokompatibel und biologisch abbaubar, weisen Zelladhäsionsmoleküle auf und ermöglichen Diffusion. Sie können so konzipiert werden, dass sie natürliche Matrix von biologischen Geweben widerspiegeln. In den letzten Jahren wurden diese Materialien auch verstärkt auf ihre Verwendungsmöglichkeit im 3D bioprinting untersucht.

Im Rahmen dieser Arbeit wurden die nötigen Materialeigenschaften von Hydrogelen für deren Verwendung als „*bioink*“ im 3D Bioprinting (Extrusion, Inkjet, *Orifice-free* Bioprinting) diskutiert. Des Weiteren wurde ein mathematisches Model entwickelt, welches die Veränderung der mechanischen Eigenschaften beschreibt, wenn das Hydrogel mit Zellen beladen wird. Einflüsse wie Zellproliferation, Zellverteilung und Zelldichte wurden hierbei untersucht. Im zweiten Teil dieser Arbeit wurde eine Methode entwickelt, die es ermöglicht auch weiche Materialien mittels Extrusion zu verdrucken. Das entwickelte Material basiert auf Hyaluronsäure und weist sowohl strukturviskose (shear-thinning) als auch selbstheilende (self-healing) Eigenschaften auf. Dies ermöglicht das Verdrucken von einem Hydrogel in ein zweites Support-Hydrogel, welches dieselben chemischen Eigenschaften aufweist (embedding gel-in-gel approach/omnidirectional printing). Da weiche Materialien aufgrund ihrer unzureichenden mechanischen Eigenschaften, schwer verdruckbar sind und die Struktur unter dem Eigengewicht kollabiert, benötigt es neue Methoden um diese zu

verarbeiten. Wir zeigen, dass mit unserer Methode stabile Strukturen auch aus weichen Hydrogelen verdruckt werden können, welches mit herkömmlichem Extrusionsverfahren nicht möglich wäre.

Im letzten Teil, wurde Methacryloyl-modifizierte Gelatine (gelMA) auf die Eignung im Bereich Knorpelregeneration, vor allem im Bereich der Osteoarthritis, untersucht. Wir konnten zeigen, dass es möglich ist bereits dedifferenzierte primäre humane Chondrozyten durch 3D Kultivierung in gelMA zu redifferenzieren. Weiters konnte durch die Applizierung von gelMA, welches mit Zellen beladen wurde, auf osteoarthritischen Knorpel und anschließender Simulation der mechanischen Belastungen im Knie gezeigt werden, dass das Hydrogel nicht nur als Zelltransporter agiert und die Zellen an gewünschter Stelle am Gewebe fixiert, sondern auch die Zellen vor mechanischem Stress, welcher im Gelenk auftritt, schützt. gelMA ist photosensitiv und injizierbar, wodurch es arthroskopisch appliziert werden könnte. Dadurch stellt es eine gute Möglichkeit dar, um Knorpeldefekte minimalinvasiv zu behandeln.

Zusammenfassend lässt sich sagen, dass es viele unterschiedliche Möglichkeiten gibt, um die Herstellung von funktionalem Gewebe zu verbessern. Mathematische Modelle stellen ein wichtiges Werkzeug dar, um die Eigenschaften der verdruckten Struktur vorauszusagen. Trotzdem braucht es die Weiterentwicklung von Materialien und deren Verarbeitungsmethoden, um unterschiedliche Gewebe nachzuahmen. Weiters ist nicht nur deren Herstellung *in vitro* von Bedeutung, sondern auch deren Eignung für klinische Anwendungen.

ABSTRACT

In vitro generation of functional tissue is a challenging task in tissue engineering. The new, or “regenerated” tissue should resemble native tissue as close as possible in structure, function, and properties. The use of scaffolds, that support the alignment of cells into desired 3-dimensional networks, and bioactive factors, proteins that aid cells in growth and differentiation, are essential for the generation of biomimetic tissue. In this work we utilize the properties of hydrogels to expand the spectrum of tissue engineering approaches to get closer to the ultimate goal of functional tissue production. We investigated their use for 3D bioprinting as well as for the treatment of defective cartilage tissue.

Hydrogels have been shown to be a powerful scaffold material as they can be generated to closely mimic the extracellular matrix of native tissue. Depending on the type of hydrogel, they are biocompatible and biodegradable, possess cell-adhesive domains, and allow diffusion of oxygen, nutrients and metabolites. Over the last years, hydrogels also have been excessively investigated for their use as a bioink in 3D bioprinting.

In the first part of this work, we determined the optimal properties that a hydrogel has to exhibit to be used as bioink for different 3D bioprinting approaches (extrusion, inkjet, and orifice-free bioprinting). We further introduce a numerical model that predicts the changes in material properties once the hydrogel is loaded with cells. We also modelled the influences of cell density, cell distribution, and cell proliferation on the structures final properties using a computational approach. In the second part, we discuss the development of a novel soft hydrogel based on dynamic coordination chemistry. This chemical strategy results in a hyaluronic acid based hydrogel with shear-thinning and self-healing properties, that allows the extrusion of one hydrogel into another supportive hydrogel (embedding gel-in-gel approach/omnidirectional printing). As the printing of soft hydrogels is especially difficult due to weak self-supportive properties of the material, it needs adapted materials and fabrication methods. We show, that with this chemistry and printing method we can fabricate stable structures out of soft hydrogel starting material, that would not be possible by regular extrusion printing.

In the third part, we examined the utility of gelatin methacryloyl (gelMA) for its clinical relevance in cartilage tissue engineering, especially for the treatment of osteoarthritic (OA) cartilage. We show that 3D cultivation of dedifferentiated primary human articular chondrocytes within gelMA yields in their redifferentiation. We further show that under simulation of the mechanical stresses occurring in the human knee joint during walking, gelMA, applied to OA cartilage, not only attaches to the defective tissue and acts as a cell transporter system, but also sufficiently protects the cells from the prevalent stresses. We thus demonstrate that this hydrogel could potentially be applied arthroscopically in a minimal invasive way, as it also gives the possibility of being injected.

In summary, we showed that there are many different areas to work on to improve the fabrication of hydrogels into 3D biomimetic scaffolds. Mathematical modelling is a strong tool to predict the outcome of printed constructs. Still, further development of materials and their processing methods has to happen, in order to mimic the versatile tissues of different origin. But not only their production *in vitro*, but also their applicability for clinical use has to be carefully considered in the process of biomimetic artificial tissue establishment.

TABLE OF CONTENT

Kurzfassung		I
Abstract		III
Acknowledgements		VI
Chapter I	Introduction	1
Chapter II	Bioink properties before, during and after 3D bioprinting	33
Chapter III	Dynamic coordination chemistry enables free directional printing of biopolymer hydrogel	53
Chapter IV	Gelatin methacryloyl as environment for chondrocytes and cell delivery to superficial cartilage defects	70
Curriculum Vitae		102

ACKNOWLEDGEMENT

I would like to thank my supervisor, Aleksandr Ovsianikov, who gave me this great opportunity to come to TU Wien and do my research in such an interesting and exciting field. I am very grateful for having been a member of his work group from the early start on and that I could experience how the group evolved and the progress we made together as the years passed by.

My special thanks go to Sylvia Nürnberger, who enabled my collaboration with the Medical University and Allgemeinem Krankenhaus (AKH) Vienna. I want to thank her for the support and expert advice in all biological matters and for the opportunity to work and further improve my skills at her institution. Furthermore, I want to thank Heinz Redl and Sandra Haudek, who supported and supervised me along the way and for taking the time to review my thesis.

I give my gratitude to Andreas Pauschitz, for the possibility to perform measurements at the AC²T Research GmbH together with Hakan Göcerler, who supported me with scientific knowledge.

I want to thank all my colleagues, who went through all this with me, who kept me motivated, and for the great time we had. Special thanks to Wolfgang Steiger, Peter Gruber, Marica Markovic, Agnes Dobos, Denise Mandt, Sara Zigon-Branc, Elise Zerobin, Maximilian Troymayer, Markus Lunzer and Marian Fürsatz for their time to discuss science as well as everyday life matters. Moreover, I am grateful that I met Sonja Baumgartner, Peter Dorfinger, Robert Gmeiner, Markus Pfaffinger, Jürgen Kollmer, Julia Schönherr, Bernhard Busetti, Bernhard Steyrer, and Malte Hartmann, who made every day a special day at the Institute of Materials Science.

The greatest thanks go to my family, who supported and encouraged me in good and not so good times. They lived this experience together with me and kept me going when needed. Without their love and support, I would not have gotten to this point. Also, many thanks to all my friends for their friendship and encouraging words.

Finally, Christoph Hofstetter, for his love and care.

Chapter I

Introduction

1 The importance of tailored hydrogels

As the world's population is ageing, there is an increasing demand for organ transplants and new or restored tissue. A lot of diseases that damage tissue and organs are treated with donor transplants, but these are rare and can be rejected by the recipient's immune system. Therefore, we need new solutions to restore tissue and organs and allow good health even at higher age.

Tissue Engineering aims to generate functional tissue to replace dead or injured native tissue. Conventionally, the use of two-dimensional (2D) cell culture techniques to build new tissue has been explored, yet it soon became evident that such approaches cannot replicate the complexities of living tissue, mainly because 2D cell behaviour and structure does not resemble the three-dimensional (3D) in vivo situation^{1,2}. Therefore, new methods involving 3D cell tissue culture techniques need to be established to better mimic the native environment of tissues, particularly that of the extracellular matrix (ECM) that surrounds and supports cells. The specific composition of ECM impacts cell morphology, colonization, migration, growth, and function and is thus of uttermost importance to assure successful tissue regeneration³.

The basic concept of tissue engineering originates from the idea to combine scaffolds (for mechanical support) and bioactive molecules (for biologic support) with cells, in which scaffolds serve as ECM to resemble living tissue. Because the microarchitecture of ECM is adjusted to the specific cell type it surrounds, it has a crucial influence on the cells itself: the cells geometry, cell-cell contacts, cellular growth and function as well as gene expression and phenotype commitment are affected^{4,5}. Therefore, the engineered ECM needs to be designed in a particular way to support the cells' specific phenotype and allow cell colonization, migration, growth and differentiation³⁻⁵. In order to best resemble the ECM of the native tissue of interest, scaffolds have to provide certain properties, such as: (a) cell-adhesive domains to allow cells to bind to the matrix; (b) allow diffusion of bioactive molecules and migration of cells to take place; (c) high biocompatibility; (d) controllable degradation kinetics; and (e) suitable mechanical properties (stiffness, porosity, etc.). Importantly, once the engineered 3D tissue is placed where needed, the scaffold should slowly degrade while the cells build up their own native ECM^{3,6}.

Hydrogels are polymeric networks that have been shown to provide some of these attributes. They consist of hydrophilic polymers that have been crosslinked either chemically or physically to form a three-dimensional network. Because of the hydrophilic polymer components, they can take up water a thousand times their dry weight inside their matrix, but do not dissolve in water in their crosslinked state. Their high water content contributes to their flexibility and certain mechanical properties as well as high permeability of nutrients, oxygen and other water-soluble metabolites. Therefore, they resemble native tissue more closely than other materials. They usually exhibit good biocompatibility and depending on the type of hydrogel, they are also biodegradable^{1,7-11}. Moreover, their mechanical properties can easily be adapted by varying the degree of polymerization or by using a combination of different hydrogels rendering them tunable for different tissues and applications. Therefore, diverse types of hydrogels have emerged as key material for generating tissue in vitro for clinical use^{6,12}.

Different methods have been developed over the years to process hydrogels to bring them into the desired 3D configuration. By using these biofabrication techniques, biomimetic scaffolds with controlled matrix parameters such as material geometries, localization of biomolecular cues and mechanical properties can be produced. Among those biofabrication techniques 3D bioprinting has become of particular interest to create structures that mimic the native ECM¹³⁻¹⁶. Bioprinting is a process in which a mixture of cells and biomaterial (“bioink”) is deposited to result in a viable structure of desired shape and size. In extrusion bioprinting, bioink is deposited through a nozzle in strands, that can be built atop of each other, whereas in inkjet bioprinting small droplets are dispensed. In adjusting cell density, and material properties (type, concentration, viscosity, crosslinking parameters, etc.) of a biomaterial, and processing it with the suitable 3D printing approach, it is possible to fabricate biomimetic structures that resemble tissue.

As many hydrogels are liquid before crosslinking, the material can easily be mixed with the cells resulting in a homogenous distribution within the bioink and therefore also within the structure. In contrast to approaches, where cells are seeded into a solid scaffold in a second step, the cells are completely surrounded by the hydrogel. This enables a close interaction between the material and the cell that is of uttermost importance for a cell’s differentiation status.

2 The extracellular matrix

Inside the body, cells are surrounded by a complex three-dimensional architecture mainly composed of water, proteins, carbohydrates and growth factors. This network is called the extracellular matrix (ECM). Its composition and organization vary over a wide range of biophysical and biochemical properties being unique for each tissue. In displaying different biochemical, physical and mechanical cues, the ECM not only gives structural support, but provides the right signals for the cells to facilitate the tissues physiological function^{17,18}.

As the ECM itself is produced by the residing cells, it is a dynamic system, which can adapt to external stimuli to maintain homeostasis. The cells are in contact with the ECM through receptors, which allow a bidirectional flow of information between cell and ECM. Therefore, the cells can modify and remodel the matrix to respond to physiological stresses caused by growth, injury or disease. In doing so, the change in ECM properties will also have an influence on the function and behaviour of neighbouring cells, regulating proliferation, migration and differentiation of cells^{17,19,20}.

The individual properties of the highly heterogenic and anisotropic ECM lead to its intrinsic functions:

- a) its microarchitecture serves as an anchoring substrate for the cells:
through inherent gradients the matrix can also attract and direct migratory cells.
- b) the ECM provides the structure and mechanical properties that are characteristic for various tissue types: cell and tissue fate are directly influenced by signals that originate from mechanotransduction
- c) it can also bind and sequester growth factors, which can be presented to the cell receptors: this allows spatio-temporal control over growth factor release. Hence, concentration gradients can be formed to direct cells²⁰.

2.1 ECM microarchitecture

To get a better understanding of how these functions emerge, one has to go deeper into ECM microarchitecture.

The ECM constitutes of three major components:

- a) insoluble collagen fibers/elastin: provide a supportive framework and mechanical resilience
- b) proteoglycans: highly hydrophilic, bind water and therefore act as a shock absorber to cushion the cells.
- c) soluble multiadhesive matrix proteins: bridges between cell receptors and ECM components

The most abundant proteins are the insoluble **collagens**²¹. There are 28 different types of collagen found in the ECM, which contain all the same characteristic element– the triple helix. With this unique structure they bind to other proteins and glycosaminoglycans (GAGs) to form supramolecular assemblies^{17,22}. In this form, they can bind and deposit growth factors and chemokines, which can be released and presented to the cell surface receptors influencing cell fate and behaviour^{17,18,20}. Moreover, the collagen family also strongly participates in signal transduction caused by mechanotransduction (translation of mechanical information into biochemical signaling). As the mechanical properties and architecture changes, the cells receive instructive signals as they are connected to the collagen fibrils^{17,22}.

Among the soluble proteins, multiadhesive matrix proteins and proteoglycans can be found. **Multiadhesive proteins** are glycoproteins such as laminin²³ and fibronectin. They have multiple binding domains and operate as bridges between structural ECM molecules, as well as cell-surface proteins and signaling molecules. Whereas the connection of structural ECM molecules with each other enhances the overall ECM network properties, the linkage of cells to the ECM and growth factors provokes cellular responses^{17,19,24}. One of the most common sequence for binding cells is the Arg-Gly-Asp (RGD) motif. This peptide structural element is responsible for the binding of many integrins and therefore for the anchorage of the cells to

the ECM²⁵. In the design of biomimetic ECM, it is often introduced to enhance the affinity of the cells to the material and to prevent cell death due to anoikis²⁶.

Proteoglycans²⁷ are also a major component of ECM, especially in connective tissue. They consist of a core protein, which is covalently bound to one or more GAGs. As they can vary in their type of core protein as well as in the number and composition of GAG chains, this group has noticeable variability resulting also in highly diverse function²⁴. The **GAG groups** contribute mainly to the characteristics that give proteoglycans their biological function. GAGs are long, repeating units of disaccharides^{20,28}. They are classified in different subtypes based on their chemical structure. The abundance of carboxyl, hydroxyl and sulfate groups is critical for their physical properties and specifies individual GAGs (e.g. keratan sulfate, heparan sulfate, chondroitin sulfate, dermatan sulfate and hyaluronan)²⁰. Their biological function results from their ability to bind water and therefore to provide tissue hydration and compressive resistance¹⁷. Due to their structure, GAGs are negatively charged, resulting in the affinity for Na⁺⁺ ions. As water is drawn in not only the mechanical properties are improved, but cell migration and the diffusion of growth factors is enabled^{20,29}. Hence, proteoglycans are responsible for the large volume of the ECM, but also connect other ECM molecules through their domains. However, proteoglycans are also present on the surface of many cells. In the case of syndecan, the core protein spans the plasma membrane and the polysaccharide domains bind to collagens and other glycoproteins on the surrounding. In this way, the proteoglycans anchor the cells to the ECM²⁴.

Taken together, all these different molecules make up a highly complex ECM (**Figure 1**). The interaction between cells and the ECM takes place at several levels, in which the right signals are provided. The organization and composition of the ECM, which brings along mechanical support and growth factors, is read by the cells. The signals presented to the cells will change their gene expression and therefore trigger certain processes like proliferation, migration and differentiation to perform the tissues' intrinsic function.

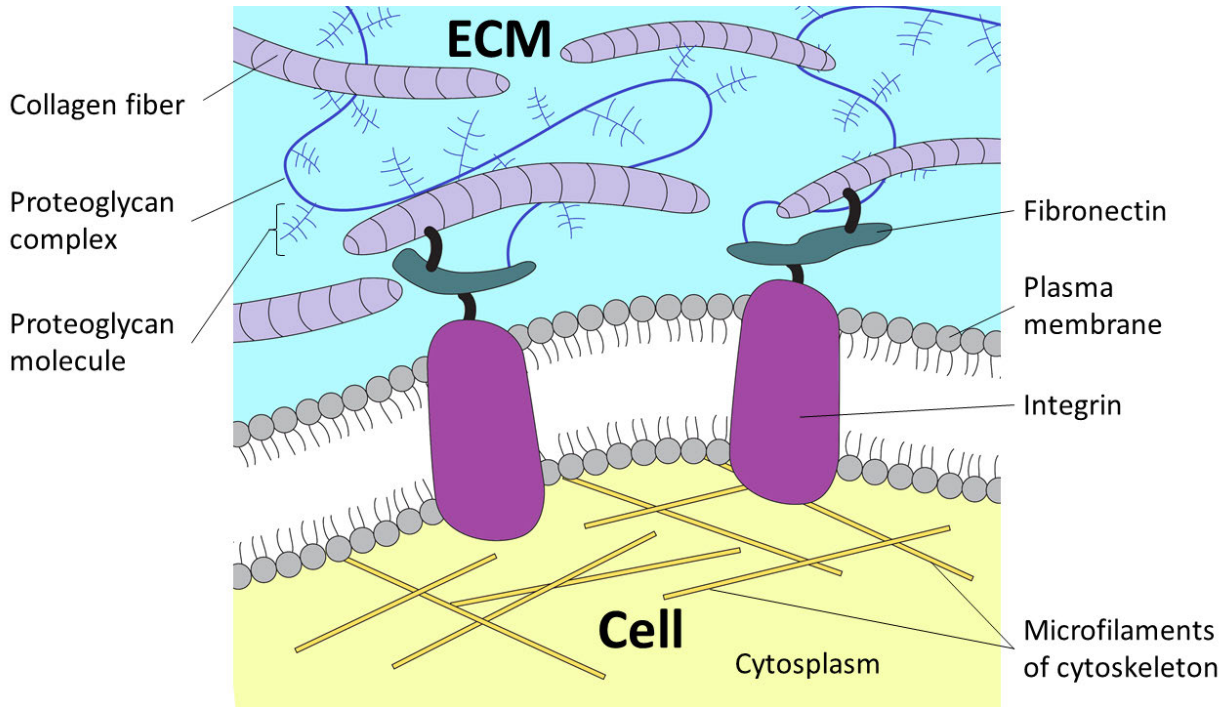


Figure 1: Schematic overview of the microarchitecture of the extracellular matrix. Collagen and elastin fibers span through the matrix and give structure and mechanical resilience. Proteoglycans are the filler substance between the insoluble protein fibers and bind water to absorb loading forces. Multiadhesive matrix proteins such as fibronectin act as bridges to connect cells via their integrin receptors to the extracellular matrix.

3 The influence of the ECM on cell fate

To design hydrogel constructs that achieve the desired cell responses to promote tissue formation one has to have a closer look at cell-ECM interactions. Although, the presence or absence of soluble growth factors is known to substantially influence the cell fate, they will not be discussed at this point. However, not all cellular responses are attributed to soluble factors, but are governed by ECM properties and cell-ECM interactions. Among other stimuli, the surrounding provides biochemical and mechanical cues, such as the nanoscale topography, ligand presentation, porosity and stiffness that trigger signal transduction. Conversely, the cells exert forces on the surrounding as they degrade and remodel the matrix. This highly dynamic phenomena, in which ECM and cell influence each other's fate is related to the field of **mechanotransduction** and is discussed in the following^{5,30}.

The influence of **nanoscale architecture** and **ligand presentation** on cell fate has been described in many studies. As the order of magnitude of nanoscale features is below that of cells, it is possible to address cell responses on the cellular receptor level. Cells interact with the surrounding matrix via special receptors called integrins²⁵. These receptors are heterodimeric transmembrane proteins that connect the ECM with the cytoskeleton of the cell. Spanning through the cell membrane the integrins bind extracellularly to various amino acid sequences (e.g. RGD) of the ECM, while intracellularly connecting to the cytoskeleton. Therefore, integrins are not only responsible for the anchorage of the cell, but also for the bidirectional flow of information provided by mechanotransduction. Consequently, the presence and spatial organization of ligands on the nanoscale level, and also the mechanical properties of the matrix where they are positioned have a strong impact on the signals received by the cells. Hence, the Spatz group³¹ could show that the spacing between ligands is an important parameter for cell attachment. They designed a non-adhesive matrix functionalized with dots of integrin binding sites (Au/RGD). The small dots of 8 nm diameter allowed the binding of only a single integrin per adhesive dot. They could show that a separation gap of >73 nm results in limited cell attachment and spreading due to restricted formation of focal adhesions³¹.

In addition to these biochemical signals, mechanical cues such as **substrate stiffness, elasticity and roughness** have been revealed to guide cell differentiation. Many studies have

already shown the different behaviour of cells when cultured on different sized posts, grates or pits³². For example, Fu et al showed that human mesenchymal stem cell (hMSC) differentiation is influenced by different heights of elastomeric microposts. Taller microposts signal the cells a softer substrate, whereas short microposts appear stiffer to the cells (**Figure 2**). This results in different cell mediated traction forces, as the cells on compliant substrate are unable to form focal adhesions. The cells cultured on the more rigid substrate are unable to deform the matrix, resulting in higher **cytoskeletal tension**, which impacts cell morphology, causing hMSC to differentiate into different pathways³³. hMSC exhibited a round morphology at tall flexible microposts and a more spreaded on small rigid posts. Gene expression analysis showed upregulation of adipogenic markers in cells growing on high microposts and upregulation of osteogenic markers in cells growing on smaller microposts.

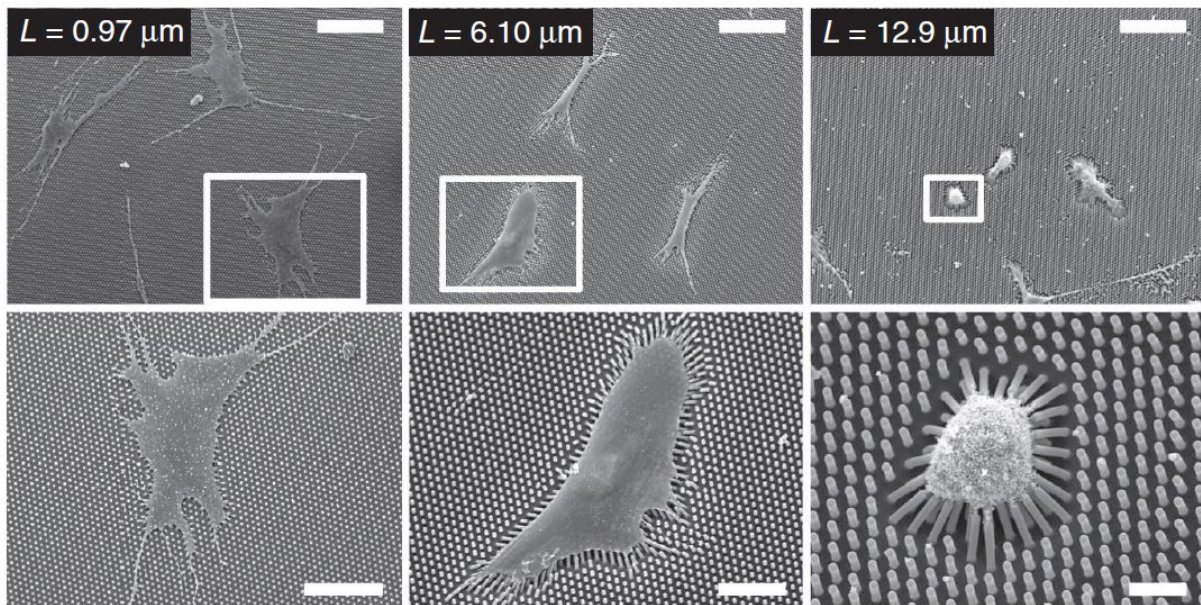


Figure 2: Human mesenchymal stem cells cultured on microposts of different heights. Short microposts signal the cells a stiffer substrate (left) wherefore the cells show a highly stretched morphology. Taller posts (right) appear softer to the cells as they can bend them with their own contraction forces. They exhibit a round morphology. Gene expression analysis showed upregulation of osteogenic markers in stretched cells attributed to their high cytoskeletal contraction and upregulation of adipogenic markers in round cells. Reprinted by permission from Springer Nature³³.

Dalby et al. showed, that not only the size, but also the **spatial arrangement of nanoscale features** can stimulate mesenchymal stem cells to differentiate into osteoblasts without any addition of osteogenic supplements. Different patterns of nanoscale pits ranging from aligned to disordered and random patterns were fabricated using electron beam lithography (see **Figure 3**). The cells, which were experiencing the slightly disordered patterns were shown to differentiate into osteoblasts³⁴.

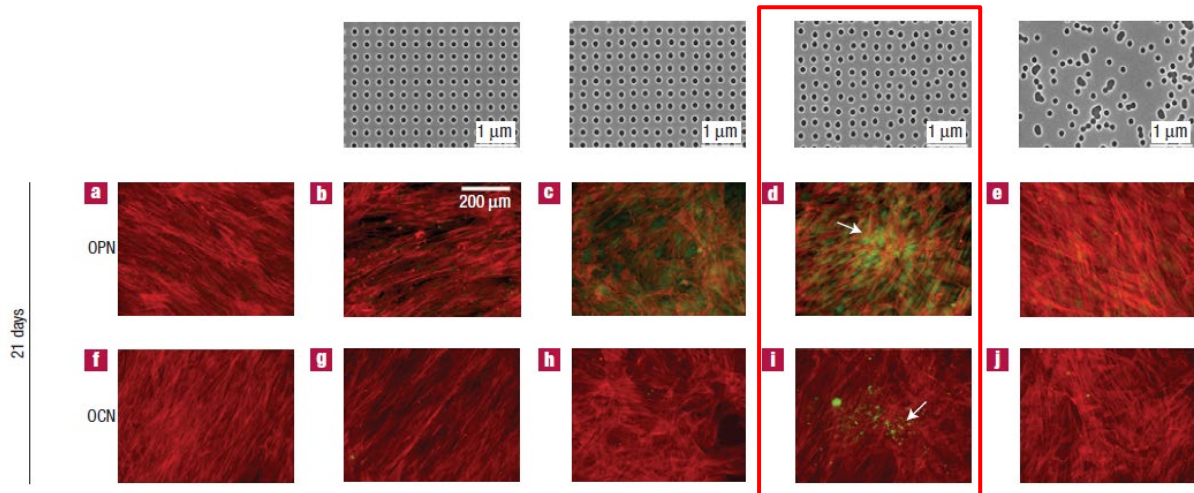


Figure 3: Mesenchymal stem cells (MSC) cultured on different patterns of nanoscale pits (diameter 120 nm, depth 100 nm) and stained for osteogenic marker genes osteopontin (OPN) and osteocalcin (OCN) after 21 days in culture. Pits were placed in squares, slightly displaced squares (± 20 nm from the true centre), strongly displaced squares (± 50 nm from the true centre) and random placements (first row from left to right). MSCs cultured on strongly displaced squares (**d+i**) stained positive for OPN and OCN and showed nodule formation (arrows). Actin = red, OPN/OCN=green. Reprinted by permission from Springer Nature³⁴.

Therefore, it is not surprising that also the surface roughness of the material was shown to guide stem cells into specific pathways. Faia-Torres et al reported the influence of different **surface-roughness** on hMSC. It has been shown, that an average roughness of already 0.93 μm can substitute soluble osteogenic supplementation. hMSC cultured in basal medium on polycaprolactone at a surface-roughness gradient ranging from 0.5 - 4.7 μm showed superior expression of osteogenic genes compared to cells on polystyrene control cultured in complete osteogenic differentiation medium³⁵.

As already implied, **cell shape** and **cytoskeletal tension** have been identified as major contributors to cell fate. McBeath et al. showed that a change in cell shape is already

sufficient enough for hMSC to change lineage commitment. hMSC cells were seeded on different sized polydimethylsiloxane substrate (PDMS) adhesive islands between non-adhesive regions. This design allowed only single-cell attachment. hMSC seeded on big islands were allowed to stretch and showed upregulation in osteogenic markers, whereas on small islands they were forced to stay in a rather round morphology and expressed adipogenic markers (see **Figure 4**)³⁶. Further investigation was performed by Kilian as well as Peng et al, who have shown that not only the size, but also cell shape is a critical parameter for directing stem cell differentiation. Peng et al revealed the importance of inherent anisotropy in stem cell lineage commitment. Under the same adhesive area, cells develop different cytoskeleton at various shaped islands (see **Figure 5**). MSC seeded on circular shape displayed an adipogenic profile, whereas cells seeded on star-shaped islands preferred osteogenic differentiation. The critical parameter was shown to be the cell perimeter, as an indicator for the local anisotropy and the non-roundness of cells³⁷. Kilian et al could show that specific geometric features that introduce increased myosin contractility stimulate osteogenesis. Hence, cells cultured in star shapes displayed larger focal adhesions and stress fibers, which promoted osteogenesis, whereas cells cultured in flower shapes showed promoted adipogenesis. The influence of cytoskeletal contractility was verified by adding pharmacological agents to the cell culture medium, which modulate the cytoskeleton. Results showed that by adding nocodazole, which increases cell contractility, osteogenesis was promoted independent of the shape. Adding other drugs that inhibit contractility were shown to increase adipogenesis. Hence, the differentiation pathway is directly dependent on the contractility of the cytoskeleton³⁸.

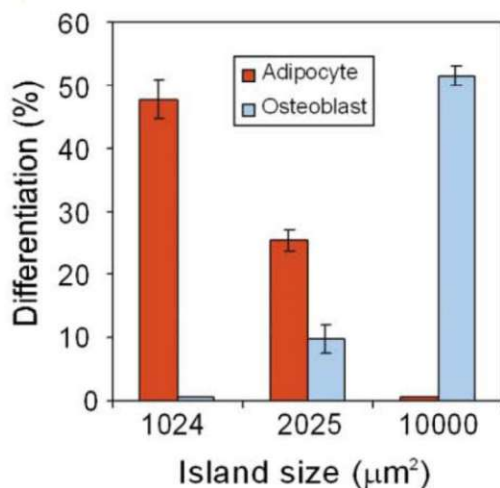


Figure 4: Influence of cell shape and cytoskeletal tension on MSC differentiation. hMSC seeded on variable sized island. hMSC cultured on smaller islands exhibited round morphology and showed adipogenic differentiation. hMSC on big islands were able to stretch and therefore committed to osteogenic differentiation pathway. Reprinted by permission from Elsevier³⁶.

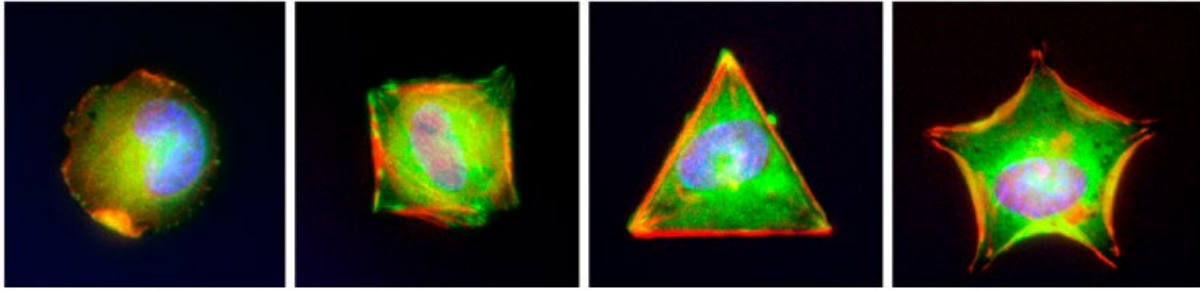


Figure 5: MSC seeded on micropatterned islands of different shape. Cells exhibit different morphological traits (focal adhesions/stress fibers) directly connected to lineage commitment of stem cells. Green: vinculin, red: actin, blue: nuclei. Reprinted by permission from Elsevier³⁷.

In addition, Yang et al. reported that stem cells have a **mechanical memory** and continue to respond to past physical environments. They cultured hMSC on stiff tissue culture polystyrene (Young's modulus $E \sim 3$ GPa) prior to culture on soft PEG hydrogels ($E \sim 2$ kPa). The cells were driven towards osteogenic lineage, although they would favour adipogenesis on the soft substrate. This effect is either reversible or irreversible depending on the culture time at initial conditions (**Figure 6**). They also cultured cells on photodegradable PEG hydrogel and switched the substrate stiffness from 10 kPa to 2 kPa observing the same behaviour. Therefore, they were able to show that cells retain some mechanical information, which effects their future stem cell fate³⁹.

4 Translation into the three-dimensional system

As described in the previous chapter, factors such as **ligand presentation**, **material stiffness** and **roughness** have already been identified as key parameters in cell differentiation in the 2D environment. Adding the third dimension present these key parameters to the entire cell-surrounding it with structural (microarchitecture, porosity, meshwork size), compositional (RGD, growth factors) and mechanical cues (stiffness, viscoelasticity, porosity) - and therefore mimicking the actual organization within native tissue. Adding also the element of time into the cell culturing system further introduces time-dependent factors, such as: **diffusion kinetics** (mass transfer), **degradation** of the biomaterial, cell-induced **matrix formation**, **stress relaxation** and cell induced **reorganization of the matrix** (Figure 6)⁴⁰.

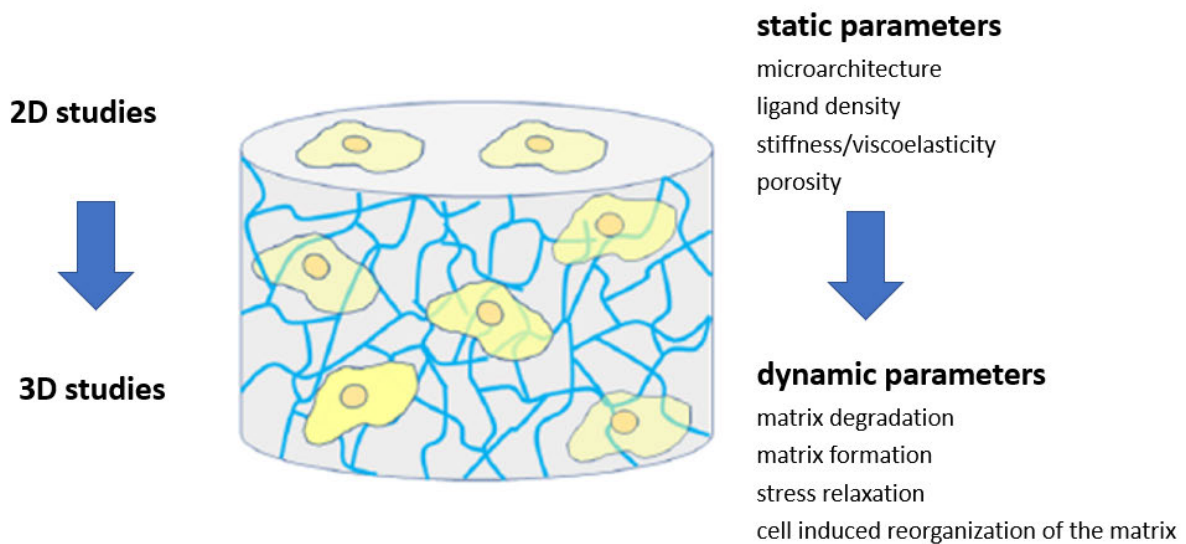


Figure 6: Schematic of the static and dynamic key parameters in the three-dimensional system. Static parameters: Structural (microarchitecture/porosity/meshwork size), compositional (ligand density, growth factors) and mechanical cues (stiffness/viscoelasticity, porosity); and dynamic parameters: matrix degradation, matrix formation, stress relaxation and cell induced reorganization of the matrix are considered key parameters in dictating stem cell fate. Figure adapted from Lee and Kim (2018)⁴⁰.

As ECM-cell interactions are known to be a highly dynamic system, it is not surprising that degradation of the hydrogel is highly influencing cell fate as the overall conditions of the surrounding are changed over time. Degradation is an important process in native tissue, as cells need to degrade their surrounding in order to remodel. The Burdick group⁴¹ reported the influences of degradation on differentiation pathway independent of cell morphology. hMSC encapsulated in hyaluronic acid hydrogels that permitted or restricted degradation showed different lineage commitment. As the cells were able to degrade the matrix, they could spread and exhibited higher cell traction forces, which resulted in osteogenesis. hMSC in hydrogels of the same elastic modulus that were restricted in cell-mediated degradation favoured adipogenesis. Furthermore, a switch from a degradation-permitted to restricted hydrogel over time resulted in a switch from osteogenesis to adipogenesis, although the cells kept their stretched morphology. This study showed the influence of cytoskeletal traction on hMSC lineage commitment, which is further dependent on matrix degradation. Hence, inhibition of the tension-mediated signaling by pharmaceuticals in the permissive hydrogels resulted in adipogenesis, whereas upregulation resulted in osteogenesis even in degradation-restricted hydrogels⁴¹.

In another paper of the Burdick group⁴², they investigated the influence of microenvironmental factors such as dimensionality, stiffness and again degradability on stem cell differentiation. Human bone marrow derived mesenchymal stem cells (BM-hMSC) were seeded either atop of a hydrogel layer (2D) or encapsulated into the hydrogel (3D) of different stiffnesses. The cells were cultured in medium, which did not contain any soluble factors that would induce differentiation. They analyzed the localization and signaling of YAP/TAZ, which are key mediators of mechanosensitive signaling. They showed, that BM-hMSC spreading is dependent on substrate stiffness and dimensionality. In fact, they showed opposing behaviour between 2D and 3D cultivated cells. With increasing stiffness BM-hMSC were able to stretch and had a big spread area in 2D. On the contrary, in 3D the cells were entrapped in the stiff hydrogel and forced to take a round morphology, which yielded to commitment into adipogenic lineage. In 3D cells were only able to spread and elongate at low stiffnesses (**Figure 7**). Regarding YAP/TAZ signaling, a higher spreading of the cells is directly connected to a higher YAP/TAZ nuclear localisation. Therefore, YAP/TAZ is increased with increasing stiffness in 2D cultured MSC, but decreased in 3D cultured cells.

Increased stiffness promotes increased YAP/TAZ in 2D, but decreased YAP/TAZ in 3D

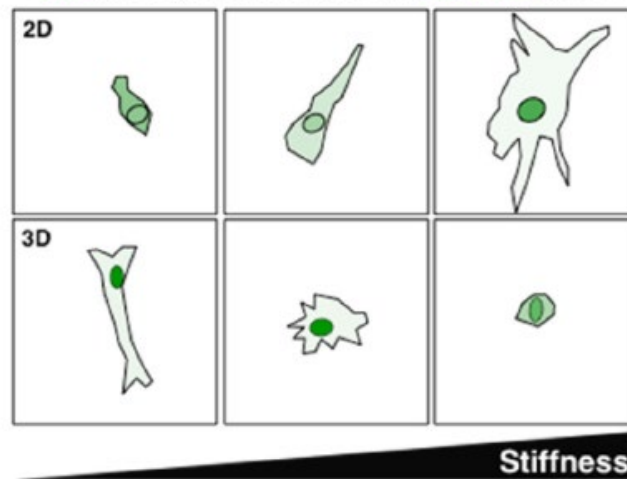


Figure 7: Influence of dimensionality and stiffness on differentiation pathways. With increasing stiffness, the cells are able to stretch out in 2D, whereas they are entrapped in 3D and forced to a round morphology. On the contrary, at lower stiffnesses the cells stay round in 2D, but are able to stretch through the hydrogel in 3D. Stretched morphology yielded in higher YAP/TAZ nuclear localization and therefore osteogenesis. Reprinted by permission from Elsevier⁴².

This shows that cells prefer an environment that allows reorganization⁴⁰ – which in this case is enabled through degradation, but can also be enabled using viscoelastic hydrogels that show stress relaxation⁴³. Non-degradable **chemically crosslinked** hydrogels usually exhibit a more **elastic** behaviour, which restricts the cells to reorganize the surrounding matrix. On the contrary, **physically crosslinked** hydrogels exhibit a more **viscoelastic** behaviour– such as found in native tissue – that allows rearrangement of ligands and thus spreading of the cell. This arises due to the weak bondings that can be broken and reorganized by cellular forces (**Figure 8**). Chaudhuri et al⁴⁴ showed that stress relaxation is an important factor, that allows matrix reorganization and therefore is guiding stem cell fate. They showed that mesenchymal stem cells (MSC) differentiation was influenced by the hydrogels stress relaxation rate. Cells were encapsulated in non-degradable alginate-based hydrogels

exhibiting different stress relaxation rates. Osteogenic differentiation was favoured in hydrogels with increasing stress relaxation rate.

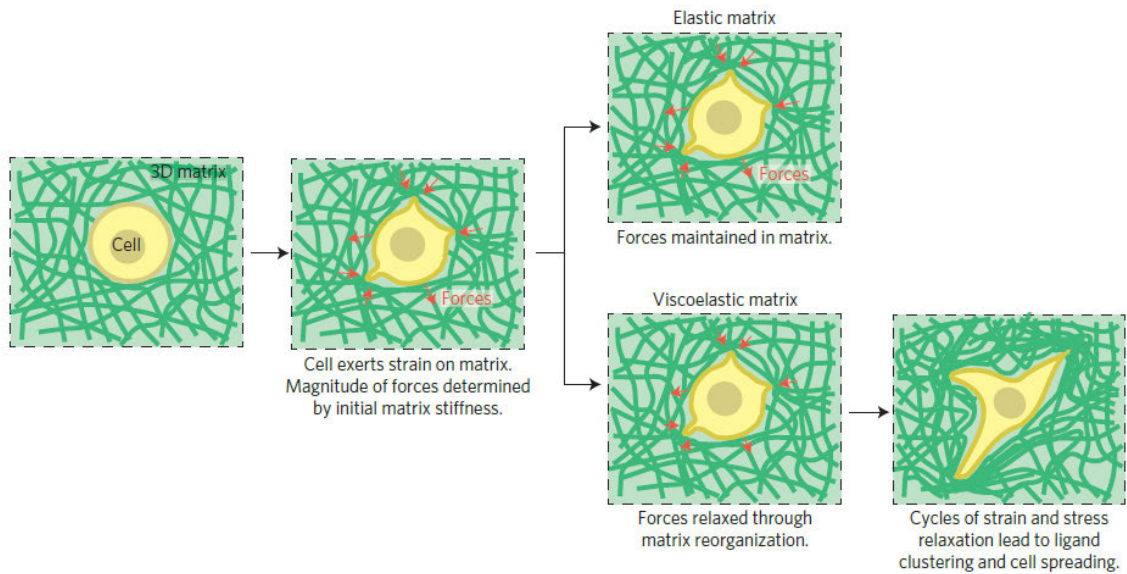


Figure 8: Schematic of how cells behave in an elastic vs viscoelastic matrix. Cells within the matrix exert traction forces by pulling on the matrix with their cytoskeletal forces. The matrix resists this strain depending on its elastic modulus. Elastic matrices never relax and therefore cannot be remodelled by a cells' cytoskeletal force. Within viscoelastic matrices, due to stress relaxation the cells can reorganize the matrix, that leads to ligand clustering and cell spreading. Reprinted by permission from Springer Nature⁴⁴.

4.1 Methods to introduce degradation

As already described in the previous chapter, the dynamical change of the matrix over time is one of the important criteria for mimicking the native ECM and has to be considered when designing a hydrogel for tissue engineering purposes. In controlling the spatiotemporal change of mechanical and biochemical properties, cell differentiation, proliferation and migration are influenced. The introduction of cleavage sites to the hydrogel system represent an attractive strategy for the control of degradation properties. They can be used to decrease the density of crosslinks, but also to release or bind incorporated growth factors. Many strategies such as ester hydrolysis, enzymatic cleavage reactions^{41,45-47} and light-mediated reactions⁴⁸⁻⁵¹ have been reported^{52,53}.

Enzymatic degradation can automatically take place in naturally derived hydrogels such as collagen or hyaluronic acid. However, by introducing cleavage sites e.g. for matrix-metalloproteinases (MMP) the degradation kinetics can be tuned. Enzymatic degradation has been widely used to investigate the influence of a dynamic microenvironment on stem cells^{41,46}. Feng and coworkers could show that the introduction of MMP sites to methacrylated hyaluronic acid hydrogels influences hMSC chondrogenesis⁴⁷.

Degradation methods employing **hydrolysis** or enzymes only allow temporal control, but lack spatial control. In contrast, **photodegradation** can also spatially control the hydrogel properties in real-time. A widely exploited chemistry is the incorporation of nitrobenzyl groups into the hydrogel⁴⁸⁻⁵⁰. The Anseth group⁴⁸ designed a photocleavable hydrogel by introducing nitrobenzyl ether moieties to a PEG hydrogel system. Embryonic stem cell-derived motor neurons (ESMNs) were encapsulated and by applying one or two-photon irradiation, the cells could be released allowing control over the extension of cell axons (**Figure 9**)⁴⁸. They also described a coumarin-based photodegradable hydrogel as an alternative to the nitrobenzyl-based system. The advantage of this chemistry is, that the by-products are biologically inert in contrast to the nitrobenzyl-based chemistry and that a broader spectrum of light, with wavelengths more suitable for cells, can be used for inducing the degradation process⁵⁴.

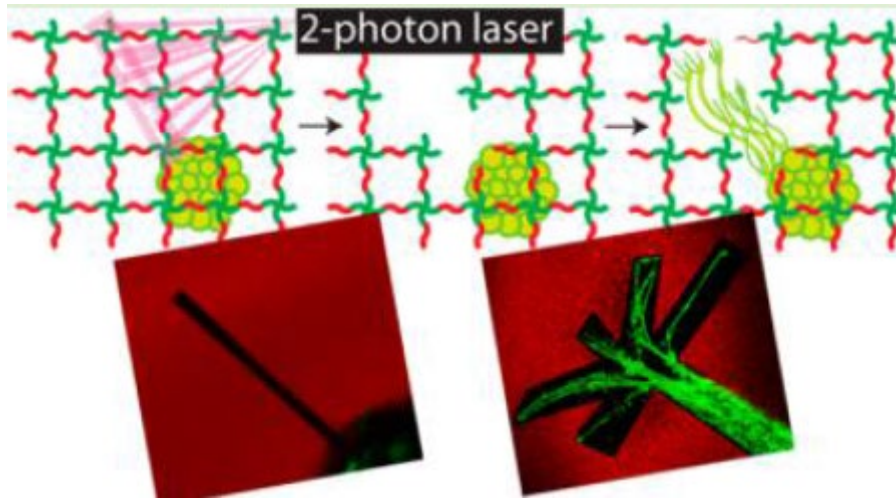


Figure 9: Photocleavable hydrogel. By introducing nitrobenzyl ether moieties, the PEG hydrogel system becomes photodegradable. Using 2-photon irradiation, covalent bonds can be cleaved to direct cells. Embryonic stem cell-derived motor neurons (ESMNs) encapsulated within this hydrogel, could be directed, as they extended their axons at locations where photocleavage had been performed. Reprinted with permission from ⁴⁸. Copyright (2014) American Chemical Society.

5 Outlook

For biofabrication of functional tissue the major challenges still remain in the design of a hydrogel, which provides the right cues within the microenvironment to guide cells to develop their intended behaviour. Limitations for the material arise due to the fact, that the hydrogel also has to have certain traits to be fabricated with current biofabrication techniques. Requirements on chemistry and viscosity, which arise due to certain process parameters, as well as desired mechanical properties and resolution of the final construct further restrict the possibilities in design. Moreover, fabrication of the cell-loaded hydrogel with the method of choice needs to maintain the viability of encapsulated cells during and after the whole process. The interplay between all these factors result in high demands on hydrogel and process design⁵⁵.

A lot of progress has been made in biomaterial design as well as development of biofabrication techniques since the advent of 3D bioprinting. Methods emerged and advanced, each bringing along its own limitations. Nevertheless, with the variety of today's possibilities to fabricate biomaterials it seems that the shortcomings of one method can be compensated with the strengths of another method. Therefore, in the future not only further development of bioink and fabrication processes have to be made, but especially advances in the combination of already existing methods might be the key to fill the persisting technological gap.

6 Summary

The aim of this work is expanding the spectrum of tissue engineering approaches by establishing tools that allow to improve the precision of biofabricated biomimetic scaffolds. To achieve the development of a certain tissue construct, the bioprinting input parameters, such as starting material, initial cell loading and construct geometry have to be optimized. By using a computational framework, it is possible to predict the behaviour of the cells within the material and to adopt these parameters for the printing process. Therefore, in this work we developed a numerical model for predicting the mechanical properties of cell-loaded hydrogels considering the effect of cell density, cell distribution and proliferation of the cells over time. Although such computational tools can be used to optimize parameters during the 3D printing process and therefore benefit the whole field of bioprinting, they currently lack attention. Hence, we propose, that computational approaches should be integrated as a pre-step in every biomimetic tissue design and fabrication to yield in the desired construct.

Within the second part we further addressed the improvement of printing precision. This time, we focused on the fabrication of soft hydrogels. For many bioinks there is a compromise between the printability of the liquid material and the mechanical properties of the final solid structure. It needs excellent fluidity of the liquid during the printing process and at the same time self-supportive mechanical properties of the solid immediately after the material is deposited so that it will not collapse under its own weight. Therefore, a fast transition from liquid to the solid state is required, but often difficult to match – also in respect to maintain uniform conditions through the whole printed structure. Hence, we developed a novel bioink exhibiting shear-thinning as well as self-healing properties for free directional printing (Embedding Gel-in-Gel Approach). This method allows to print a soft hydrogel (which is not self-supportive) into another hydrogel (that serves as a support material) that share the same chemistry. Therefore, deformation and collapse of the 3D printed construct is prevented. By further adding the ability to additionally crosslink one of those hydrogels photochemically, self-supportive 3-dimensional structures can be obtained and the non-covalently bound supportive hydrogel can be washed away. This chemistry also provides the possibility to incorporate chemically attached ligands in specific locations that serve as biological cues for cells. The presented biomaterial and fabrication method are suitable for cell encapsulation. Therefore, by using this material in combination with the

presented printing approach, we further expanded the toolbox of fabricating soft hydrogels for tissue engineering approaches.

Lastly, in the third part, we investigated the suitability of methacryloyl-modified gelatin (gelMA) for cartilage tissue engineering. We showed, that dedifferentiated chondrocytes can be redifferentiated by 3D culture within gelMA hydrogel. We further investigated its potential use to treat osteoarthritic cartilage (OA). Coating of rough OA cartilage (*ex vivo*) yielded in smoothing of the surface, filling up the defects and delivering cells for treatment. After crosslinking gelMA attaches to the defect tissue and withstands mechanical stress. Therefore, in a next step we simulated the mechanical stresses present in the human knee joint during walking to investigate the stability of the hydrogel. The hydrogel stayed intact and encapsulated cells stayed viable. Therefore, we propose that gelMA might be a great material to treat cartilage defects, especially osteoarthritis. It allows easy application of the cells to the defect site and shields the cells against prevalent mechanical stresses whilst promoting differentiation.

Taken together, this work shows that there are many different construction areas along the road to the ultimate goal of producing functional tissue. Mathematical modelling, material and process development and the matching with the final clinical approach - all contribute to establishment of processes to regenerate defective tissues.

6.1 Bioink properties before, during and after 3D bioprinting

In the first publication, we discuss key properties of bioinks before, during and after 3D bioprinting using the most popular bioprinting approaches as examples. We give an overview of the bioprinting methodologies - such as inkjet, orifice-free, and extrusion bioprinting - along with the suitable bioinks. We further present commercially available bioprinters and bioink materials. Lastly, we identified a numerical approach that allows to predict the mechanical properties of a cell-loaded hydrogel considering the effect of cell density, distribution, and proliferation within the hydrogel. Therefore, we performed the following experiments:

1) We investigated the changes in mechanical properties of methacrylamide-modified gelatin, in the presence of mouse-calvaria-derived preosteoblast cells (MC3T3-E1). Using rheological measurements, we showed that higher cell numbers resulted in the reduction of mechanical properties.

2) We designed a numerical model based on experimental data to predict hydrogel properties, when loaded with cells. A representative volume element (RVE) was loaded with cells modeled as spheres with a diameter of 30 μm , a Young's modulus of 1.5 kPa, and 5% cell contraction (eigenstrain). The hydrogel was modeled based on the data obtained from the previous rheological measurements of acellular samples (storage modulus and loss modulus). The RVE was then loaded with 10% shear loading to simulate the rheological testing conditions. The predicted shear modulus, calculated by the mathematical model, was shown to be in agreement with the experimental obtained data.

Therefore, we modelled further influences, such as various cell distributions within the gelMA hydrogel and the change in hydrogel properties due to proliferation of cells over time.

3) When designing a biomimetic construct, it has to be considered that cells proliferate, migrate, and differentiate within the hydrogel and also interact with it. This will change the hydrogel's material properties over time. As cells proliferate, they can form clusters or distribute within the hydrogel evenly. This not only depends on the cell type, but also on the properties of the hydrogel used (porosity, stiffness, cell binding motifs, etc.). We modelled

three different variations of cell distribution (at constant cell density): random distributed, cluster formation in the corners of RVE and cluster formation within the center of RVE. We showed, that gelMA loaded with cells, which were organized in clusters, were softer compared to randomly distributed samples. Moreover, mechanical stresses experienced by the cells were higher, when cells were clustered and therefore, cells might have been more prone to damage.

4) Cell proliferation within the 3D printed construct is inevitable. Therefore, the effect of cell growth has to be considered and predicted during the design of a 3D printed scaffold. Numerical modeling was performed on cell-loaded hydrogels simulating cluster formation as a result of cell proliferation. It showed that the mechanical properties decreased when cells proliferate over time.

In conclusion, in order to fabricate a biomimetic construct with the desired final properties, one has to take a lot of different parameters into account in the estimation. The described numerical model does not take into account all the parameters of cell-material interaction. To get a more precise prediction of the resulting material properties, the model has to be fed with more data based on the knowledge of further parameters such as material degradation rate and matrix remodeling. Nevertheless, numerical models help to predict the behaviour of cells within the material and will help to optimize the fabrication parameters to yield in the production of the desired structure. Therefore, we propose that computational approaches, as the one presented within this work, should be integrated as a pre-step in biomimetic tissue design and biofabrication.

My contribution: Generation of data for the numerical model, rheological measurements of cell-loaded hydrogels, parts of writing/structuring

6.2 Dynamic Coordination Chemistry Enables Free Directional Printing of Biopolymer Hydrogel

In the second paper, we focus on the challenges of extrusion based bioprinting systems. As has already been discussed in the first paper, there are several limitations when it comes to extrusion based bioprinting systems. It is possible to print with materials that exhibit high viscosity, but due to pressure drops which are generated during the extrusion process, the cells might be harmed. On the other hand, extruding a material, which is low in viscosity will not yield in stable structures and might deform and collapse. Therefore, there is always a compromise between printability of the fluid material and good mechanical properties.

To enable easy extrusion of the material and mechanical supportive structures, the bioink needs to undergo a sharp transition from the liquid to the solid state. To control this process and to guarantee a uniform condition amongst the 3D printed structure still remains challenging. New materials and strategies are necessary to surpass these limitations.

In this work, we introduce a new chemistry which allows omnidirectional embedding of one hydrogel into another support hydrogel that share the same chemistry. Bisphosphonate groups (BP) were conjugated on hyaluronic acid (HA) to exploit the complexing capacity of BP in the presence of calcium ions (Ca^{2+}). Due to the reversibility of these coordination bonds, the material develops shear-thinning as well as self-healing properties. These properties allow to extrude one soft hydrogels, into a supportive hydrogel bath, thereby avoiding the deformation and collapse of the structure (Embedding Gel-in-Gel Approach). With further addition of acrylamide groups (Am) to the HA-BP derivative (Am-HA-BP) the material becomes also photosensitive. Therefore, it is possible to chemically crosslink the hydrogel using UV light in a second step. This improves the mechanical stability of the constructs. In summary, the combination of these two materials, HA-BP and Am-HA-BP, using an embedding gel-in-gel approach (free directional printing technology) and post UV-crosslinking, allows the production of complex tubular shapes, voids, and tunnel systems (depending on which hydrogel is washed away).

We further added a bioactive group, Arg-Gly-Asp-Ser-Cys (RGDSC), to the bioink and extruded it into the support hydrogel Am-HA-BP. This procedure allowed spatial controlled immobilization of the extruded bioactive molecules. In tissue engineering the spatial control

over bioactive molecules like drugs, growth factors, and cytokines would be key to fabricate biomimetic scaffolds that resemble not only the topography, but also the biochemical composition of the native ECM. Therefore, this material and its fabrication method expands the spectrum of possibilities to recreate native tissue.

In the last step, we demonstrated that our fabrication method was also suitable when cells are present. Mouse pre-osteoblast cells (MC3T3-E1) and hTERT immortalized human adipose-derived mesenchymal stem cells (ASC/TERT1) were encapsulated within the material and showed great viability when crosslinked physically as well photochemically.

In conclusion, we developed a material that approaches the basic concept of tissue engineering in combining a suitable biomaterial with growth factors and cells to create biomimetic scaffolds. This material shows great potential as a bioink to construct biomimetic scaffolds via 3D bioprinting application.

My contribution: Experimental work and analysis of cell culture experiments.

6.3 Gelatin methacryloyl as environment for chondrocytes and cell delivery to superficial cartilage defects

In the third paper, we investigated the clinical relevance of a hydrogel material for cartilage tissue engineering. Gelatin methacryloyl (gelMA) was used to encapsulate dedifferentiated human articular chondrocytes (hAC) to provide a 3D environment that allows redifferentiation to happen. The influence of various amounts of transforming growth factor β 3 (TGF- β 3) on cells in different passages was investigated along with the influence of different hydrogel stiffness.

When chondrocytes are expanded in a conventional monolayer cell culture, they start to lose their phenotype, as characterized by the downregulation of chondrogenic specific genes, such as collagen type II (COL2) and aggrecan (ACAN), and the upregulation of collagen type I (COL1)⁵⁶⁻⁵⁹. As such, chondrocytes become more fibroblast-like. For clinical application, this process needs to be either prevented or methods have to be developed that redifferentiate these cells back to the chondrocyte phenotype, as the implantation of dedifferentiated chondrocytes might yield to the formation of mechanical inferior fibrocartilage^{60,61}.

Culturing cells in a 3D environment that mimics the natural ECM has been shown to support the cell's original phenotype. Herein, we used gelMA as it exhibits many beneficial material properties: a) it is derived from collagen, which is also the major component of cartilage; b) it is biocompatible; c) it features cell-binding motifs, such as the protein sequence RGD (Arg-Gly-Asp) for cell adhesion and d) it exhibits sequences where matrix metalloproteinases can cut, rendering the material biodegradable. Gelatin-type-B from bovine skin was modified with methacryloyl groups to make it photosensitive. Therefore, the material becomes tunable in its mechanical properties by controlling the degree of substitution, concentrations of polymer, photoinitiator, and irradiation conditions⁶². Furthermore, as the final application will be *in vivo*, the photochemical crosslinking provides a superior stability within the body's physiological conditions in contrast to physical crosslinked hydrogels.

The rheological properties of gelMA were investigated and biocompatibility for chondrocyte encapsulation was determined. Cell culture for three weeks within different stiffnesses of gelMA resulted in different morphology for samples cultured in 0 ng/mL and 1 ng/mL TGF- β 3

as shown via live-dead staining. Within the softer gelMA, cells adapted to a stretched morphology, whereas in the stiffer gelMA round morphology dominated. When cultured within 10 ng/mL TGF- β 3 the cells adapted their morphology to an overall round shape with small cell processes independently of the gelMA stiffness. This indicates the strong influence of TGF- β 3 on chondrocyte phenotype.

We further examined gene expression profiles using quantitative PCR and comparison with standard micromass pellet culture. The presence of cartilage specific matrix proteins, such as glycoaminoglycans (GAGs) and collagen type 2, were analysed using histology techniques. We showed, that chondrocytes in late passage 5 were able to redifferentiate using gelMA 3D culture. The redifferentiation potential was directly influenced by the concentration of TGF- β 3. No preference among one hydrogel stiffness could be observed.

To test the feasibility of the hydrogel for osteoarthritic (OA) cartilage treatment, we simulated the mechanical stresses prevalent in the human knee joint during walking. Samples of OA cartilage were coated with the cell-loaded gelMA and force was applied using a tribometer. Results showed, that the cell-loaded hydrogel attached to the defective tissue, filled up the voids and smoothed its superficial surface roughness. We showed, that gelMA delivers cells effectively to sites of tissue damage and protects the cells from mechanical stress emerging during human gait.

We concluded, that gelMA is a material suitable for the redifferentiation of human articular chondrocytes. It promotes the chondrogenic phenotype even at late passage (P5). Furthermore, it is easily applied and forms a stable film when applied to defect tissue. As was shown in *ex vivo* simulation, gelMA adheres to the defect cartilage tissue and acts as a cell transporter matrix and simultaneously protects the encapsulated cells from mechanical stresses occurring in the joint during movement. Therefore, gelMA presents a material which is highly promising for cartilage tissue engineering.

My contribution: I wrote the whole paper, performed experimental work (except statistics and histological staining) and analysed the results.

7 REFERENCES

1. Slaughter, B. V., Khurshid, S. S., Fisher, O. Z., Khademhosseini, A. & Peppas, N. A. Hydrogels in Regenerative Medicine. *Adv. Mater. Deerfield Beach Fla* **21**, 3307–3329 (2009).
2. Pampaloni, F., Reynaud, E. G. & Stelzer, E. H. K. The third dimension bridges the gap between cell culture and live tissue. *Nat. Rev. Mol. Cell Biol.* **8**, 839–845 (2007).
3. Melchels, F. P. W. *et al.* Additive manufacturing of tissues and organs. *Prog. Polym. Sci.* **37**, 1079–1104 (2012).
4. Guilak, F. *et al.* Control of Stem Cell Fate by Physical Interactions with the Extracellular Matrix. *Cell Stem Cell* **5**, 17–26 (2009).
5. Walters, N. J. & Gentleman, E. Evolving insights in cell–matrix interactions: Elucidating how non-soluble properties of the extracellular niche direct stem cell fate. *Acta Biomater.* **11**, 3–16 (2015).
6. Zhu, J. & Marchant, R. E. Design properties of hydrogel tissue-engineering scaffolds. *Expert Rev. Med. Devices* **8**, 607–626 (2011).
7. Lee, J., Cuddihy, M. J. & Kotov, N. A. Three-Dimensional Cell Culture Matrices: State of the Art. *Tissue Eng. Part B Rev.* **14**, 61–86 (2008).
8. Drury, J. L. & Mooney, D. J. Hydrogels for tissue engineering: scaffold design variables and applications. *Biomaterials* **24**, 4337–4351 (2003).
9. Geckil, H., Xu, F., Zhang, X., Moon, S. & Demirci, U. Engineering hydrogels as extracellular matrix mimics. *Nanomed.* **5**, 469–484 (2010).
10. Zhu, J. & Marchant, R. E. Design properties of hydrogel tissue-engineering scaffolds. *Expert Rev. Med. Devices* **8**, 607–626 (2011).
11. Hunt, N. C. & Grover, L. M. Cell encapsulation using biopolymer gels for regenerative medicine. *Biotechnol. Lett.* **32**, 733–742 (2010).
12. Annabi, N. *et al.* 25th anniversary article: Rational design and applications of hydrogels in regenerative medicine. *Adv. Mater. Deerfield Beach Fla* **26**, 85–123 (2014).
13. Mironov, V., Reis, N. & Derby, B. Review: Bioprinting: A Beginning. *Tissue Eng.* **12**, 631–634 (2006).
14. Murphy, S. V. & Atala, A. 3D bioprinting of tissues and organs. *Nat. Biotechnol.* **32**, 773–785 (2014).

-
15. Jungst, T., Smolan, W., Schacht, K., Scheibel, T. & Groll, J. Strategies and Molecular Design Criteria for 3D Printable Hydrogels. *Chem. Rev.* **116**, 1496–1539 (2016).
 16. Qin, X.-H., Ovsianikov, A., Stampfl, J. & Liska, R. Additive manufacturing of photosensitive hydrogels for tissue engineering applications. *BioNanoMaterials* **15**, (2014).
 17. Mouw, J. K., Ou, G. & Weaver, V. M. Extracellular matrix assembly: a multiscale deconstruction. *Nat. Rev. Mol. Cell Biol.* **15**, 771–785 (2014).
 18. Aizawa, Y., Owen, S. C. & Shoichet, M. S. Polymers used to influence cell fate in 3D geometry: New trends. *Prog. Polym. Sci.* **37**, 645–658 (2012).
 19. Bowers, S. L. K., Banerjee, I. & Baudino, T. A. The extracellular matrix: at the center of it all. *J. Mol. Cell. Cardiol.* **48**, 474–482 (2010).
 20. Rozario, T. & DeSimone, D. W. The extracellular matrix in development and morphogenesis: A dynamic view. *Dev. Biol.* **341**, 126–140 (2010).
 21. Gordon, M. K. & Hahn, R. A. Collagens. *Cell Tissue Res.* **339**, 247 (2009).
 22. Ricard-Blum, S. The Collagen Family. *Cold Spring Harb. Perspect. Biol.* **3**, (2011).
 23. Durbeej, M. Laminins. *Cell Tissue Res.* **339**, 259–268 (2010).
 24. Lodish, H. *et al.* Noncollagen Components of the Extracellular Matrix. *Mol. Cell Biol.* 4th Ed. (2000).
 25. Barczyk, M., Carracedo, S. & Gullberg, D. Integrins. *Cell Tissue Res.* **339**, 269–280 (2010).
 26. Chiarugi, P. & Giannoni, E. Anoikis: A necessary death program for anchorage-dependent cells. *Biochem. Pharmacol.* **76**, 1352–1364 (2008).
 27. Schaefer, L. & Schaefer, R. M. Proteoglycans: from structural compounds to signaling molecules. *Cell Tissue Res.* **339**, 237 (2009).
 28. Esko, J. D., Kimata, K. & Lindahl, U. Proteoglycans and Sulfated Glycosaminoglycans. in *Essentials of Glycobiology* (eds. Varki, A. *et al.*) (Cold Spring Harbor Laboratory Press, 2009).
 29. Afratis, N. *et al.* Glycosaminoglycans: key players in cancer cell biology and treatment. *FEBS J.* **279**, 1177–1197 (2012).
 30. Murphy, W. L., McDevitt, T. C. & Engler, A. J. Materials as stem cell regulators. *Nat. Mater.* **13**, 547–557 (2014).

-
31. Arnold, M. *et al.* Activation of Integrin Function by Nanopatterned Adhesive Interfaces. *ChemPhysChem* **5**, 383–388 (2004).
 32. Anselme, K. & Biggerelle, M. Role of materials surface topography on mammalian cell response. *Int. Mater. Rev.* **56**, 243–266 (2011).
 33. Fu, J. *et al.* Mechanical regulation of cell function with geometrically modulated elastomeric substrates. *Nat. Methods* **7**, 733–736 (2010).
 34. Dalby, M. J. *et al.* The control of human mesenchymal cell differentiation using nanoscale symmetry and disorder. *Nat. Mater.* **6**, 997–1003 (2007).
 35. Faia-Torres, A. B. *et al.* Osteogenic differentiation of human mesenchymal stem cells in the absence of osteogenic supplements: A surface-roughness gradient study. *Acta Biomater.* **28**, 64–75 (2015).
 36. McBeath, R., Pirone, D. M., Nelson, C. M., Bhadriraju, K. & Chen, C. S. Cell shape, cytoskeletal tension, and RhoA regulate stem cell lineage commitment. *Dev. Cell* **6**, 483–495 (2004).
 37. Peng, R., Yao, X. & Ding, J. Effect of cell anisotropy on differentiation of stem cells on micropatterned surfaces through the controlled single cell adhesion. *Biomaterials* **32**, 8048–8057 (2011).
 38. Kilian, K. A., Bugarija, B., Lahn, B. T. & Mrksich, M. Geometric cues for directing the differentiation of mesenchymal stem cells. *Proc. Natl. Acad. Sci. U. S. A.* **107**, 4872–4877 (2010).
 39. Yang, C., Tibbitt, M. W., Basta, L. & Anseth, K. S. Mechanical memory and dosing influence stem cell fate. *Nat. Mater.* **13**, 645–652 (2014).
 40. Lee, J.-H. & Kim, H.-W. Emerging properties of hydrogels in tissue engineering. *J. Tissue Eng.* **4**.
 41. Khetan, S. *et al.* Degradation-mediated cellular traction directs stem cell fate in covalently crosslinked three-dimensional hydrogels. *Nat. Mater.* **12**, 458–465 (2013).
 42. Caliarì, S. R., Vega, S. L., Kwon, M., Soulas, E. M. & Burdick, J. A. Dimensionality and spreading influence MSC YAP/TAZ signaling in hydrogel environments. *Biomaterials* **103**, 314–323 (2016).
 43. Chaudhuri, O. *et al.* Substrate stress relaxation regulates cell spreading. *Nat. Commun.* **6**, 1–7 (2015).

-
44. Chaudhuri, O. *et al.* Hydrogels with tunable stress relaxation regulate stem cell fate and activity. *Nat. Mater.* **15**, 326–334 (2016).
45. Amer, L. D., Holtzinger, A., Keller, G., Mahoney, M. J. & Bryant, S. J. Enzymatically degradable poly(ethylene glycol) hydrogels for the 3D culture and release of human embryonic stem cell derived pancreatic precursor cell aggregates. *Acta Biomater.* **22**, 103–110 (2015).
46. Chung, C., Beecham, M., Mauck, R. L. & Burdick, J. A. The Influence of Degradation Characteristics of Hyaluronic Acid Hydrogels on In Vitro Neocartilage Formation by Mesenchymal Stem Cells. *Biomaterials* **30**, 4287–4296 (2009).
47. Feng, Q., Zhu, M., Wei, K. & Bian, L. Cell-Mediated Degradation Regulates Human Mesenchymal Stem Cell Chondrogenesis and Hypertrophy in MMP-Sensitive Hyaluronic Acid Hydrogels. *PLoS ONE* **9**, (2014).
48. McKinnon, D. D., Brown, T. E., Kyburz, K. A., Kiyotake, E. & Anseth, K. S. Design and Characterization of a Synthetically Accessible, Photodegradable Hydrogel for User-Directed Formation of Neural Networks. *Biomacromolecules* **15**, 2808–2816 (2014).
49. Griffin, D. R., Patterson, J. T. & Kasko, A. M. Photodegradation as a mechanism for controlled drug delivery. *Biotechnol. Bioeng.* **107**, 1012–1019 (2010).
50. Griffin, D. R. & Kasko, A. M. Photodegradable macromers and hydrogels for live cell encapsulation and release. *J. Am. Chem. Soc.* **134**, 13103–13107 (2012).
51. DeForest, C. A. & Anseth, K. S. Cytocompatible Click-based Hydrogels with Dynamically-Tunable Properties Through Orthogonal Photoconjugation and Photocleavage Reactions. *Nat. Chem.* **3**, 925–931 (2011).
52. Kharkar, P. M., Kiick, K. L. & Kloxin, A. M. Designing degradable hydrogels for orthogonal control of cell microenvironments. *Chem. Soc. Rev.* **42**, 7335–7372 (2013).
53. Hilderbrand, A. M. *et al.* Biomaterials for 4D stem cell culture. *Curr. Opin. Solid State Mater. Sci.* **20**, 212–224 (2016).
54. Azagarsamy, M. A., McKinnon, D. D., Alge, D. L. & Anseth, K. S. Coumarin-Based Photodegradable Hydrogel: Design, Synthesis, Gelation, and Degradation Kinetics. *ACS Macro Lett.* **3**, 515–519 (2014).
55. Sun, W. *et al.* The bioprinting roadmap. *Biofabrication* **12**, 022002 (2020).
56. Kang, S.-W., Yoo, S. P. & Kim, B.-S. Effect of chondrocyte passage number on histological aspects of tissue-engineered cartilage. *Biomed. Mater. Eng.* **17**, 269–276 (2007).

-
57. Benya, P. D., Padilla, S. R. & Nimni, M. E. Independent regulation of collagen types by chondrocytes during the loss of differentiated function in culture. *Cell* **15**, 1313–1321 (1978).
58. Caron, M. M. J. *et al.* Redifferentiation of dedifferentiated human articular chondrocytes: comparison of 2D and 3D cultures. *Osteoarthritis Cartilage* **20**, 1170–1178 (2012).
59. von der Mark, K., Gauss, V., von der Mark, H. & Müller, P. Relationship between cell shape and type of collagen synthesised as chondrocytes lose their cartilage phenotype in culture. *Nature* **267**, 531–532 (1977).
60. Karuppal, R. Current concepts in the articular cartilage repair and regeneration. *J. Orthop.* **14**, A1–A3 (2017).
61. Bhosale, A. M. & Richardson, J. B. Articular cartilage: structure, injuries and review of management. *Br. Med. Bull.* **87**, 77–95 (2008).
62. Van Den Bulcke, A. I. *et al.* Structural and rheological properties of methacrylamide modified gelatin hydrogels. *Biomacromolecules* **1**, 31–38 (2000).

Chapter II

Bioink properties before, during and after 3D bioprinting

Authors:

HÖLZL, K., LIN S., TYTGAT, L., VAN VLIERBERGHE, S., GU, L. and OVSIANIKOV, A.

Published in:

BIOFABRICATION 2016; 8 (3)

Contribution:

Generation of data for the numerical model, rheological measurements of cell-loaded hydrogels, parts of writing/structuring

Biofabrication



TOPICAL REVIEW

Bioink properties before, during and after 3D bioprinting

OPEN ACCESS

RECEIVED

24 March 2016

REVISED

6 June 2016

ACCEPTED FOR PUBLICATION

20 July 2016

PUBLISHED

23 September 2016

Katja Hölzl^{1,2,7}, Shengmao Lin^{3,6,7}, Liesbeth Tytgat^{4,5}, Sandra Van Vlierberghe^{4,5}, Linxia Gu³ and Aleksandr Ovsianikov^{1,2}

¹ Institute of Materials Science and Technology, Technical University Vienna, Austria

² Austrian Cluster for Tissue Regeneration, Austria

³ Department of Mechanical & Materials Engineering, University of Nebraska Lincoln, USA

⁴ Polymer Chemistry and Biomaterials Group, Ghent University, Belgium

⁵ Brussels Photonics Team, Vrije Universiteit Brussel, Belgium

⁶ School of Civil Engineering and Architecture, Xiamen University of Technology, China

⁷ Both authors contributed equally to this paper.

E-mail: Aleksandr.Ovsianikov@tuwien.ac.at

Keywords: tissue engineering, bioprinting, hydrogels, scaffold, numerical modeling, bioink, 3D printing

Original content from this work may be used under the terms of the [Creative Commons Attribution 3.0 licence](https://creativecommons.org/licenses/by/3.0/).

Any further distribution of this work must maintain attribution to the author(s) and the title of the work, journal citation and DOI.



Abstract

Bioprinting is a process based on additive manufacturing from materials containing living cells. These materials, often referred to as bioink, are based on cytocompatible hydrogel precursor formulations, which gel in a manner compatible with different bioprinting approaches. The bioink properties before, during and after gelation are essential for its printability, comprising such features as achievable structural resolution, shape fidelity and cell survival. However, it is the final properties of the matured bioprinted tissue construct that are crucial for the end application. During tissue formation these properties are influenced by the amount of cells present in the construct, their proliferation, migration and interaction with the material. A calibrated computational framework is able to predict the tissue development and maturation and to optimize the bioprinting input parameters such as the starting material, the initial cell loading and the construct geometry. In this contribution relevant bioink properties are reviewed and discussed on the example of most popular bioprinting approaches. The effect of cells on hydrogel processing and vice versa is highlighted. Furthermore, numerical approaches were reviewed and implemented for depicting the cellular mechanics within the hydrogel as well as for prediction of mechanical properties to achieve the desired hydrogel construct considering cell density, distribution and material–cell interaction.

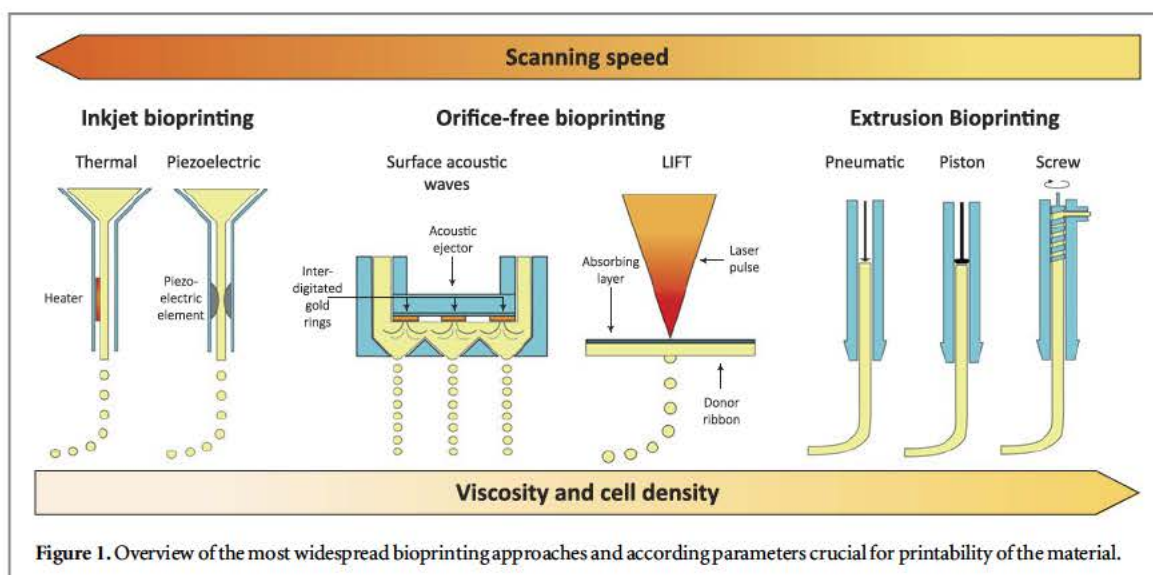
1. Introduction

Fabrication of scaffolds by employing additive manufacturing technologies (AMT) also referred to as three-dimensional (3D) printing, has been widely used in tissue engineering to restore, replace or regenerate defective tissues [1, 2]. Bioprinting can be considered an additive manufacturing technique during which cells and biomaterials, often referred to as 'bioink', are deposited simultaneously [3, 4]. Bioprinting allows to skip the cell seeding procedure, which often proved to be challenging for classical scaffold-based tissue engineering. Moreover, it provides a possibility to distribute different cell types at desired locations within the bioprinted construct and achieve high initial cell densities. A number of comprehensive reviews, book chapters and books, discussing the

relevant technologies and materials have been published over the years [3, 5–21]. In order, to achieve the desired tissue construct, it is essential to understand the properties of bioprinted hydrogel matrix and identify its key parameters (cell density, geometry, stiffness, etc) influencing tissue development and maturation.

In this review, recent progress in bioprinting and relevant bioink properties with focus on the interaction between hydrogel materials and cells is summarized. The properties of the hydrogel, which are required for the printing process as well as to ensure cell survival are discussed along with the influence of cells on the hydrogel properties itself.

We also describe a numerical approach allowing the estimation of the mechanical properties of a cell-containing hydrogel. The effect of cell densities and



distributions within the hydrogel was discussed, which might help to design the bioprinted constructs in a way to achieve the desired properties.

2. Overview of bioprinting methodologies and suitable bioink materials

The physico-chemical parameters of a hydrogel precursor including the rheological behavior, the swelling properties, the surface tension and the gelation kinetics are important factors for its printability. This especially applies for biofabrication techniques that rely on bioink dispensing. Therefore, different hydrogel properties are essential depending on the particular bioprinting technique to be applied. With regard to that, such processing methodologies can be subdivided into three groups including extrusion bioprinting (pneumatic and mechanical), orifice-free bioprinting (laser-induced forward transfer (LIFT) and printing by surface acoustic waves) and inkjet bioprinting (piezoelectric and thermal) (see figure 1).

2.1. Inkjet bioprinting

An inkjet bioprinter delivers small droplets of bioink (1–100 picoliters; 10–50 μm diameter) [16, 22] on predefined locations of a substrate. The two most commonly used methods for inkjet printing of cells are piezoelectric and thermal inkjet bioprinting [6, 23, 24]. The piezoelectric inkjet printer uses piezoelectric crystals to produce acoustic waves to force the liquid in small amounts through the nozzle [16, 25–28]. The thermal inkjet system produces pulses of pressure by vaporizing the bioink around the heating element expelling the droplets out from the printing head. Several studies have already indicated that cells are not affected by the local high temperature of the heating element up to 300 $^{\circ}\text{C}$ due to the short period of exposure (2 μs) during the printing process [29–32].

In inkjet bioprinting the surface tension is an important parameter that determines to what extent the processing technology will result in the formation of droplets or a jet. Surface tension is the result of the cohesive forces existing between the compounds present in the liquid. When the charges on the surface of the bioink are weaker than the surface tension, droplets are formed. Conversely, a jet is produced. The surface tension decreases with increasing cell concentration in the bioink, because more cells are adsorbed to the liquid-gas interface. Therefore, the total free energy is reduced, resulting in a smaller surface tension [33].

Gelation methods including physical [27, 34], chemical and photo-crosslinking [35] are used to ensure the stability of bioprinted constructs. Gelation of the bioink should occur *in situ* after the material exits the nozzle and simultaneously with the printing process (e.g. by photopolymerization) [32], because when it already takes place inside the printing head, blockages are created in the nozzle [23]. When hydrogel formation does not occur rapidly *in situ* the bioprinted construct might be compromised due to possible spreading of non crosslinked bioink solution. Furthermore, the shear stress characteristic to this process can negatively influence the cell viability [36]. As a result, the bioink must exhibit low viscosities (<10 mPa s) and cell densities (<10⁶ cells ml⁻¹) (see figure 1 and table 1) [29, 37, 38]. These conditions result in limitations for the printing process. Despite the disadvantages, inkjet bioprinters are successfully applied with a micrometer resolution (10–50 μm) [23, 28, 39] for the deposition of cells and are compatible with various bioinks [23, 29, 40].

2.2. Orifice-free bioprinting

LIFT is also known as laser-assisted bioprinting and biological laser printing. In LIFT a pulsed laser beam is focused and scanned over a donor substrate that is

Table 1. Overview of crucial bioink parameters, which are characteristic for the discussed bioprinting approaches. Adapted from [40].

	Orifice free bioprinting		Inkjet bioprinting [23, 29, 30, 37, 38, 61]	Extrusion bioprinting [7, 36, 53, 54, 57, 62–66]
	LIFT [41, 67, 68]	Acoustic [19, 48, 69]		
Viscosity bioink	1–300 mPa s	1–18 mPa s	<10 mPa s	$30–6 \times 10^7$ mPa s
Cell density	Medium (10^8 cells ml ⁻¹)	Low ($<16 \times 10^6$ cells ml ⁻¹)	Low $<10^6$ cells ml ⁻¹	High, cell spheroids
Resolution	10–100 μ m	3–200 μ m	10–50 μ m	200–1000 μ m
Single cell control	Medium	High	Low	Medium
Fabrication speed	Medium (200–1600 mm s ⁻¹)	Fast 1–10 000 droplets s ⁻¹	Fast (100 000 droplets s ⁻¹)	Slow (700 mm s ⁻¹ –10 μ m s ⁻¹)
Cell viability	>95%	89.8%	>85%	80%–90%

coated with an absorbing layer (e.g. gold or titanium) and a layer of bioink [41]. The focal point of the laser causes local evaporation of the absorbing layer thereby creating a high-pressure bubble that propels small portions of bioink towards a collector platform. The bioink jet extends towards the collector before separating from the donor substrate, by this way creating a temporary connection between both substrates [42–45]. This bioprinting technique is nozzle-free and is therefore not affected by clogging problems. Another substantial advantage is that the shear stress caused by the material passing through a nozzle (inkjet) or a needle (extrusion) is avoided. The resolution of LIFT is in the range of 10–100 μ m [41, 45]. It is influenced by various factors, such as the laser parameters, the air gap between the donor substrate and the collector platform, the thickness and viscosity of the bioink layer [44]. LIFT is suitable for bioinks with a viscosity ranging from 1 to 300 mPa s and medium cell densities of $\sim 10^8$ cells ml⁻¹ (table 1) [40, 41, 46, 47]. Understandably, bioprinting of well-defined 3D structures from low viscosity bioinks might be quite challenging. For the fabrication of the pre-designed 3D constructs at high spatial resolution the bioink must exhibit fast crosslinking. Among the suitable cross-linking mechanisms, ionic crosslinking of sodium alginate containing bioink is frequently used. Also the temperature dependent gelation of Matrigel or enzymatic driven polymerization of fibrinogen were demonstrated [41, 42, 46].

Another elegant orifice-free bioprinting technique is relying on surface acoustic waves [19, 48]. The latter are produced by an acoustic ejector, which uses a surface acoustic wave piezoelectric substrate (e.g. lithium niobate, quartz, etc) with interdigitated gold rings placed on top of the substrate. Due to the circular geometry of the waves, an acoustic focal plane is generated at the air-liquid interface in the microfluidic channel. As a result, the bioink droplets are ejected from the microfluidic channel. The diameter of the droplets is uniform and can be set between 3 and 200 μ m by changing the wavelength of the acoustic ejector. The

embedded cells are not exposed to nozzle geometry, heat or high pressure, which results in a high cell viability (>89.8%). Furthermore, bioinks with various surface tensions and viscosities can be ejected [19, 48].

2.3. Extrusion bioprinting

Perhaps the most widespread method for the fabrication of 3D cell-laden constructs is extrusion bioprinting [41, 49]. For extrusion bioprinting, the bioink is generally inserted in disposable plastic syringes and dispensed either pneumatically or mechanically (piston- or screw-driven) on the receiving substrate [15]. In contrast with a LIFT or an inkjet bioprinter, an extrusion bioprinter does not dispense small bioink droplets but rather larger hydrogel filaments (approximately 150–300 μ m in diameter) [16, 50–54]. A piston-driven system may provide more direct control over the flow of the bioink, when compared to pneumatic-based systems, prone to delays associated with the compressed gas volume. Screw-based deposition provides more spatial control and is capable of dispensing bioinks exhibiting higher viscosities [12]. However, the larger pressure drops generated by this extrusion method can be harmful for the suspended cells due to possible disruption of the cell membranes which results in cell death [55]. Because of the possibility to adjust the air pressure, pneumatic deposition can be used for a broad range of bioink types and viscosities. Advantages of extrusion bioprinting include the ability to print viscous bioinks ($30–6 \times 10^7$ mPa s) with very high cell densities, and even cell spheroids, into 3D scaffolds (see figure 1 and table 1) [40, 56]. The drawbacks related to this approach are its inferior resolution (200–1000 μ m), potential nozzle clogging and the decreased cell viability due to shear stress [12, 40, 57]. The cross-linking pathways for fixation include physical (shear thinning and thermally induced), chemical (e.g. Michael addition reactions, click chemistry, etc) and photo-induced crosslinking [16, 40].

Another common aspect is that bioink formulations having adequate mechanical properties for

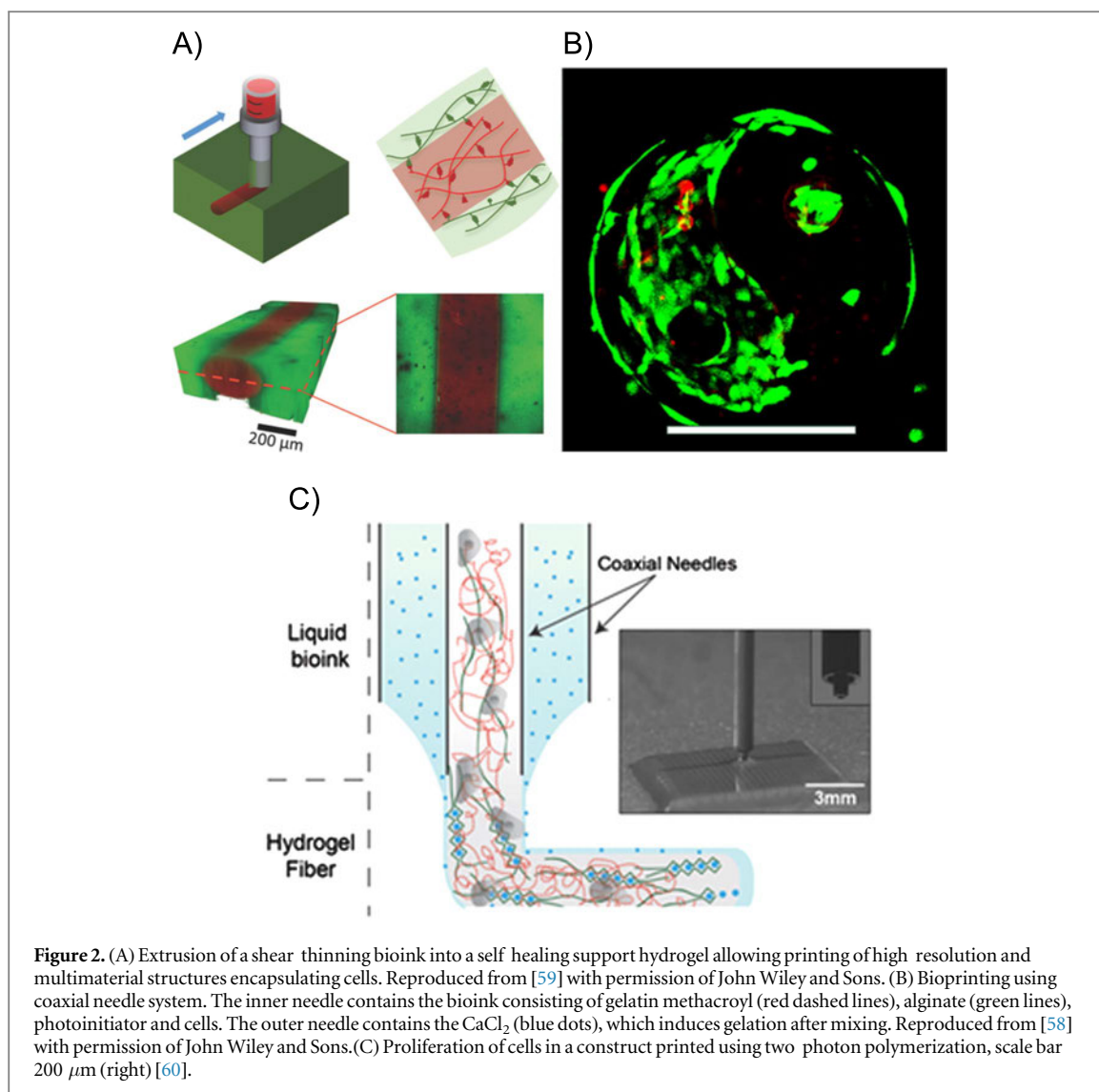


Figure 2. (A) Extrusion of a shear thinning bioink into a self healing support hydrogel allowing printing of high resolution and multimaterial structures encapsulating cells. Reproduced from [59] with permission of John Wiley and Sons. (B) Bioprinting using coaxial needle system. The inner needle contains the bioink consisting of gelatin methacryl (red dashed lines), alginate (green lines), photoinitiator and cells. The outer needle contains the CaCl_2 (blue dots), which induces gelation after mixing. Reproduced from [58] with permission of John Wiley and Sons. (C) Proliferation of cells in a construct printed using two photon polymerization, scale bar 200 μm (right) [60].

fabrication of stable 3D constructs at good bioprinting accuracy often present suboptimal environment for cell migration and spreading [12]. A new bioprinting approach, which might overcome some of these drawbacks was reported recently by [58, 59]. In this gel-in-gel bioprinting method bioink is extruded into a volume of self-healing hydrogel acting as a support material. The support hydrogel deforms upon the injection of bioink and heals immediately after deposition enclosing the printed structure inside (see figure 2a). By using photocrosslinking as secondary stabilization step the mechanical properties of the printed construct can further be improved. Moreover, in combination with photocrosslinking, where either the bioink or the support hydrogel is photosensitive, freestanding 3D structures or structures with voids can be generated, by washing away the unstabilized hydrogel. This gel-in-gel printing method also opens up the possibility to print multiple materials and as the hydrogels are shear thinning also printing of cells results in a high viability (>90%).

2.4. Methods for hydrogel gelation

Hydrogel fixation (i.e. ‘gelation’) is an important aspect in preserving the shape of a bioprinted constructs thereby minimizing structure collapse [12]. The different gelation mechanisms can be subdivided into two categories being physical and chemical crosslinking. The network formation of a physical hydrogel is reversible and is the result of the occurrence of ionic interactions, high molecular chain entanglements, hydrogen bonds and/or hydrophobic interactions [70, 71]. Physically crosslinked hydrogels are usually associated with poor mechanical stability [55]. To overcome this limitation, chemical functionalities can be introduced to improve the mechanical strength of the hydrogel by creating covalent crosslinks, thereby resulting in an irreversibly crosslinked network [72, 73]. An irreversible network can be achieved by Michael-type addition reactions [74], click chemistry [75], enzymatic reactions [76] and photo-induced polymerization [77]. Li *et al* recently reported the development of a two-component bioink based on a supramolecular polypeptide–DNA hydrogel

Table 2. Overview of commercially available bioprinters.

Bioprinter and manufacturer	Fabrication technique	Specified resolution	Recommended materials
3Dn300TE, NScrypt	Extrusion based	Line widths 20–100 μm	Not specified (viscosity range: 0.001–1000 Pa s)
3D Bioplotter [®] , Envisiontec ^a	Extrusion based	Minimum strand diameter 100 μm	Hydrogels, ceramic, metal pastes, thermoplasts
Bioscaffolder [®] , Gesim ^a	Extrusion based	Not specified	Hydrogels, biopolymers (collagen, alginate) bone, cement paste, biocompatible silicones and melting polymers (CPL, PLA)
Biobot 1, Biobots ^a	Extrusion based	Layer resolution 100 μm	Hydrogels, biopolymers (viscosity range: 100–10 ⁴ Pa s, see table 3 for more details)
Inkredible+, Cellink ^a	Extrusion based	Layer resolution 50–100 μm	Hydrogels (see table 3)
Biofactory [®] , RegenHU ^a	Extrusion based Inkjet	Not specified	Bioink, Osteoink (see table 3 for more details)
Revolution, Ourobotics	Extrusion based	Not specified	Collagen, gelatin, alginates, chitosan
Bio3D Explorers, Bio3D technologies ^a	Extrusion based	Not specified	Not specified
CellJet Cell Printer, Digilab		Droplet size 20 nl 4 μl	Water based, hydrogels, alginate, polyethylene glycol
BioAssemblyBot, advanced solutions	Extrusion based	Not specified	Not specified
Regenova, Cyfuse	Spheroid assembly	Related to spheroid diameter	Cells only (scaffold/biomaterial free approach)
NovoGen MMX, Organovo ^b	Inkjet	20 μm	Cellular hydrogels
Dimatix Materials Printer, Fujifilm	Inkjet	20 μm	Water based, solvent, acidic or basic fluids
Poietis ^b	LIFT	20 μm	Not specified

^a Light curing system.

^b Not for sale, but utilized for bioprinting human tissue.

[78]. A combination of both physical as well as chemical crosslinking can also be pursued [72, 79]. Physical crosslinking is generally used for biofabrication processes, since chemical crosslinking is often associated with stringent control over the crosslinking kinetics to avoid blocking of the nozzle [12]. Therefore, chemical crosslinking is frequently used as post-processing fixation and stabilization of the printed 3D constructs [55]. For example, Billiet *et al* already reported on the application of methacrylamide-modified gelatin which was exposed to post-processing photo-induced crosslinking to produce mechanically stable 3D-constructs [63]. Sometimes a two-step photopolymerization approach is used to create a viscous, yet printable bioink and then the printed construct is fully photopolymerized to obtain the final shape of crosslinked scaffold. Skardal *et al* used this two-step photopolymerization method to create 3D scaffolds based on a methacrylated ethanamide derivative of gelatin and methacrylated hyaluronic acid for tissue engineering applications. First, the gelatin and hyaluronic acid derivatives were partially photocrosslinked to obtain a gel-like bioink. Then the desired constructs were printed and photocrosslinked completely to fix their shape [80].

Colosi *et al* has recently reported the use of low-viscosity bioink blend of alginate and gelatin methacryloyl (GelMA) with a coaxial dispensing system [81]. GelMA at low concentrations (<5% w/v) exhibits favourable properties for cells, but is not printable. Combining it with alginate results in a bioink

mechanically stabilized by physically cross-linked fibers. Coaxial needle system (figure 2c) allows to precisely tune the gelation kinetics of this bioink by adjusting concentrations of alginate and CaCl₂. After bioprinting the hydrogel construct is further reinforced by UV cross-linking of GelMA.

2.5. Commercialization of bioprinting

The recent progress along with the increased attention to the field of bioprinting lead to intensified commercialization of devices and materials. Table 2 provides an overview of some commercially available bioprinters with their specifications and typical printing materials. Currently there is no standard way for defining the resolution of the printing process. Hence, manufacturers provide different parameters to describe it. For future evaluation, standardized parameters have to be defined in order to reasonably compare different printing methods.

While most of these printing devices rely on a single biofabrication method, RegenHU offers the selection between different fabrication technologies or combinations thereof. Very often bioprinters are also equipped with an additional light source enabling photo-induced polymerization, also referred to as curing, of the specialized bioinks.

As bioprinting has been commercialized, companies also start to offer their own bioinks. Among these, materials based on various cross-linking

Table 3. Overview of commercially available bioinks.

Company	Bioink	Material	Features
Bioink Solutions, Inc.	Gel4Cell [®]	Gelatin based	UV crosslinkable Cell viability > 90%
	Gel4Cell [®] BMP	Conjugated with different growth factors	Osteoinductive
	Gel4Cell [®] VEGF		Angiogenic
	Gel4Cell [®] TGF		Chondrogenic
CELLINK	CELLINK	Nano cellulose/alginate mixture	Shear thinning Fast crosslinking For soft tissue engineering
RegenHU	BioInk [®]	PEG/gelatin/hyaluronic acid based	Good cell adhesion properties Biodegradable Mimics the natural ECM Possible combination with Osteoink [™]
	Osteoink [™]	Calcium phosphate paste	Osteoconductive Chemical composition similar to human bone For hard tissue engineering
Biobot	Bio127	Pluronic F127 based	Gels at room temperature Dissolves when cooled
	BioGel	Gelatin Methacrylate based	When combined with GelKey it Covalently crosslinks when exposed to light

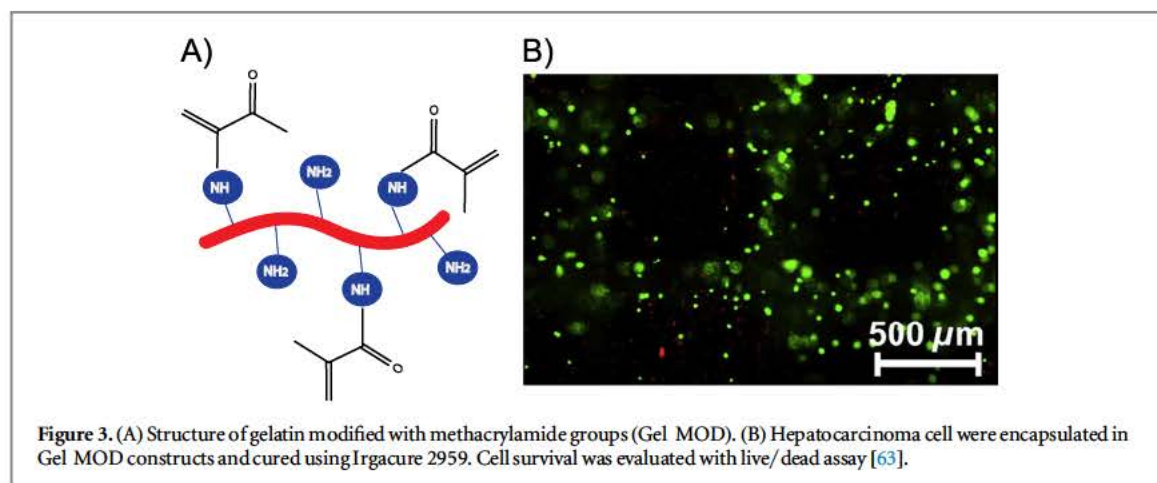


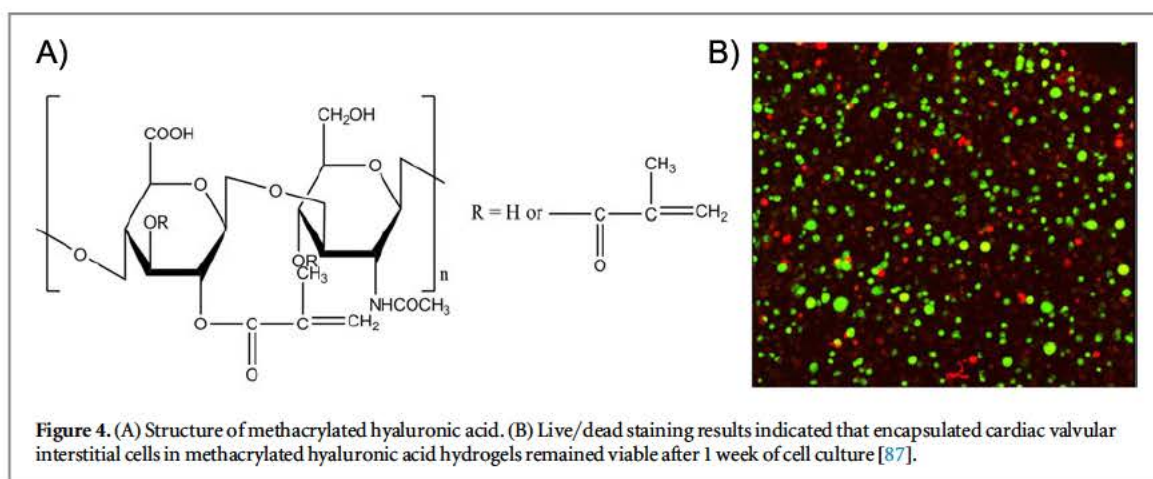
Figure 3. (A) Structure of gelatin modified with methacrylamide groups (Gel MOD). (B) Hepatocarcinoma cell were encapsulated in Gel MOD constructs and cured using Irgacure 2959. Cell survival was evaluated with live/ dead assay [63].

mechanisms and specified for different applications can be found (table 3). For example Bioink Solutions, Inc. offers gelatin-based bioinks containing growth factors that are specific for the printing of different tissue types.

Rheological properties of these bioinks are mostly not indicated by the manufacturer. Therefore, they might only be suitable in combination with the companies own bioprinter and would have to be adapted for other printing techniques.

Generally, these bioinks are constituted from natural and/or synthetic polymers including collagen/gelatin, hyaluronic acid, PEG, etc. Collagen is the most abundant protein present in the extracellular matrix (ECM) of many tissues [82]. This protein forms a hydrogel at physiological conditions by triple helix formation. Collagen is a suitable material for cell encapsulation purposes because of the presence of

cell-interactive RGD (Arginine-Glycine-Aspartic acid) sequences in their backbone, which stimulate cell adhesion. For example, Xu *et al* have mixed rat embryonic hippocampal neurons with neutralized collagen and placed the cell-laden solution subsequently in the incubator at 37 °C to induce hydrogel formation [83]. The degradation of the triple helix of collagen by acidic or basic hydrolysis results in the production of gelatin [71]. Gelatin is a thermo-responsive protein with a sol-gel temperature of around 30 °C depending on the gelatin concentration applied. By cooling a gelatin solution below 30 °C, hydrogel formation is induced (cfr. upper critical solution temperature behavior) [84]. This protein is often employed for tissue engineering and regenerative medicine because various functional groups corresponding with constituting amino acids can be easily modified with (meth)acrylate groups to prevent



liquefying of gelatin at physiological temperature [60, 63, 77]. In addition, gelatin is bio-interactive due to the presence of RGD sequences (figure 3).

Not only proteins are present in the ECM, but also glycosaminoglycans including hyaluronic acid, which is a biodegradable, biocompatible and non-immunogenic biopolymer. The modification of hydroxyl and carboxylic acid functional groups of hyaluronic acid enable the introduction of photocrosslinkable moieties which can be photopolymerized in the presence of cells [85, 86]. Masters *et al* for example investigated the effect of photocrosslinkable methacrylated hyaluronic acid hydrogels on the cell response of encapsulated cardiac valvular interstitial cells (figure 4). Results showed that after 1 week, the embedded cells were still viable indicating the potential of these materials for tissue engineering purposes [87].

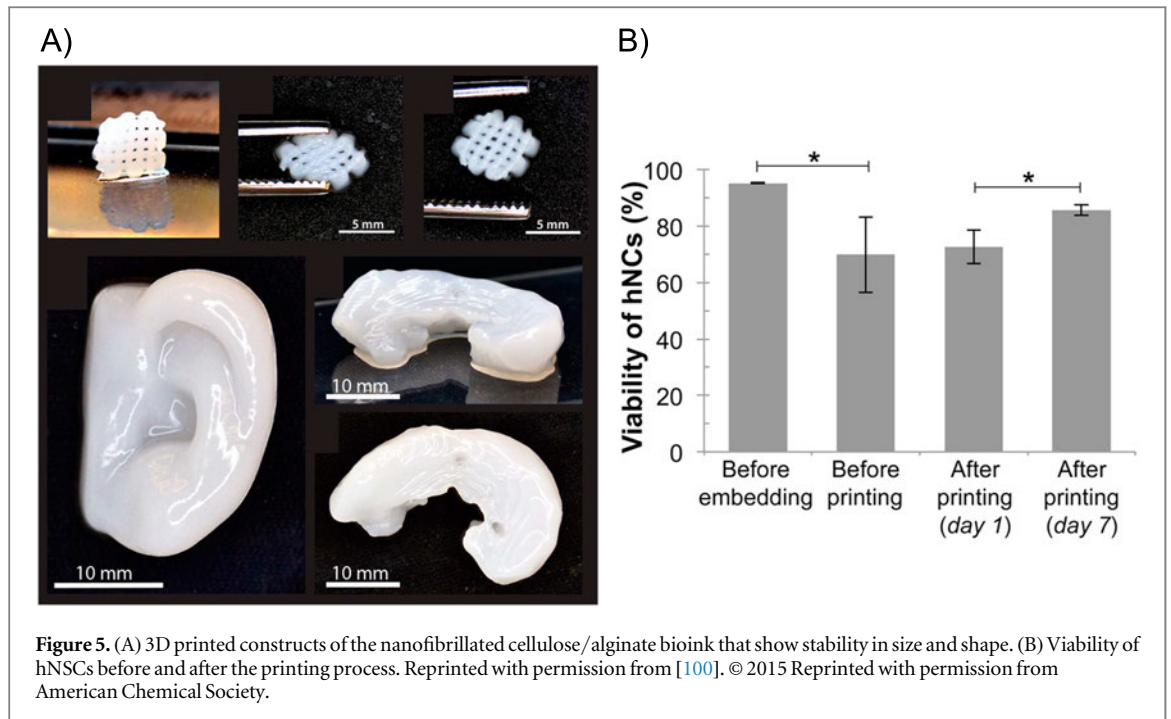
Also synthetic polymers such as PEG-based hydrogel precursors have already been frequently used for cell encapsulation because their mechanical, swelling and diffusion properties can be easily controlled by varying the crosslinking degree. On the other hand, these hydrogels lack inherent binding sequences, like the common RGD motif, for cell attachment and are not degradable. To make them more suitable for cells, these hydrogels have to be modified with the necessary binding peptides and enzymatically degradable groups. For example, Bryant *et al* developed PEG diacrylate hydrogels and incorporated RGD sequences in the backbone to enhance the cell-interactive properties of the hydrogel [88].

2.6. Summary

Each bioprinting technique has its own set of 'ideal requirements' with respect to the bioink properties, in order to achieve designed 3D geometries with the desired resolution and a high viability of the embedded cells (see table 1). In addition, process peculiarities might necessitate more specific material characteristics. A plethora of rheological parameters (i.e. viscosity, shear thinning and thixotropy) can be distinguished, which inherently affect the bioprinting

process [12]. Viscosity is determined by temperature, the polymer concentration and its molecular weight. A bioink exhibiting a high viscosity is associated with an increased shear stress during the printing process, which can cause cell damage [89]. A previous study has already shown that the viscosity of a cell-laden hydrogel influences shape fidelity after deposition. Low-viscosity bioink forms strands which spread out on the receiving platform, while higher viscosity bioinks leads to the formation of filaments on the collecting substrate [90]. The viscosity of shear thinning materials decreases with increasing shear rate. This property results in high printing fidelity, because the applied pressure in the nozzle causes a decrease in viscosity thereby facilitating the deposition of the bioink. As the shear stress is removed after exiting the orifice, the viscosity increases sharply [18, 64]. This effect also takes place for thixotropic biomaterials, for which the decrease in viscosity is reversible and time-dependent [91]. Therefore, these phenomena are extremely useful for nozzle-based applications.

For example, inkjet bioprinting exhibits limitations regarding the material viscosity, while extrusion-based techniques may require shear-thinning properties to reduce the shear stress on the embedded cells to increase the cell viability [92]. The low viscosity bioinks for inkjet bioprinting require fast crosslinking mechanisms to facilitate the layering of the 3D-printed constructs. Conversely, crosslinking in extrusion bioprinting can be executed after fabrication, because the high viscosity bioinks maintain their 3D shape after deposition [12, 40]. However, the resolution of extrusion bioprinting is directly related to the diameter of the needle, which might result in some restrictions on material viscosity and affect the shear-stress induced during the dispensing process. Another interesting option is gel-in-gel bioprinting, allowing to extrude soft cell-friendly bioinks into the support gel. It remains to be seen how the supporting gel volume displaced by deposited bioink would affect the bioprinted construct in case when a large bioink quantity is used. By using a combination where one of the two



hydrogels is photopolymerizable, gel-in-gel printing allows to create constructs with localized photosensitivity. As a result a photopolymerizable part of the construct can be crosslinked, while the rest of the material is washed away to reveal the desired structure. A similar outcome is achieved by lithography-based 3D printing technologies. In this case it is not necessary to combine different properties, instead the same hydrogel is crosslinked selectively by controlling the material-light interaction volume [17]. Somewhat higher spatial resolution and true 3D structuring, without the necessity to deposit material layer-by-layer, is possible with multi-photon processing [93]. For example gelatin-based bioinks, already in their physical gel state, can be locally cross-linked by two-photon polymerization (figure 2c) [60].

In the case of LIFT and inkjet bioprinting techniques bioinks also encounter localized heating, which can further affect the viability of cells. Therefore, bioinks with a low thermal conductivity may be applied, to facilitate cell viability and superior cell function after the printing process [94].

3. Hydrogel properties before and after bioprinting

The characteristics of the bioink should meet the mechanical requirements for the bioprinting process and at the same time ensure cell survival within the produced construct [95, 96]. Therefore, cytocompatibility of a bioink is another critical aspect concomitant with bioprinting. Hydrogels are commonly used for tissue engineering and biofabrication because of their high water content and low toxicity rendering them excellent mimics of the ECM [97, 98]. Several studies

have already demonstrated that 3D hydrogels produced by a bioprinting technology, provide an excellent matrix for encapsulated cells [63, 99–101]. Malda *et al* gives a good overview of the cytocompatibility of different hydrogels when fabricated with different methods [12]. For example, 3D printed cell-encapsulating methacrylamide-modified gelatin hydrogels with a substitution degree of 62% resulted in a cell survival of >97% and maintained cell expression of the liver-specific functions.

Thus, the cell viability was not impaired due to the printing process (e.g. needle type, temperature, etc) and the exposure to increased fluid shear stresses [63]. In addition, Hsieh *et al* have shown that neural stem cells embedded in 20%–30% polyurethane hydrogels exhibit excellent proliferation and differentiation due to the low matrix stiffness. The developed hydrogel was anticipated to mimic the microenvironment of the brain, resulting in an excellent niche for neural stem cells [99]. Markstedt *et al* studied the use of a bioink that combined the outstanding shear thinning properties of nanofibrillated cellulose with the fast crosslinking ability of alginate. The printed constructs were stable in their shape and size and the embedded human chondrocytes exhibited a cell viability of 86% 7 d after printing (see figure 6). They stated that the bioink was suitable for 3D printing in the presence of living cells for inducing the growth of cartilage tissue [100]. Furthermore, Das *et al* assessed the differentiation potential of human nasal inferior turbinate tissue-derived mesenchymal progenitor cells embedded in silk fibroin-gelatin. In the latter, bioink gelation was induced via enzymatic crosslinking by mushroom tyrosinase and physical crosslinking via sonication (see figure 5). The results showed that the constructs

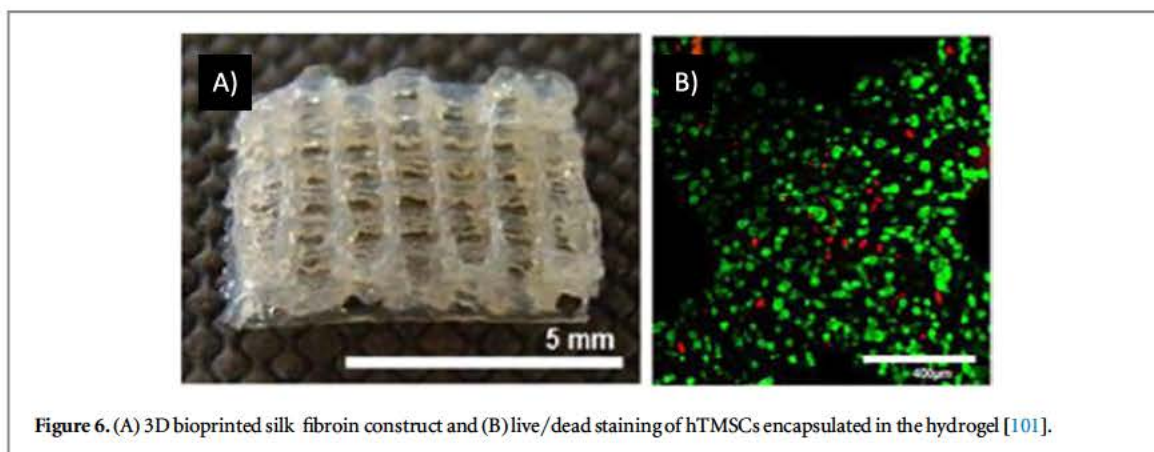


Figure 6. (A) 3D bioprinted silk fibroin construct and (B) live/dead staining of hTMSCs encapsulated in the hydrogel [101].

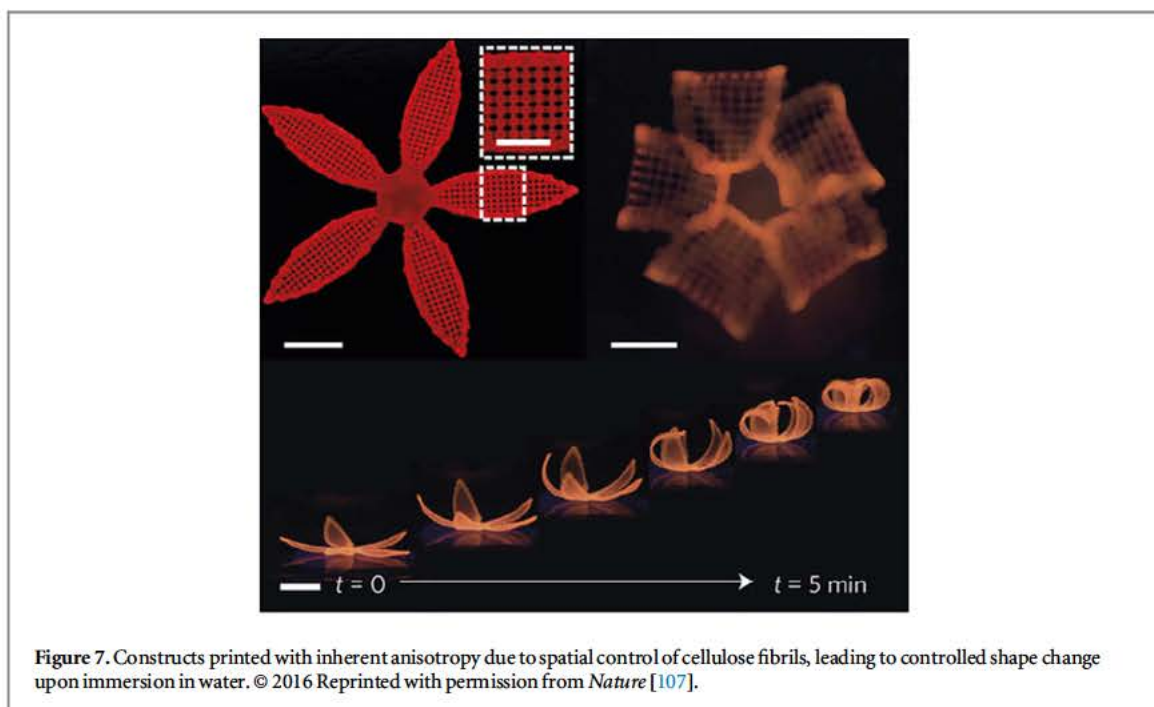


Figure 7. Constructs printed with inherent anisotropy due to spatial control of cellulose fibrils, leading to controlled shape change upon immersion in water. © 2016 Reprinted with permission from *Nature* [107].

supported multilineage differentiation of the encapsulated stem cells and specific tissue formation [101].

In clinical applications direct injection of cells within a carrier solution often leads to a low cell viability due to mechanical disruption of cell membrane. Mechanical properties of a hydrogel carrier can be designed in a way that protects cells during injection. Aguado *et al* shows the protective effect of crosslinked alginate hydrogel with different storage modulus on encapsulated cells. The cell viability after injection was significantly higher in all the crosslinked hydrogel carriers with G' ranging from 0.33 to 58.1 Pa compared to control samples where a cell suspension in PBS was injected. Cells encapsulated in the hydrogel with a storage modulus of 29.6 Pa showed the highest viability demonstrating the impact of cell carrier mechanics on the cell viability [89]. Also Yan *et al* investigated the flow profile of a β -hairpin peptide-based hydrogel and could show their big potential as cell carriers for injection due to their shear-thinning and self-healing

properties [102]. Moreover, Burdick group designed a Dock-and-Lock mechanism to obtain a self-assembling, self-healing and shear-thinning hydrogel for needle injection. Encapsulated mesenchymal stem cells showed a viability of $>90\%$ and remained homogeneously distributed in the gel after needle injection [103].

Another important physico-chemical parameter for the fidelity of bioprinted constructs is the swelling behavior of hydrogels, which is mainly determined by the crosslinking extent and the charge densities [104]. This characteristic influences the final shape and the size of the printed 3D construct [90].

Moreover, the use of high levels of crosslinking result in lower swelling ratios thereby reducing the diffusion of oxygen and nutrients required for the cells to survive as a result of the reduced pore sizes [105]. Diffusion of waste products away from the cells encapsulated in the hydrogel is also managed in this context [97]. In addition, highly cross-linked hydrogels,

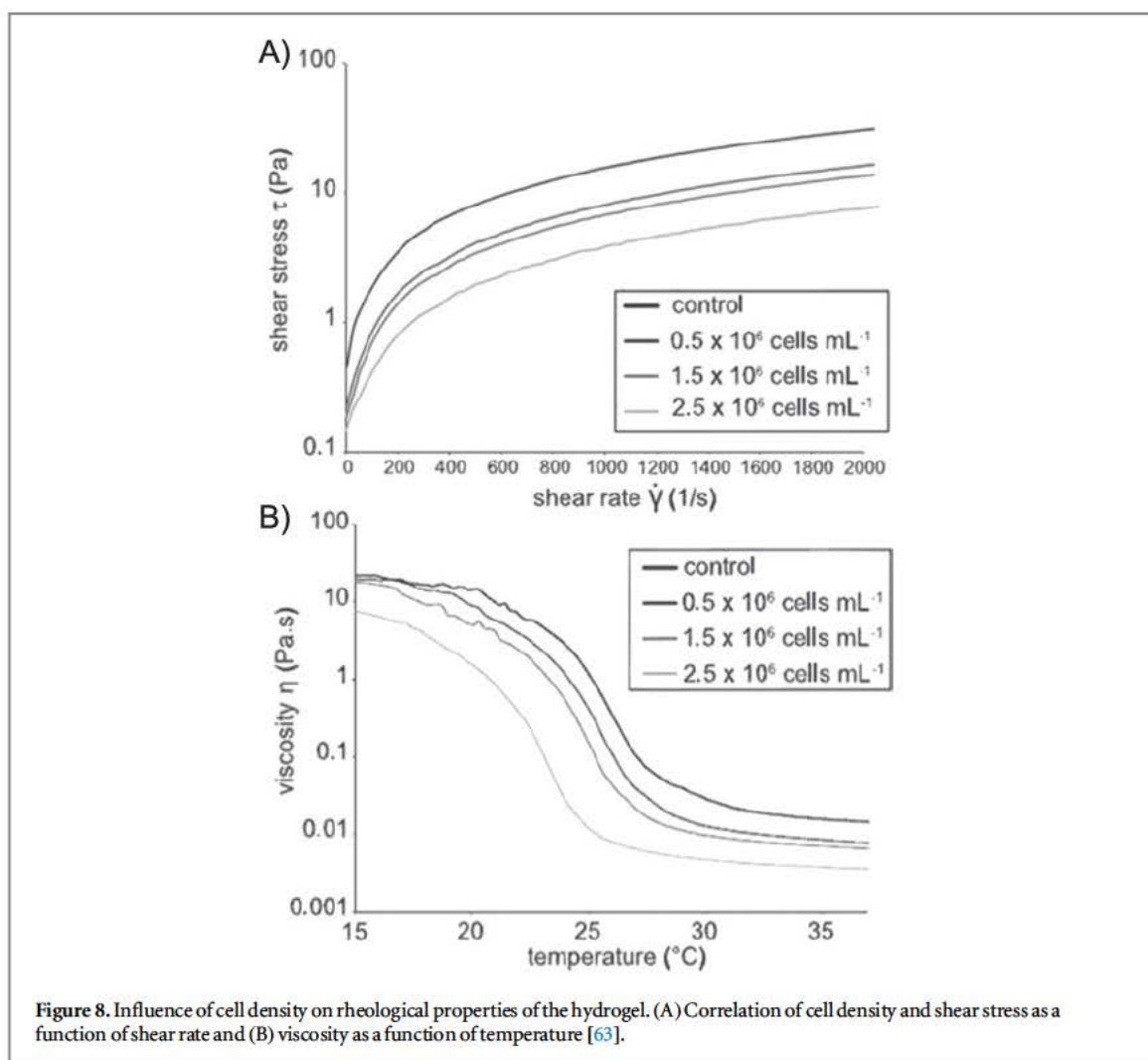


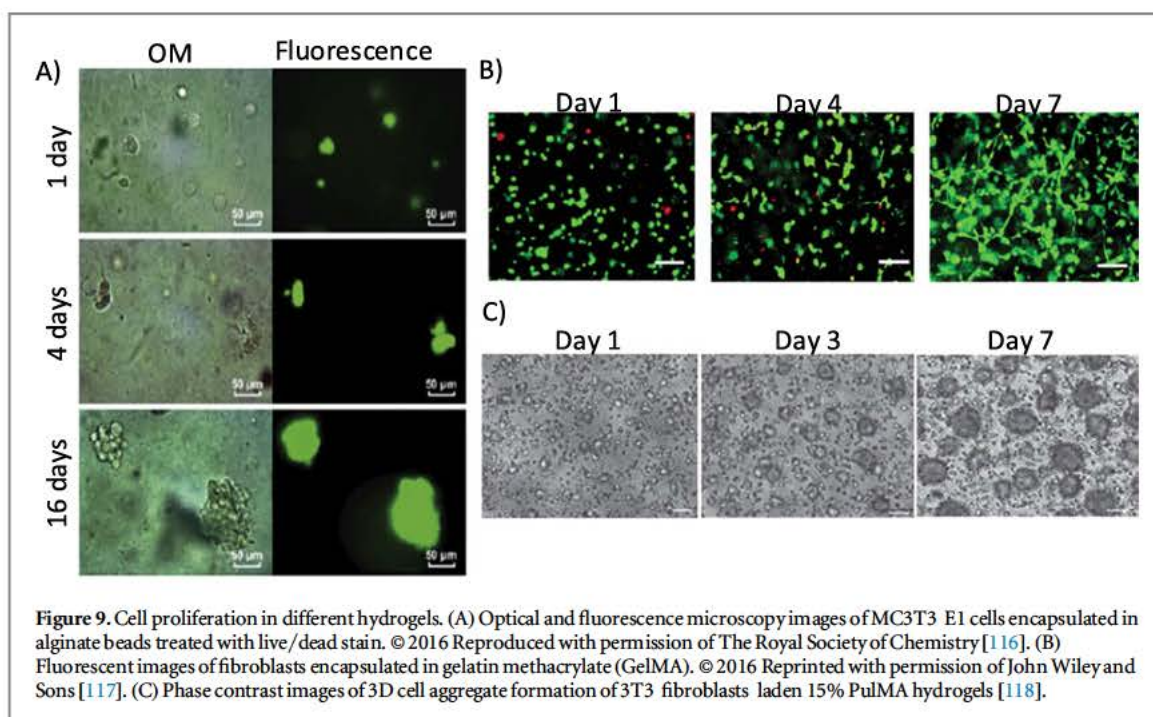
Figure 8. Influence of cell density on rheological properties of the hydrogel. (A) Correlation of cell density and shear stress as a function of shear rate and (B) viscosity as a function of temperature [63].

providing good shape fidelity after bioprinting, might not always be optimal from biological perspective due to impairment of cell migration and proliferation [12]. The requirements towards the properties of a hydrogel with regard to bioprinting process and cell culture are often opposing. A possible solution to this issue is combining hydrogels optimized for cell culture with materials providing mechanical stability and facilitating shape fidelity [106].

In a method referred to as 4D-Printing, Lewis *et al* demonstrated that by controlling swelling anisotropies within a hydrogel construct it can deform in controllable manner. Swelling anisotropy was introduced during printing by spatial control over the orientation of the cellulose fibrils inside the hydrogel. Upon immersion in water the structure swells and acquires its final shape over time (see figure 7) [107]. In general every bioprinting process has a 4D printing character since, it is likely that the geometry and properties will change in long term, unless completely isotropic constructs are built. For example the change in the geometry induced by swelling of zonal hydrogel constructs with different mechanical properties in separate layers has to be taken into account if swelling would occur after bioprinting [108].

4. Effect of cell content on material processing

It is expected that high initial density of cells in the bioprinted construct will lead to faster tissue formation. However, the presence of cells significantly affects the printability of bioinks. Indeed, Billiet *et al* have compared the processing potential of methacrylamide-modified gelatin (Gel-MOD) with and without hepatocarcinoma cells. It was demonstrated that the incorporation of the cells altered the rheological properties. As such, this parameter will affect the printing process since the viscosity is altered. For temperatures above the gelation point, the viscosity was reduced by a factor of 2, up to a cell density of 1.5×10^6 cells ml⁻¹. Increasing the cell density further to 2.5×10^6 cells ml⁻¹ resulted in a further viscosity decrease up to a factor of 4 (see figure 8) [63]. Furthermore, Skardal *et al* have assessed the effect of the presence of human intestinal epithelial cells on hyaluronan-based hydrogels which were crosslinked using tetrahedral polyethylene glycol tetracrylate. Their report states that cell densities above a certain threshold, interfere with hydrogel formation. Bioink with cell densities up to 25×10^6 cells ml⁻¹ formed



hydrogels within 20 min. At higher cell densities the hydrogels did not form under the applied conditions [109].

The equilibrium and dynamic modulus at 1 Hz of agarose hydrogels with chondrocyte density at 0, 10, 40 million cells ml⁻¹ were presented in the study by Buckley *et al* [110]. By maintaining the effective concentration of agarose as constant, both the equilibrium modulus and dynamics modulus at 40 million cells ml⁻¹ were lower than acellular constructs. This result could be explained by the Young's modulus of a chondrocyte, which has been reported as approximately 0.6 kPa [111], an order of magnitude lower than that of agarose. In this case, a larger cell-seeding density would reduce the modulus of cell seeded agarose.

5. Predicting properties of hydrogels containing living cells

There was a certain amount of effort dedicated to predicting properties of the 3D printed scaffolds [112–115]. The mechanical properties of scaffolds were mainly considered with regard to construct compliance, but also in terms of cell-material interaction.

In case of bioinks one has to consider the presence of living cells not only with regard to bioprinting, but also in terms of possible long-term changes of bio-printed construct properties due to cell proliferation, migration and interaction with hydrogel material (cell traction, enzymatic degradation matrix remodeling). As shown in figures 9(A)–(C) there are different ways for cells to proliferate inside the hydrogel construct. For example MC3T3-E1 cells were found to grow in

clusters when encapsulated in alginate hydrogel. In contrast, fibroblasts encapsulated in methacrylated gelatin were able to spread through the hydrogel over time, whereas they were found to grow in aggregates in pullulan methacrylate [116–118]. This behavior is not only attributed to the cell type, but also to the properties of the hydrogels, such as porosity, stiffness and most important the presence of ligands facilitating cell attachment.

The relationship between the density of encapsulated cells and mechanical properties of the resulting hydrogels was investigated by Mauck *et al* [119]. In their work, chondrocyte-seeded agarose hydrogels were cultured in free-swelling and dynamic loading conditions over a 2 month culture period. Constructs containing 10 million cells ml⁻¹ were initially twice stiffer than the ones seeded with 60 million cells ml⁻¹. After culturing 56 d, the constructs seeded with more cells showed similar Young's modulus with the lower cell density one under the condition of free-swelling (85.1 ± 15 kPa versus 78 ± 1.5 kPa). This indicated that higher cell-seeding density accelerates the hydrogel remodeling. This observation was confirmed by Chang *et al* [120], who demonstrated that a higher cell density led to a larger equilibrium modulus of tissue implants after 30 weeks of culture. In addition, the dynamic loading condition resulted in a much larger Young's modulus for the hydrogel containing higher cell density (186.2 ± 11.3 kPa versus 91.5 ± 11.6 kPa). The loading condition induced dynamic modulus followed the same trend. The interesting observations were that both proteoglycan and collagen density remained the same regardless of free-swelling or dynamics loading. This was speculated that the loading condition promoted the production of linker

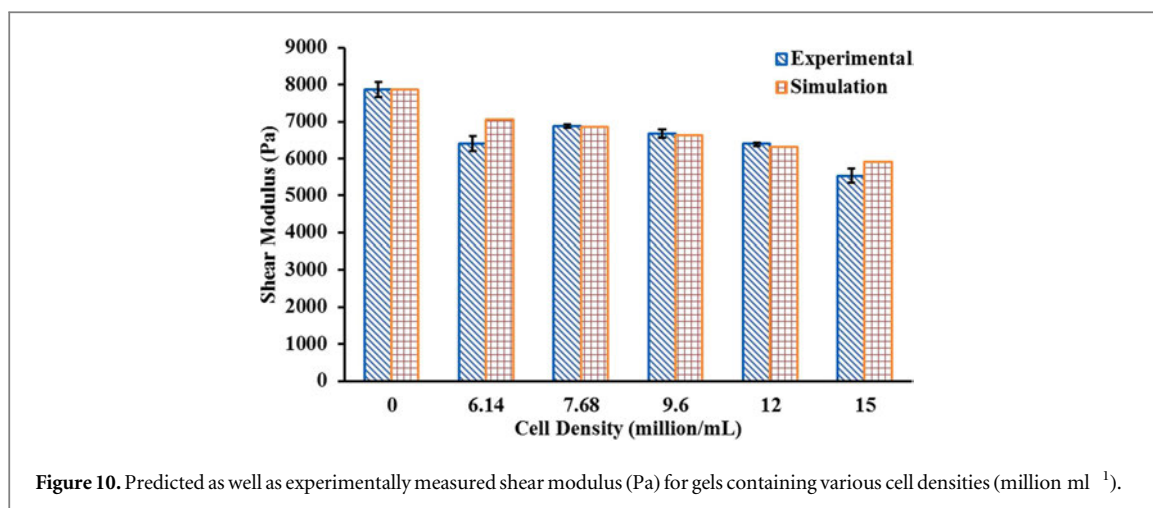


Figure 10. Predicted as well as experimentally measured shear modulus (Pa) for gels containing various cell densities (million ml⁻¹).

molecules and/or the aggregation of macromolecular proteoglycan. This work indicated that various cell densities encapsulated in the 3D hydrogel could promote material remodeling depending on external loading conditions. The experimental data reported in literature is generally obtained following different protocols, which makes it difficult to guide hydrogel design and optimization. Numerical models have the potential to predict mechanical properties of a construct with different cell density under various protocols. It is especially appealing considering the multitude of bioinks used by different groups and the diversity of their properties. Guilak *et al* [121] developed a finite element model of chondrocytes within an explant of cartilage to understand the interactions between cell and matrix, which differ by nearly three-order of magnitude in terms of their Young's modulus. This material mismatch resulted in stress concentrations at the cell-matrix interface. The consideration of a thin layer of pericellular matrix could alter the local mechanical environment of chondrocytes, suggesting a functional biomechanical role for the pericellular matrix. Another numerical model developed by Chang *et al* [122] provides a good base to evaluate mechanical properties of the hydrogel containing living cells. A strain energy density based damage criterion was proposed to correlate cellular viability with external loadings. However, the effect of cell density on the mechanical properties of the resulting construct as well as the cellular viability remains unclear.

Owing to the influence of loading the hydrogel construct with cells, we have studied this effect on the example of methacrylamide-modified gelatin (Gel-MOD) photopolymerized with the photoinitiator LiTPO-L. The Gel-MOD loaded with different densities of MC3T3-E1 cells, ranging from 15 to 6.14×10^6 cells ml⁻¹, was characterized compared to acellular hydrogels using a photorheometer. The details of experimental procedure are similar to the ones reported previously by our group [123]. In short, the cells were directly resuspended in a 10% (w/w)

Gel-MOD solution. Measurement of the storage modulus G' and the loss modulus G'' were taken with a photorheometer (Anton Paar MCR 302 WESP) during a dynamic time sweep at a frequency of 10 Hz and strain of 10% during 10 min of photopolymerization with a 320–500 nm light source.

Our results presented here (previously unpublished) show that the stiffness of hydrogel drops by 13% when the cell density is increased from 12 to 15 million cells ml⁻¹ (figure 10). Calibrated by the aforementioned experimental data, numerical models were developed to predict mechanical properties of hydrogels containing different cell densities and the corresponding cellular mechanics.

A representative volume element (RVE) of the hydrogel with side length of 150 μm was used to represent hydrogels containing different cell densities (figure 11). The encapsulated cells were modeled as solid sphere with 30 μm in diameter and 1.5 kPa in Young's modulus, which was adopted from the previous experimental observation on MC3T3-E1 cells [124]. Based on the aforementioned experimental measurements, the shear storage modulus and loss modulus of the acellular hydrogel was 7870 Pa and 11 Pa, respectively. In the model, the material behaviors of hydrogel were then defined by the magnitude of shear modulus and the Poisson's ratio of 0.49. A 10% shear loading was applied on the RVE to mimic the testing condition. Nonlinear finite element models were solved using ABAQUS 6.12 (Simulia, Providence, RI, USA). Different cell densities varying from 6.14 to 15 million ml⁻¹, corresponding to the volume fraction of 8.68% to 21.2%, were considered in the RVE. The estimated shear modulus of the RVE was found to be in good agreement with experimental measurements (figure 10). Both experiment and simulation demonstrated that higher cell density led to reduced modulus of the hydrogel. These findings are also consistent with experimental observations reported by other groups [63, 110, 119].

As cells are not always distributed homogeneously, but might be present in clusters inside the hydrogel,

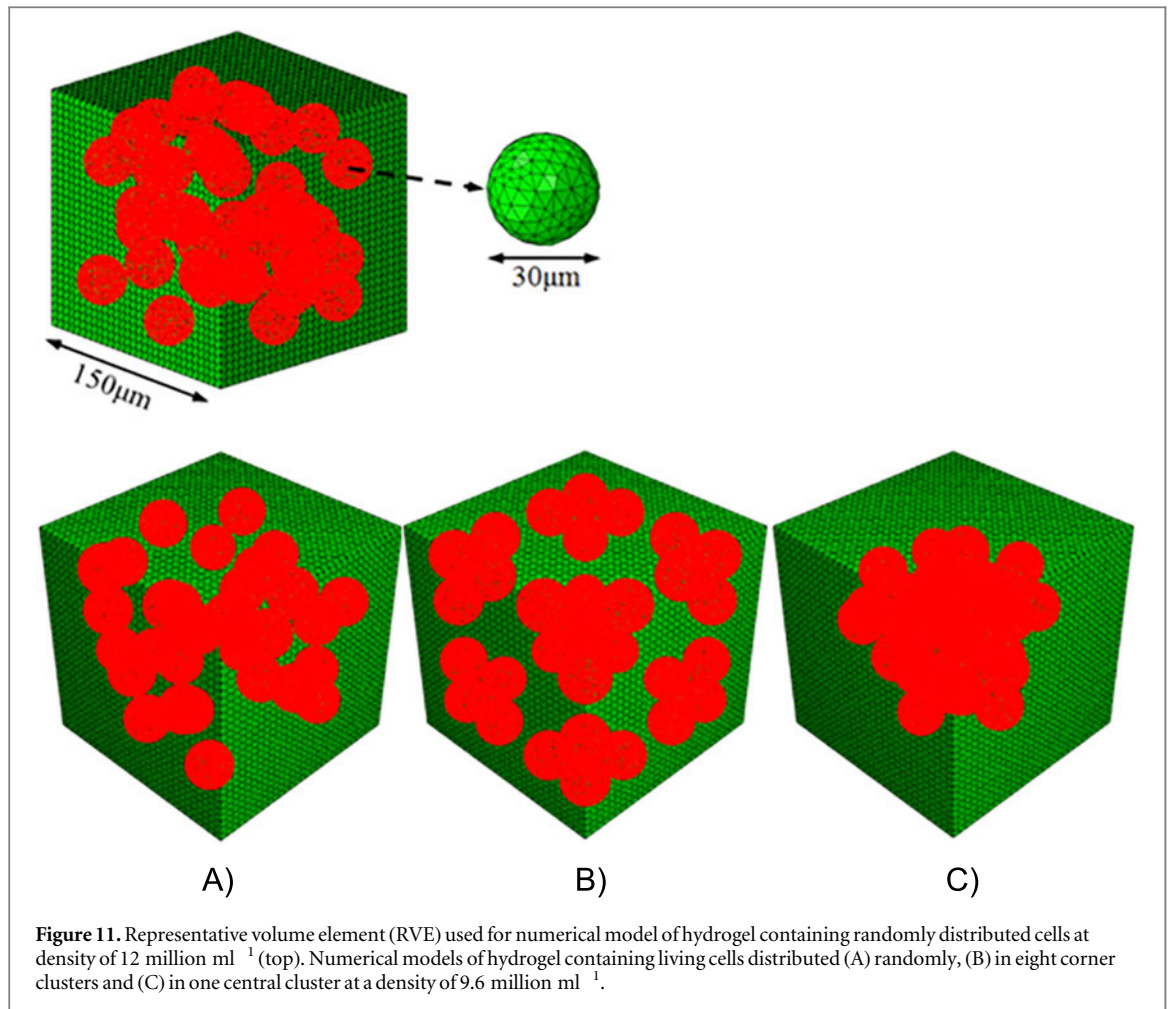
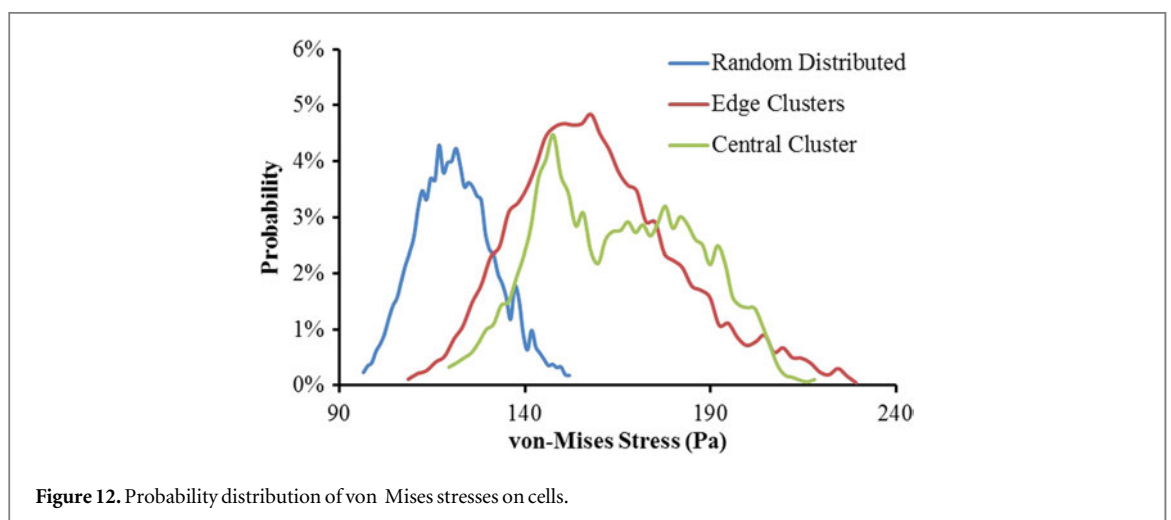


Table 4. Mechanical performance of hydrogel with different cell distribution.

	Random distributed	Edge clusters	Central cluster
Shear modulus (Pa)	6628	6141 (7.3%)	6221 (6.1%)

the effect of different cell distributions on the hydrogel properties was also investigated. This was illustrated by comparison of three different cellular distributions (random distributed, corner clusters and central cluster) at the same cell density of 9.6 million ml^{-1} as shown in figure 11. The obtained shear modulus from finite element models was summarized in table 4. It is clear that the samples with cell clusters are softer compared to the ones without randomly distributed cells.



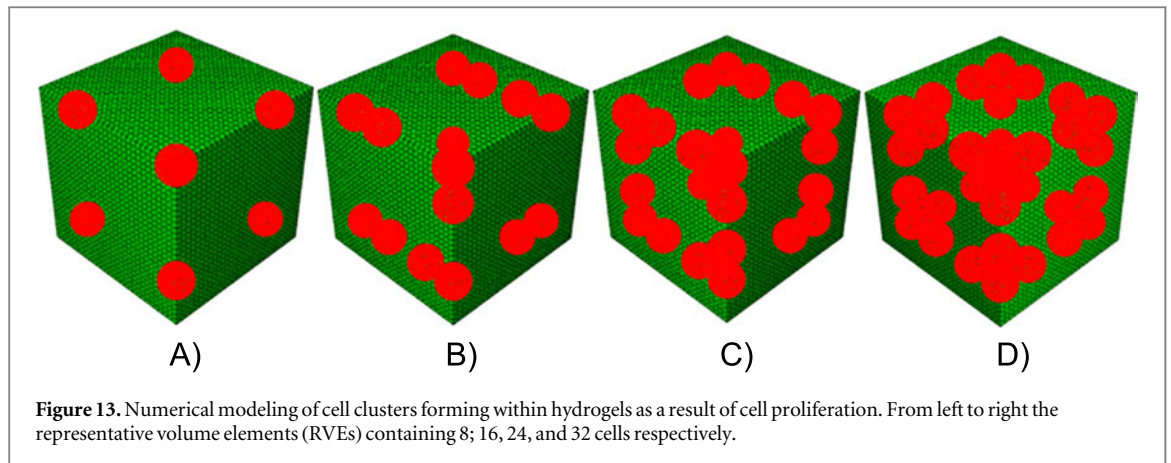


Figure 13. Numerical modeling of cell clusters forming within hydrogels as a result of cell proliferation. From left to right the representative volume elements (RVEs) containing 8; 16, 24, and 32 cells respectively.

Table 5. Mechanical performance of hydrogel with cell proliferation.

	Base	Double	Triple	Quadruple
Shear modulus (Pa)	7425	7010 (5.6%)	6610 (11.0%)	6141 (17.3%)

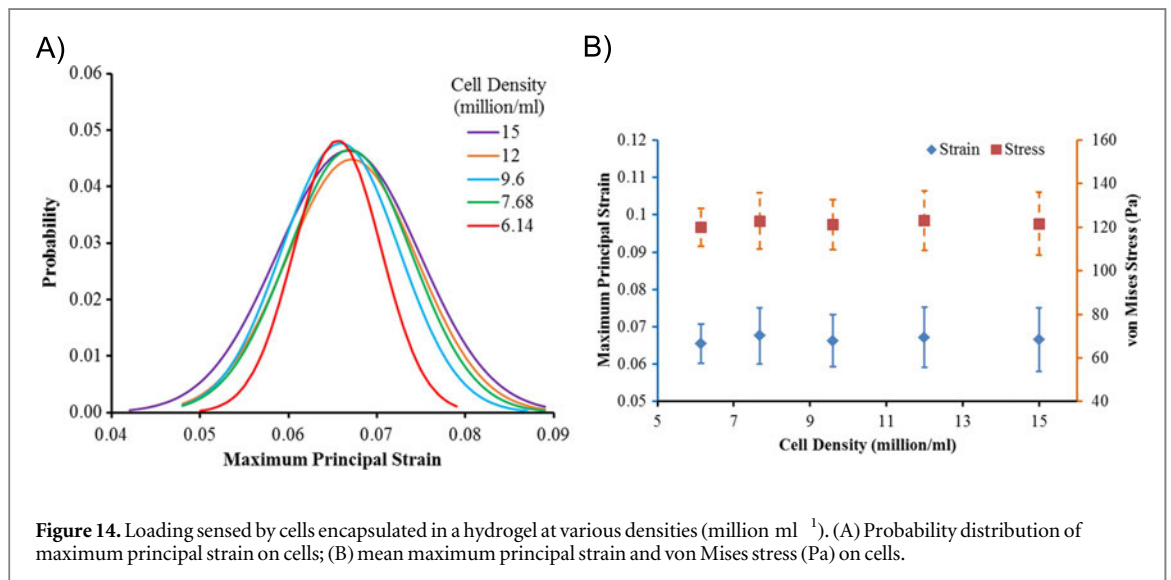


Figure 14. Loading sensed by cells encapsulated in a hydrogel at various densities (million ml^{-1}). (A) Probability distribution of maximum principal strain on cells; (B) mean maximum principal strain and von Mises stress (Pa) on cells.

The shear modulus for edge clusters and central cluster are 7.3% and 6.1% less than the Gel-MOD samples with random distributed cells. The minimal difference between two cluster distributions could be explained by the average distance between cells, which are close enough resulting in similar cell–cell interactions. The mechanical stresses sensed by cells embedded in Gel-MOD were depicted as probability curves in figure 12. It is obvious that cell clusters shifted probability distribution curve to a higher stress region. This implied that cells in cluster state are more prone to damage and therefore also more susceptible to mechanical stimulation. This behavior might be beneficial considering the matrix design for cartilage tissue engineering [125].

Moreover, multiple edge clusters shared a little larger loadings than the one central cluster, as indicated by the shapes of probability curves. However, in general the cluster distribution has minimal impact on the accumulated cellular loadings.

The formation of cell clusters inside the hydrogel might also result from proliferation of encapsulated cells (see figure 9). In order to estimate to what extent clusters might influence the temporal properties of the construct, the effect of cell proliferation was investigated by simulating four different situations related to cell division: initial distribution of single cells (8 cells per RVE), cell doubling (16 cells) etc (figure 13). Although this model might be not taking into account all the aspects of the cell–material interaction, it estimated that within the simulated range the shear modulus decreased from 7.425 to 6.141 kPa as a results of cell proliferation (see table 5). Since cell proliferation is imperative to most bioprinting methods it is important to be able to estimate the final mechanical properties of the construct based on the knowledge of initial material, cell density and proliferation rate. In addition, the appropriate numerical models should be capable of predicting the effect of material degradation, matrix remodeling etc [126].

The loadings sensed by cells are relevant to their behavior, including cellular viability, differentiation, and damage etc. We have delineated the maximum principal strain sensed by cells encapsulated in hydrogel as probability curves (figure 14a). It is clear that the cellular strain tends to be more inhomogeneous as the cell density increased. Higher strain regions were observed at the interface between the cell and hydrogel. This could be explained by the material mismatch between cell and hydrogel and the cell–cell interactions. Stress concentration was observed at the interface between cell and hydrogel, where there existed the material mismatch. Previous reports speculated, that this inhomogeneity is correlated with cellular damages as cells are more prone to be damaged at higher strain [122]. It is interesting to note though that mean stress and strain sensed by cells as a whole has no significant difference among various cell densities (figure 14b).

Another potentially important aspect of cell–material interaction, which might have an effect on the hydrogel construct, is cell contraction. Our modeling results assuming the 5% cell contraction (implemented as eigenstrain, which was estimated from the traction force microscopy data) showed only minimal effect on the mechanical properties of the hydrogel. Specifically, for the case of hydrogel containing 9.6 million cells, the cell contraction altered the shear modulus of the hydrogel from 6.628 to 6.631 kPa.

6. Future perspectives

The dawn of bioprinting enabled the generation and transplantation of several tissues, including multi-layered skin, bone, vascular grafts, tracheal splints, heart tissue and cartilaginous structures [40]. Bioprinting has come a long way with the portfolio of bioinks designed for different technologies and applications expanding rapidly. Hydrogel properties relevant to the process of bioprinting have been systematically investigated and adapted to match different technologies. The development of the bioprinted construct into a tissue is gathered by a multitude of factors such as cell proliferation, material degradation, matrix remodeling etc. Although modern computational approaches should be capable of predicting these processes and benefiting the field of bioprinting, their development is currently lacking attention. Availability of according modeling tools would be highly advantageous, especially taking into account the diversity of bioink properties, expenditures associated with experimental optimization of bioprinted tissue constructs and the possibility to apply these tools to different geometries, e.g. patient-specific cases, in the future. This work reviewed the recent efforts aiming at predicting the properties of cell containing materials and constructs. Furthermore, we present an own model

allowing to estimate the mechanical properties of hydrogels containing different cell densities and distributions. This model provides a fundamental framework for designing bioprinted constructs considering the impact of cell density to achieve desired mechanical properties. The model could be extended to incorporate complex 3D construct architectures, which has demonstrated great influence on their mechanical environments [127]. The predicted mechanical response of cells in various printed hydrogel architectures, integrated with experimental data, could be used to determine the cellular loadings, its damage threshold, as well as the longitudinal behaviors. In addition, the bioprinting process-induced mechanical disturbances has also been found to affect the cell viability [36]. Numerical modeling could be also used to mimic the mechanics during the fabrication process. Optimized parameters such as printing speed or nozzle diameter might be obtained for certain mechanical properties of hydrogel containing cells. In perspective, such computational tools can be directly integrated with modeling of tissue and organ development [128].

Disclosure of interests

We declare no potential conflicts of interest relevant to this article.

Acknowledgments

The authors acknowledge the financial support of the European Research Council (Starting Grant-307701, AO) and the National Science Foundation Faculty Early Career Development (award CBET-1254095: LG). We would like to thank The Research Foundation Flanders (FWO, Belgium) for providing a PhD fellowship to Liesbeth Tytgat. This work was also supported in part by FWO (G008413N, G044516N, G005616N, G0F0516N, FWOKN273), BELSPO IAP Photonics@be, the Methusalem and Hercules foundations, Flanders Make, the OZR of the Vrije Universiteit Brussel (VUB) and Ghent University (UGent). We would like to thank Prof. Jürgen Groll (Universitätsklinikum Würzburg) and Prof. Jürgen Stampfl (Technische Universität Wien) for their valuable comments, and Wolfgang Steiger (Technische Universität Wien) for his help with preparation of Figure 1.

References

- [1] Chan B P and Leong K W 2008 Scaffolding in tissue engineering: general approaches and tissue specific considerations *Eur. Spine J.* **17** 467–79
- [2] Langer R and Tirrell D A 2004 Designing materials for biology and medicine *Nature* **428** 487–92
- [3] Mironov V, Reis N and Derby B 2006 Review: bioprinting: a beginning *Tissue Eng.* **12** 631–4

- [4] Groll J et al 2016 Biofabrication: reappraising the definition of an evolving field *Biofabrication* **8** 13001
- [5] Atala A and Yoo J J 2015 *Essentials of 3D Biofabrication and Translation* (London: Elsevier)
- [6] Campbell P G and Weiss L E 2007 Tissue engineering with the aid of inkjet printers *Expert Opin. Biol. Ther.* **7** 1123–7
- [7] Chang C C, Boland E D, Williams S K and Hoying J B 2011 Direct write bioprinting three dimensional biohybrid systems for future regenerative therapies *J. Biomed. Mater. Res. B* **98B** 160–70
- [8] Cho D W, Lee J S, Jang J, Jung J W, Park J H and Pati F 2015 *Organ Printing* (Bristol: IOP)
- [9] Chua C K and Yeong W Y 2015 *Bioprinting: Principles and Applications* (NJ: World Scientific)
- [10] Husár B, Hatzenbichler M, Mironov V, Liska R, Stampfl J and Ovsianikov A 2014 Photopolymerization based additive manufacturing for the development of 3D porous scaffolds *Biomaterials for Bone Regeneration* (Amsterdam: Elsevier) pp 149–201
- [11] Jakab K, Norotte C, Marga F, Murphy K, Vunjak Novakovic G and Forgacs G 2010 Tissue engineering by self assembly and bio printing of living cells *Biofabrication* **2** 22001
- [12] Malda J, Visser J, Melchels F P, Jüngst T, Hennink W E, Dhert W J A, Groll J and Huttmacher D W 2013 25th anniversary article: engineering hydrogels for biofabrication *Adv. Mater.* **25** 5011–28
- [13] Mironov V, Visconti R P, Kasyanov V, Forgacs G, Drake C J and Markwald R R 2009 Organ printing: tissue spheroids as building blocks *Biomaterials* **30** 2164–74
- [14] Narayan R 2014 *Rapid prototyping of biomaterials: principles and applications* (Cambridge: Woodhead)
- [15] Ozbolat I T and Hospodiuk M 2016 Current advances and future perspectives in extrusion based bioprinting *Biomaterials* **76** 321–43
- [16] Pereira R F and Bártolo P J 2015 3D bioprinting of photocrosslinkable hydrogel constructs *J. Appl. Polym. Sci.* **132** n/a–n/a
- [17] Qin X H, Ovsianikov A, Stampfl J and Liska R 2014 Additive manufacturing of photosensitive hydrogels for tissue engineering applications *BioNanoMaterials* **15** 49–70
- [18] Skardal A and Atala A 2015 Biomaterials for integration with 3D bioprinting *Ann. Biomed. Eng.* **43** 730–46
- [19] Tasoglu S and Demirci U 2013 Bioprinting for stem cell research *Trends Biotechnol.* **31** 10–9
- [20] Forgacs G and Sun W 2013 *Biofabrication: Micro and Nano Fabrication, Printing, Patterning, and Assemblies* (Amsterdam; Boston: Elsevier/WA, William Andrew is an imprint of Elsevier)
- [21] Jüngst T, Smolan W, Schacht K, Scheibel T and Groll J 2016 Strategies and molecular design criteria for 3D printable hydrogels *Chem. Rev.* **116** 1496–539
- [22] Nakamura M, Kobayashi A, Takagi F, Watanabe A, Hiruma Y, Ohuchi K, Iwasaki Y, Horie M, Morita I and Takatani S 2005 Biocompatible inkjet printing technique for designed seeding of individual living cells *Tissue Eng.* **11** 1658–66
- [23] Saunders R E and Derby B 2014 Inkjet printing biomaterials for tissue engineering: bioprinting *Int. Mater. Rev.* **59** 430–48
- [24] Calvert P and Boland T 2012 *Biopolymers and Cells Inkjet Technology for Digital Fabrication* ed I M Hutchings and G D Martin (New York: Wiley) pp 275–305
- [25] Lorber B, Hsiao W K, Hutchings I M and Martin K R 2014 Adult rat retinal ganglion cells and glia can be printed by piezoelectric inkjet printing *Biofabrication* **6** 15001
- [26] Saunders R E, Gough J E and Derby B 2008 Delivery of human fibroblast cells by piezoelectric drop on demand inkjet printing *Biomaterials* **29** 193–203
- [27] Arai K, Iwanaga S, Toda H, Genci C, Nishiyama Y and Nakamura M 2011 Three dimensional inkjet biofabrication based on designed images *Biofabrication* **3** 34113
- [28] Phillippi J A, Miller E, Weiss L, Huard J, Waggoner A and Campbell P 2008 Microenvironments engineered by inkjet bioprinting spatially direct adult stem cells toward muscle and bone like subpopulations *Stem Cells* **26** 127–34
- [29] Xu T, Jin J, Gregory C, Hickman J J and Boland T 2005 Inkjet printing of viable mammalian cells *Biomaterials* **26** 93–9
- [30] Cui X, Dean D, Ruggeri Z M and Boland T 2010 Cell damage evaluation of thermal inkjet printed Chinese hamster ovary cells *Biotechnol. Bioeng.* **106** 963–9
- [31] Cui X and Boland T 2009 Human microvasculature fabrication using thermal inkjet printing technology *Biomaterials* **30** 6221–7
- [32] Gao G, Yonezawa T, Hubbell K, Dai G and Cui X 2015 Inkjet bioprinted acrylated peptides and PEG hydrogel with human mesenchymal stem cells promote robust bone and cartilage formation with minimal printhead clogging *Biotechnol. J.* **10** 1568–77
- [33] Xu C, Zhang M, Huang Y, Ogale A, Fu J and Markwald R R 2014 Study of droplet formation process during drop on demand Inkjetting of living cell laden bioink *Langmuir* **30** 9130–8
- [34] Xu T, Zhao W, Zhu J M, Albanna M Z, Yoo J J and Atala A 2013 Complex heterogeneous tissue constructs containing multiple cell types prepared by inkjet printing technology *Biomaterials* **34** 130–9
- [35] Cui X, Breitenkamp K, Finn M G, Lotz M and D’Lima D D 2012 Direct human cartilage repair using three dimensional bioprinting technology *Tissue Eng. A* **18** 1304–12
- [36] Nair K, Gandhi M, Khalil S, Yan K C, Marcolongo M, Barbee K and Sun W 2009 Characterization of cell viability during bioprinting processes *Biotechnol. J.* **4** 1168–77
- [37] Calvert P 2001 Inkjet printing for materials and devices *Chem. Mater.* **13** 3299–305
- [38] Kim J D, Choi J S, Kim B S, Chan Choi Y and Cho Y W 2010 Piezoelectric inkjet printing of polymers: stem cell patterning on polymer substrates *Polymer* **51** 2147–54
- [39] Campbell P G, Miller E D, Fisher G W, Walker L M and Weiss L E 2005 Engineered spatial patterns of FGF 2 immobilized on fibrin direct cell organization *Biomaterials* **26** 6762–70
- [40] Murphy S V and Atala A 2014 3D bioprinting of tissues and organs *Nat. Biotechnol.* **32** 773–85
- [41] Guillotin B et al 2010 Laser assisted bioprinting of engineered tissue with high cell density and microscale organization *Biomaterials* **31** 7250–6
- [42] Unger C, Gruene M, Koch L, Koch J and Chichkov B N 2011 Time resolved imaging of hydrogel printing via laser induced forward transfer *Appl. Phys. A* **103** 271–7
- [43] Catros S, Guillotin B, Bačáková M, Fricain J C and Guillemot F 2011 Effect of laser energy, substrate film thickness and bioink viscosity on viability of endothelial cells printed by laser assisted bioprinting *Appl. Surf. Sci.* **257** 5142–7
- [44] Guillemot F, Souquet A, Catros S and Guillotin B 2010 Laser assisted cell printing: principle, physical parameters versus cell fate and perspectives in tissue engineering *Nanomedicine* **5** 507–15
- [45] Duocastella M, Colina M, Fernández Pradas J M, Serra P and Morenza J L 2007 Study of the laser induced forward transfer of liquids for laser bioprinting *Appl. Surf. Sci.* **253** 7855–9
- [46] Guillemot F et al 2010 High throughput laser printing of cells and biomaterials for tissue engineering *Acta Biomater.* **6** 2494–500
- [47] Barron J A, Wu P, Ladouceur H D and Ringeisen B R 2004 Biological laser printing: a novel technique for creating heterogeneous 3 dimensional cell patterns *Biomed. Microdevices* **6** 139–47
- [48] Demirci U and Montesano G 2007 Single cell epitaxy by acoustic picolitre droplets *Lab. Chip* **7** 1139
- [49] Chung J H Y, Naficy S, Yue Z, Kapsa R, Quigley A, Moulton S E and Wallace G G 2013 Bio ink properties and printability for extrusion printing living cells *Biomater. Sci.* **1** 763

- [50] Shor L, Güçeri S, Chang R, Gordon J, Kang Q, Hartsock L, An Y and Sun W 2009 Precision extruding deposition (PED) fabrication of polycaprolactone (PCL) scaffolds for bone tissue engineering *Biofabrication* **1** 15003
- [51] Fedorovich N E, De Wijn J R, Verbout A J, Alblas J and Dhert W J A 2008 Three dimensional fiber deposition of cell laden, viable, patterned constructs for bone tissue printing *Tissue Eng. A* **14** 127–33
- [52] Fedorovich N E, Schuurman W, Wijnberg H M, Prins H J, van Weeren P R, Malda J, Alblas J and Dhert W J A 2012 Biofabrication of osteochondral tissue equivalents by printing topologically defined, cell laden hydrogel scaffolds *Tissue Eng. C* **18** 33–44
- [53] Smith C M, Stone A L, Parkhill R L, Stewart R L, Simpkins M W, Kachurin A M, Warren W L and Williams S K 2004 Three dimensional bioassembly tool for generating viable tissue engineered constructs *Tissue Eng.* **10** 1566–76
- [54] Campos D F D, Blaeser A, Weber M, Jäkel J, Neuss S, Wilhelm J D and Fischer H 2013 Three dimensional printing of stem cell laden hydrogels submerged in a hydrophobic high density fluid *Biofabrication* **5** 15003
- [55] Dababneh A B and Ozolat I T 2014 Bioprinting technology: a current state of the art review *J. Manuf. Sci. Eng.* **136** 61016
- [56] Peltola S M, Melchels F P W, Grijpma D W and Kellomäki M 2008 A review of rapid prototyping techniques for tissue engineering purposes *Ann. Med.* **40** 268–80
- [57] Chang R, Nam J and Sun W 2008 Effects of dispensing pressure and nozzle diameter on cell survival from solid freeform fabrication based direct cell writing *Tissue Eng. A* **14** 41–8
- [58] Wu W, DeConinck A J and Lewis J A 2011 Omnidirectional printing of 3d microvascular networks *Adv. Mater.* **23** H178–83
- [59] Highley C B, Rodell C B and Burdick J A 2015 Direct 3d printing of shear thinning hydrogels into self healing hydrogels *Adv. Mater.* **27** 5075–9
- [60] Ovsianikov A et al 2014 Laser photofabrication of cell containing hydrogel constructs *Langmuir* **30** 3787–94
- [61] Li J, Rossignol F and Macdonald J 2015 Inkjet printing for biosensor fabrication: combining chemistry and technology for advanced manufacturing *Lab Chip* **15** 2538–58
- [62] Marga F, Jakab K, Khatiwala C, Shepherd B, Dorfman S, Bradley H, Colbert S and Forgacs G 2012 Toward engineering functional organ modules by additive manufacturing *Biofabrication* **4** 22001
- [63] Billiet T, Gevaert E, De Schryver T, Cornelissen M and Dubruel P 2014 The 3D printing of gelatin methacrylamide cell laden tissue engineered constructs with high cell viability *Biomaterials* **35** 49–62
- [64] Melchels F P W, Dhert W J A, Huttmacher D W and Malda J 2014 Development and characterisation of a new bioink for additive tissue manufacturing *J. Mater. Chem. B* **2** 2282
- [65] Gao Q, He Y, Fu J, Liu A and Ma L 2015 Coaxial nozzle assisted 3D bioprinting with built in microchannels for nutrients delivery *Biomaterials* **61** 203–15
- [66] Tan E Y S and Yeong W Y 2015 Concentric bioprinting of alginate based tubular constructs using multi nozzle extrusion based technique *Int. J. Bioprint.* **1** 49–65
- [67] Hopp B, Smausz T, Kresz N, Barna N, Bor Z, Kolozsvári L, Chrisey D B, Szabó A and Nográdi A 2005 Survival and proliferative ability of various living cell types after laser induced forward transfer *Tissue Eng.* **11** 1817–23
- [68] Guillotin B and Guillemot F 2011 Cell patterning technologies for organotypic tissue fabrication *Trends Biotechnol.* **29** 183–90
- [69] Fang Y, Frampton J P, Raghavan S, Sabahi Kaviani R, Luker G, Deng C X and Takayama S 2012 Rapid generation of multiplexed cell cocultures using acoustic droplet ejection followed by aqueous two phase exclusion patterning *Tissue Eng. C* **18** 647–57
- [70] Mignon A, Graulus G J, Snoeck D, Martins J, De Belie N, Dubruel P and Van Vlierberghe S 2015 pH sensitive superabsorbent polymers: a potential candidate material for self healing concrete *J. Mater. Sci.* **50** 970–9
- [71] Van Vlierberghe S, Dubruel P and Schacht E 2011 Biopolymer based hydrogels as scaffolds for tissue engineering applications: a review *Biomacromolecules* **12** 1387–408
- [72] Ullah F, Othman M B H, Javed F, Ahmad Z and Akil H M 2015 Classification, processing and application of hydrogels: a review *Mater. Sci. Eng. C* **57** 414–33
- [73] Vlierberghe S V, Schacht E and Dubruel P 2011 Reversible gelatin based hydrogels: finetuning of material properties *Eur. Polym. J.* **47** 1039–47
- [74] Fu Y and Kao W J 2011 *In situ* forming poly(ethylene glycol) based hydrogels via thiol maleimide Michael type addition *J. Biomed. Mater. Res. A* **98A** 201–11
- [75] Sivashanmugam A, Arun Kumar R, Vishnu Priya M, Nair S V and Jayakumar R 2015 An overview of injectable polymeric hydrogels for tissue engineering *Eur. Polym. J.* **72** 543–65
- [76] Moreira Teixeira L S, Feijen J, van Blitterswijk C A, Dijkstra P J and Karperien M 2012 Enzyme catalyzed crosslinkable hydrogels: emerging strategies for tissue engineering *Biomaterials* **33** 1281–90
- [77] Ovsianikov A, Deiwick A, Van Vlierberghe S, Pflaum M, Wilhelmi M, Dubruel P and Chichkov B 2011 Laser fabrication of 3D gelatin scaffolds for the generation of bioartificial tissues *Materials* **4** 288–99
- [78] Li C et al 2015 Rapid formation of a supramolecular polypeptide dna hydrogel for *in situ* three dimensional multilayer bioprinting *Angew. Chem., Int. Ed. Engl.* **54** 3957–61
- [79] Graulus G J, Mignon A, Van Vlierberghe S, Declercq H, Fehér K, Cornelissen M, Martins J C and Dubruel P 2015 Cross linkable alginate graft gelatin copolymers for tissue engineering applications *Eur. Polym. J.* **72** 494–506
- [80] Skardal A, Zhang J, McCoard L, Xu X, Oottamasathien S and Prestwich G D 2010 Photocrosslinkable hyaluronan gelatin hydrogels for two step bioprinting *Tissue Eng. A* **16** 2675–85
- [81] Colosi C, Shin S R, Manoharan V, Massa S, Costantini M, Barbeta A, Dokmeci M R, Dentini M and Khademhosseini A 2016 Microfluidic bioprinting of heterogeneous 3D tissue constructs using low viscosity bioink *Adv. Mater.* **28** 677–84
- [82] Choi Y C, Choi J S, Kim B S, Kim J D, Yoon H I and Cho Y W 2012 Decellularized extracellular matrix derived from porcine adipose tissue as a xenogeneic biomaterial for tissue engineering *Tissue Eng. C* **18** 866–76
- [83] Xu T, Molnar P, Gregory C, Das M, Boland T and Hickman J J 2009 Electrophysiological characterization of embryonic hippocampal neurons cultured in a 3D collagen hydrogel *Biomaterials* **30** 4377–83
- [84] Van Den Bulcke A I, Bogdanov B, De Rooze N, Schacht E H, Cornelissen M and Berghmans H 2000 Structural and rheological properties of methacrylamide modified gelatin hydrogels *Biomacromolecules* **1** 31–8
- [85] Collins M N and Birkinshaw C 2013 Hyaluronic acid based scaffolds for tissue engineering – a review *Carbohydr. Polym.* **92** 1262–79
- [86] Oudshoorn M H M, Rissmann R, Bouwstra J A and Hennink W E 2007 Synthesis of methacrylated hyaluronic acid with tailored degree of substitution *Polymer* **48** 1915–20
- [87] Masters K S, Shah D N, Leinwand L A and Anseth K S 2005 Crosslinked hyaluronan scaffolds as a biologically active carrier for valvular interstitial cells *Biomaterials* **26** 2517–25
- [88] Bryant S J, Nicodemus G D and Villanueva I 2008 Designing 3D photopolymer hydrogels to regulate biomechanical cues and tissue growth for cartilage tissue engineering *Pharm. Res.* **25** 2379–86
- [89] Aguado B A, Mulyasmita W, Su J, Lampe K J and Heilshorn S C 2012 Improving viability of stem cells during syringe needle flow through the design of hydrogel cell carriers *Tissue Eng. A* **18** 806–15

- [90] Schuurman W, Levett P A, Pot M W, van Weeren P R, Dhert W J A, Huttmacher D W, Melchels F P W, Klein T J and Malda J 2013 Gelatin methacrylamide hydrogels as potential biomaterials for fabrication of tissue engineered cartilage constructs: gelatin methacrylamide hydrogels as potential biomaterials for fabrication ... *Macromol. Biosci.* **13** 551–61
- [91] Mihaila S M, Gaharwar A K, Reis R L, Marques A P, Gomes M E and Khademhosseini A 2013 Photocrosslinkable kappa carrageenan hydrogels for tissue engineering applications *Adv. Healthc. Mater.* **2** 895–907
- [92] Guvendiren M, Lu H D and Burdick J A 2011 Shear thinning hydrogels for biomedical applications *Soft Matter* **8** 260–72
- [93] Ovsianikov A, Mironov V, Stampfl J and Liska R 2012 Engineering 3D cell culture matrices: multiphoton processing technologies for biological and tissue engineering applications *Expert Rev. Med. Devices* **9** 613–33
- [94] Talbot E L, Berson A, Brown P S and Bain C D 2012 Evaporation of picoliter droplets on surfaces with a range of wettabilities and thermal conductivities *Phys. Rev. E* **85** 61604
- [95] Levato R, Visser J, Planell J A, Engel E, Malda J and Mateos Timoneda M A 2014 Biofabrication of tissue constructs by 3D bioprinting of cell laden microcarriers *Biofabrication* **6** 35020
- [96] Skardal A et al 2015 A hydrogel bioink toolkit for mimicking native tissue biochemical and mechanical properties in bioprinted tissue constructs *Acta Biomater.* **25** 24–34
- [97] Van Hoorick J, Declercq H, De Muynck A, Houben A, Van Hoorebeke L, Cornelissen R, Van Erps J, Thienpont H, Dubruel P and Van Vlierberghe S 2015 Indirect additive manufacturing as an elegant tool for the production of self supporting low density gelatin scaffolds *J. Mater. Sci., Mater. Med.* **26** 247
- [98] Van Vlierberghe S, Dubruel P, Lippens E, Masschaele B, Van Hoorebeke L, Cornelissen M, Unger R, Kirkpatrick C J and Schacht E 2008 Toward modulating the architecture of hydrogel scaffolds: curtains versus channels *J. Mater. Sci., Mater. Med.* **19** 1459–66
- [99] Hsieh F Y, Lin H H and Hsu S 2015 3D bioprinting of neural stem cell laden thermoresponsive biodegradable polyurethane hydrogel and potential in central nervous system repair *Biomaterials* **71** 48–57
- [100] Markstedt K, Mantas A, Tournier I, Martínez Ávila H, Hägg D and Gatenholm P 2015 3D bioprinting human chondrocytes with nanocellulose alginate bioink for cartilage tissue engineering applications *Biomacromolecules* **16** 1489–96
- [101] Das S, Pati F, Choi Y J, Rijal G, Shim J H, Kim S W, Ray A R, Cho D W and Ghosh S 2015 Bioprintable, cell laden silk fibroin gelatin hydrogel supporting multilineage differentiation of stem cells for fabrication of three dimensional tissue constructs *Acta Biomater.* **11** 233–46
- [102] Yan C, Mackay M E, Czymbek K, Nagarkar R P, Schneider J P and Pochan D J 2012 Injectable solid peptide hydrogel as a cell carrier: effects of shear flow on hydrogels and cell payload *Langmuir* **28** 6076–87
- [103] Lu H D, Charati M B, Kim I L and Burdick J A 2012 Injectable shear thinning hydrogels engineered with a self assembling Dock and Lock mechanism *Biomaterials* **33** 2145–53
- [104] Okay O 2009 *General Properties of Hydrogels Hydrogel Sensors and Actuators* ed G Gerlach and K F Arndt vol 6 (Berlin, Heidelberg: Springer) pp 1–14
- [105] Bencherif S A, Srinivasan A, Horkay F, Hollinger J O, Matyjaszewski K and Washburn N R 2008 Influence of the degree of methacrylation on hyaluronic acid hydrogels properties *Biomaterials* **29** 1739–49
- [106] Shim J H, Kim J Y, Park M, Park J and Cho D W 2011 Development of a hybrid scaffold with synthetic biomaterials and hydrogel using solid freeform fabrication technology *Biofabrication* **3** 34102
- [107] Gladman A S, Matsumoto E A, Nuzzo R G, Mahadevan L and Lewis J A 2016 Biomimetic 4D printing *Nat. Mater.* **12** 413–8
- [108] Klein T J, Rizzi S C, Reichert J C, Georgi N, Malda J, Schuurman W, Crawford R W and Huttmacher D W 2009 Strategies for zonal cartilage repair using hydrogels *Macromol. Biosci.* **9** 1049–58
- [109] Skardal A, Zhang J and Prestwich G D 2010 Bioprinting vessel like constructs using hyaluronan hydrogels crosslinked with tetrahedral polyethylene glycol tetracrylates *Biomaterials* **31** 6173–81
- [110] Buckley C T, Thorpe S D, O'Brien F J, Robinson A J and Kelly D J 2009 The effect of concentration, thermal history and cell seeding density on the initial mechanical properties of agarose hydrogels *J. Mech. Behav. Biomed. Mater.* **2** 512–21
- [111] Guilak F, Jones W R, Ting Beall H P and Lee G M 1999 The deformation behavior and mechanical properties of chondrocytes in articular cartilage *Osteoarthr. Cartil. OARS Osteoarthr. Res. Soc.* **7** 59–70
- [112] Almeida H A and Bártolo P J 2013 Numerical simulations of bioextruded polymer scaffolds for tissue engineering applications: numerical simulations of bioextruded polymer scaffolds *Polym. Int.* **62** 1544–52
- [113] Chantarapanich N, Puttawibul P, Sucharitpatskul S, Jeamwattananachai P, Inglam S and Sitthiseripratip K 2012 Scaffold library for tissue engineering: a geometric evaluation *Comput. Math. Methods Med.* **2012** 1–14
- [114] Hollister S J 2005 Porous scaffold design for tissue engineering *Nat. Mater.* **4** 518–24
- [115] Huttmacher D W, Sittinger M and Risbud M V 2004 Scaffold based tissue engineering: rationale for computer aided design and solid free form fabrication systems *Trends Biotechnol.* **22** 354–62
- [116] Bae H, Ahari A F, Shin H, Nichol J W, Hutson C B, Masaali M, Kim S H, Aubin H, Yamanlar S and Khademhosseini A 2011 Cell laden microengineered pullulan methacrylate hydrogels promote cell proliferation and 3D cluster formation *Soft Matter* **7** 1903
- [117] Cha C, Shin S R, Gao X, Annabi N, Dokmeci M R, Tang X S and Khademhosseini A 2014 Controlling mechanical properties of cell laden hydrogels by covalent incorporation of graphene oxide *Small* **10** 514–23
- [118] Lee B H, Li B and Guelcher S A 2012 Gel microstructure regulates proliferation and differentiation of MC3T3 E1 cells encapsulated in alginate beads *Acta Biomater.* **8** 1693–702
- [119] Mauck R L, Wang C B, Oswald E S, Ateshian G A and Hung C T 2003 The role of cell seeding density and nutrient supply for articular cartilage tissue engineering with deformational loading *Osteoarthr. Cartil.* **11** 879–90
- [120] Chang S C, Rowley J A, Tobias G, Genes N G, Roy A K, Mooney D J, Vacanti C A and Bonassar L J 2001 Injection molding of chondrocyte/alginate constructs in the shape of facial implants *J. Biomed. Mater. Res.* **55** 503–11
- [121] Guilak F and Mow V C 2000 The mechanical environment of the chondrocyte: a biphasic finite element model of cell matrix interactions in articular cartilage *J. Biomech.* **33** 1663–73
- [122] Chang Yan K, Nair K and Sun W 2010 Three dimensional multi scale modelling and analysis of cell damage in cell encapsulated alginate constructs *J. Biomech.* **43** 1031–8
- [123] Markovic M, Van Hoorick J, Hölzl K, Tromayer M, Gruber P, Nürnberger S, Dubruel P, Van Vlierberghe S, Liska R and Ovsianikov A 2015 Hybrid tissue engineering scaffolds by combination of three dimensional printing and cell photoencapsulation *J. Nanotechnol. Eng. Med.* **6** 21004
- [124] Takai E, Costa K D, Shaheen A, Hung C T and Guo X E 2005 Osteoblast elastic modulus measured by atomic force microscopy is substrate dependent *Ann. Biomed. Eng.* **33** 963–71
- [125] Steinmetz N J, Aisenbrey E A, Westbrook K K, Qi H J and Bryant S J 2015 Mechanical loading regulates human MSC differentiation in a multi layer hydrogel for osteochondral tissue engineering *Acta Biomater.* **21** 142–53
- [126] Carlier A, Geris L, Lammens J and Van Oosterwyck H 2015 Bringing computational models of bone regeneration to the clinic: bringing computational models of bone

- regeneration to the clinic *Wiley Interdiscip. Rev. Syst. Biol. Med.* **7** 183–94
- [127] Eshraghi S and Das S 2012 Micromechanical finite element modeling and experimental characterization of the compressive mechanical properties of polycaprolactone hydroxyapatite composite scaffolds prepared by selective laser sintering for bone tissue engineering *Acta Biomater.* **8** 3138–43
- [128] Diaz Zuccarini V and Lawford P V 2010 An in silico future for the engineering of functional tissues and organs *Organogenesis* **6** 245–51

Chapter III

Dynamic coordination chemistry enables free directional printing of biopolymer hydrogel

Authors:

SHI, L., CARSTENSEN, H., HÖLZL, K., LUNZER, M., LI, H., HILBORN, J., OVSIANIKOV, A., OSSIPOV, D.A.

Published in:

CHEMISTRY OF MATERIALS 2017; 29(14), pp. 5816-5823

Contribution:

Experimental work and analysis: cell culture experiment

Chapter IV

Gelatin methacryloyl as environment for chondrocytes and cell delivery to superficial cartilage defects

Authors:

HÖLZL, K., FÜRSATZ, M., GÖCERLER, H., SCHÄDL, B., ZIGON-BRANC, S., MARKOVIC, M., GAHLEITNER, C., VAN HOORICK, J., VAN VLIERBERGHE, S., KLEINER, A., BAUDIS, S., PAUSCHITZ, A., REDL, H., OVSIANIKOV, A. and NÜRNBERGER, S.

Published in:


JOURNAL OF TISSUE ENGINEERING AND REGENERATIVE MEDICINE 2021; 1-16

Contribution:

Writing, experimental work and analysis

RESEARCH ARTICLE

Gelatin methacryloyl as environment for chondrocytes and cell delivery to superficial cartilage defects

Katja Hölzl¹ | Marian Fürsatz^{2,3}  | Hakan Göcerler⁴ | Barbara Schädler^{3,5,6} | Sara Žigon-Branc¹ | Marica Markovic^{1,6} | Claudia Gahleitner² | Jasper Van Hoorick⁷ | Sandra Van Vlierberghe⁷ | Anne Kleiner² | Stefan Baudis^{6,8} | Andreas Pauschitz⁹ | Heinz Redl^{3,6} | Aleksandr Ovsianikov^{1,6} | Sylvia Nürnberger^{2,3,6}

¹Institute of Materials Science and Technology, 3D Printing and Biofabrication Group, TU Wien, Vienna, Austria

²Department of Orthopedics and Trauma-Surgery, Division of Trauma-Surgery, Medical University of Vienna, Vienna, Austria

³Ludwig Boltzmann Institute for Traumatology, The Research Center in Cooperation with AUVA, Vienna, Austria

⁴Institute of Engineering Design and Product Development, TU Wien, Vienna, Austria

⁵University Clinic of Dentistry, Medical University of Vienna, Vienna, Austria

⁶Austrian Cluster for Tissue Regeneration, Vienna, Austria

⁷Centre of Macromolecular Chemistry, Polymer Chemistry and Biomaterials Group, Ghent University, Ghent, Belgium

⁸Institute of Applied Synthetic Chemistry, TU Wien, Vienna, Austria

⁹AC2T Research GmbH, Wiener Neustadt, Austria

Correspondence

Sylvia Nürnberger, Department of Orthopedics and Trauma-Surgery, Division of Trauma-Surgery, Medical University of Vienna, Vienna, Austria.

Email: sylvia.nuernberger@meduniwien.ac.at

Funding information

COMET XTribology, Grant/Award Number: 849109; European Research Council, Grant/Award Number: 307701

Abstract

Cartilage damage typically starts at its surface, either due to wear or trauma. Treatment of these superficial defects is important in preventing degradation and osteoarthritis. Biomaterials currently used for deep cartilage defects lack appropriate properties for this application. Therefore, we investigated photo-crosslinked gelatin methacryloyl (gelMA) as a candidate for treatment of surface defects. It allows for liquid application, filling of surface defects and forming a protective layer after UV-crosslinking, thereby keeping therapeutic cells in place. gelMA and photoinitiator lithium phenyl-2,4,6-trimethyl-benzoylphosphinate (Li-TPO) concentration were optimized for application as a carrier to create a favorable environment for human articular chondrocytes (hAC). Primary hAC were used in passages 3 and 5, encapsulated into two different gelMA concentrations (7.5 wt% (soft) and 10 wt% (stiff)) and cultivated for 3 weeks with TGF- β 3 (0, 1 and 10 ng/mL). Higher TGF- β 3 concentrations induced spherical cell morphology independent of gelMA stiffness, while low TGF- β 3 concentrations only induced rounded morphology in stiff gelMA. Gene expression did not vary across gel stiffnesses. As a functional model gelMA was loaded with two different cell types (hAC and/or human adipose-derived stem cells [ASC/TERT1]) and applied to human osteochondral osteoarthritic plugs. GelMA attached to the cartilage, smoothed the surface and retained cells in place. Resistance against shear forces was tested using a tribometer, simulating normal human gait and revealing maintained cell viability. In conclusion gelMA is a versatile, biocompatible material with good bonding capabilities to cartilage matrix, allowing sealing and smoothing of superficial cartilage defects while simultaneously delivering therapeutic cells for tissue regeneration.

Katja Hölzl and Marian Fürsatz should be considered joint first authors.

This is an open access article under the terms of the Creative Commons Attribution-NonCommercial-NoDerivs License, which permits use and distribution in any medium, provided the original work is properly cited, the use is non-commercial and no modifications or adaptations are made.

© 2021 The Authors. Journal of Tissue Engineering and Regenerative Medicine published by John Wiley & Sons Ltd.

KEYWORDS

biocompatible materials, cartilage, chondrocytes, gelatin methacryloyl, hydrogel, osteoarthritis, stem cells

1 | INTRODUCTION

Regeneration of articular cartilage has been a major focus of regenerative medicine and tissue engineering over the past decades. Articular cartilage is a load-bearing tissue (Bhosale & Richardson, 2008), and is often damaged due to injury or wear as aging proceeds. It has a limited self-healing capability, as chondrocytes are not able to migrate from their surrounding matrix in sufficient numbers to repair the defect (Akkiraju & Nohe, 2015; Sophia Fox et al., 2009). The isolation from adjacent tissues (e.g., bone marrow, synovial membrane) and lack of vascularization does not allow sufficient ingrowth of regenerative cells (e.g., stem cells) (Zhang et al., 2009).

Deep traumatic defects in an otherwise healthy knee joint have multiple treatment options mainly based on the implantation of cells sometimes supported by scaffold biomaterials (e.g., microfracture, [matrix-associated] autologous chondrocyte implantation) (Brittberg et al., 1994; Enea et al., 2012; Hunziker et al., 2015). The intact surrounding cartilage protects from load and allows stabilization and fixation of the biomaterials. In contrast, damage as a consequence of erosion (e.g., osteoarthritis (OA)) and some traumata result in a defect too shallow to shield the implanted biomaterial from load, thereby preventing the use of scaffold materials routinely used in clinics.

Treatment approaches which rely on injection of cell suspensions (e.g., intra-articular stem cell injection) have shown some improvement in long-term clinical studies in osteoarthritic patients. However, they still lead to incomplete recovery and often late deterioration (Garza et al., 2020; Migliorini et al., 2020; Song et al., 2018). One of the reasons for this sub-optimal outcome might be the lack of cell engraftment, either by not adhering or by not being protected from the mechanical forces inside the joint. Indeed, only a fraction of cells were seen to remain in the defect in animal studies after the intra-articular injection of stem cells (Muñoz-Criado et al., 2017; Toupet et al., 2013). Therefore the concept of protecting cells with a biomaterial, also serving as a delivery vehicle to the superficial defects, is of growing interest. This biomaterial needs to withstand loads and shear forces, while promoting differentiation of therapeutic cells and production of their own matrix. In principle, hydrogels are potential candidates, as they can be arthroscopically applied, smoothly fill the rough defects, be polymerized at the defect (e.g., by temperature change, UV-crosslinking). In addition, they can even be loaded with therapeutics for an initial boost in differentiation (Koh et al., 2020). However, hydrogels used so far do not sufficiently satisfy these conditions. Alginate, a natural biomaterial frequently used in cartilage research (Häuselmann et al., 1996; Lee et al., 2003), is not suitable for intra-articular application and cannot be degraded by cells to be replaced by new matrix. Fibrin, often used as a tissue glue and for cell encapsulation (Fürsatz et al., 2021; Perka

et al., 2000; Salam et al., 2018), can be easily applied but bears low mechanical stability and degrades rapidly.

In contrast, gelatin derived from collagen - a principal constituent of cartilage tissue - exhibits many beneficial properties arising from its chemical structure. Similar to fibrin or collagen, the polymer structure of gelatin includes necessary cell-binding motifs (e.g., Arginine-Glycine-Aspartate [RGD]), allowing for cell adhesion (Van Hoorick et al., 2019). It further provides cleavage-sequences for matrix metalloproteinases rendering the hydrogel biodegradable. Notably, the material is biocompatible, inexpensive, and can be easily modified (Yue et al., 2017). However, as gelatin is soluble at a physiological temperature of 37°C, it needs to be modified and/or cross-linked using functional groups such as methacrylamide, acrylamide, or norbornene to ensure stability at body temperature (Van Hoorick et al., 2019). Of those, methacrylamide-modified gelatin methacryloyl (gelMA) is most interesting, as it is more stable and biocompatible than, for example, acrylamide and less prone to premature crosslinking than, for example, norbornene, in addition to being photo-crosslinkable. This property renders the material tuneable in its rheological properties by controlling the degree of substitution (DS) (i.e., degree of methacrylation), polymer concentration, photoinitiator, and irradiation conditions (Van Den Bulcke et al., 2000; Van Hoorick et al., 2015). GelMA allows for injection and in situ (photo-)polymerization, which is highly beneficial and contributes to ease of use when clinically applied. Our recent work showed that gelMA supports long-term cell culture and differentiation of adipose-derived stromal/stem cell microspheroids produced from immortalized human cells (Žigon-Branc et al., 2019).

While gelMA has been evaluated for the use in cartilage regeneration, many studies rely on the use of cell lines (Zhou et al., 2018), animal derived cells (L. Han et al., 2017; M.-E. Han et al., 2017; Mouser, 2018; Wang et al., 2021) or very young donors (Boere et al., 2014) thus making them less applicable for translational research. Other studies using human chondrocyte sources (Brown et al., 2017; Gu et al., 2020) often focus on material characterization and only superficially describe effects on the cellular level. Also comparisons of differentiation capacity gelMA embedded cells to culture systems routinely used to assess the differentiation potential of cells (e.g., pellet culture), which is especially important for older human donors and later passages is seldomly shown. Furthermore little is known about the use of cell-laden gelMA for the treatment of superficial cartilage damage, for example, found in osteoarthritis (OA).

Therefore this study examines the suitability of gelMA for chondrocyte differentiation, cartilage regeneration and temporal reconstitution of the gliding surface of superficially damaged cartilage. Specifically, we investigated the viability and extracellular matrix generation potential (on mRNA and protein level) of human articular chondrocytes (hAC) within gelMA and in comparison to

standard pellet culture. The performance on the damaged cartilage surface was assessed on human osteoarthritic cartilage as an ex vivo model under simulated human gait.

2 | METHODS

2.1 | Chondrocyte isolation procedure and cell culture

With written informed consent and approval of the local (Medical University of Vienna; approval number 2127/2017) ethical board hAC were isolated from femoral heads of three donors (male, age: 51–66) undergoing joint-replacement surgery due to trauma. Pieces of macroscopically intact cartilage were cut from the bone and washed in phosphate-buffered saline 1X (PBS, Sigma) containing 10 µg/mL amphotericin B (Gibco) and 0.5 mg/mL gentamicin (Gibco) for 30 min. Subsequently, the pieces were digested for another 30 min in 1 mg/mL hyaluronidase solution (Sigma) and for 1 h in 1 mg/mL pronase solution (Gibco). Then, the cartilage was digested for 3 days in a mixture of enzymes containing 200 U/mL collagenase II (Gibco) and 1 U/mL papain (Sigma) in Dulbecco's Modified Eagle Medium - High Glucose (DMEM-HG; Gibco). The isolated cells were expanded as passage 0 in chondrogenic proliferation medium (CM) under standard cell culture conditions (37°C, 5% CO₂, humidified atmosphere). This medium contained Dulbecco's Modified Eagle Medium - High Glucose (DMEM-HG) (Gibco) supplemented with 10% newborn calf serum (NBCS; Gibco), 2 mM L-glutamine (Sigma), 2 µg/mL amphotericin B, 100 µg/mL gentamicin, 50 µg/mL L-ascorbic acid 2-phosphate (Sigma), 10 mM HEPES (Corning) and 5 µg/mL insulin (Sigma). Medium was exchanged twice a week. Cells were passaged using Trypsin-EDTA (0.05%, Gibco) at a confluence of 90% and used for encapsulation in passages 3 and 5 (P3 and P5).

2.2 | gelMA preparation

Gelatin methacryloyl was produced as described previously (Ovsianikov et al., 2011; Van Den Bulcke et al., 2000; Van Hoorick et al., 2018). Briefly, gelMA was synthesized using gelatin-type-B from bovine skin as a starting material. To obtain photosensitive material, the amine side groups were chemically substituted with methacrylamide groups through reaction with 1 equivalent methacrylic anhydride yielding a DS of 60%. Purification occurred via dialysis exploiting a cut-off of 12,000–14,000 Da, followed by isolation through lyophilization.

For encapsulation experiments, the photoinitiator lithium phenyl-2,4,6-trimethyl-benzoylphosphinate (Li-TPO) was used. It was synthesized as described in literature (Majima et al., 1991; Markovic et al., 2015).

The precursor solution was prepared by dissolving gelMA in CM at 37°C with occasional vortexing. The photoinitiator, dissolved in PBS, was added to yield a final concentration of 0.3, 0.6, or 1.2 mM.

Experiments containing the light-sensitive photoinitiator were performed protected from light.

2.3 | Phototoxicity of Li-TPO

In order to evaluate the optimal biocompatible concentration phototoxicity testing of the photoinitiator Li-TPO was performed on hAC. Li-TPO concentration was selected as the highest possible concentration that is not harmful to the cells, yet allows for the highest stiffness and fastest crosslinking of gelMA. Human articular chondrocytes in P3 were seeded in two 96-well plates at a cell density of 7000 cells per well and incubated at 37°C overnight. The next day, medium was removed and the cells were exposed to 100 µL/well of 1.2 mM, 0.6 and 0.3 mM Li-TPO dissolved in CM ($n = 8$). Cells in control wells received either CM without Li-TPO (positive control) or CM with 50% Dimethylsulfoxide (DMSO, negative control; Sigma). One plate was exposed to ultraviolet (UV) light in a UV-chamber (UV-A, 365 nm, 25 mW/cm² in a Lite-Box G136, NK-OPTIK, at room temperature) for 10 min to activate the photoinitiator while at the same time the second plate was incubated in the dark at room temperature. Hence, one plate represents the photo-toxicity effect that the irradiated photoinitiator has on the cells and the second plate shows the effects that the inactive photoinitiator might have on the cells by itself.

Thereafter, both plates were incubated for 2 h at standard cell culture conditions and then the solutions of all wells were exchanged with fresh CM. After 24 h of cell resting period, Presto Blue Metabolic Viability Reagent (Life Technologies) was used to determine the metabolic activity and therefore the degree of phototoxicity. The reagent was diluted 1:10 in CM and 100 µL were added per well. After 1 h of incubation the fluorescence was measured using a plate reader (Synergy H1 BioTek, excitation 560 nm, emission 590 nm). Background fluorescence was corrected according to sample blank, which contained Presto Blue reagent in CM. Cell metabolism of control cells (no Li-TPO; no UV) was defined as 100% cell viability and other conditions were normalized to this control to calculate individual viability for each condition.

2.4 | Photorheology

To characterize the photo-crosslinking characteristics and viscoelastic properties of gelMA, oscillatory shear measurements were performed with aqueous solutions of gelMA with 5%, 7.5%, 10% as well as 12.5% (w/w) of gelMA (in the presence of 0.6 mM Li-TPO as photo-initiator) by means of a photorheometer (MCR 302 WESP, Anton Paar) with a light source of 320–500 nm wavelength and an intensity of 6 mW cm⁻² (Omnicure) (Gorsche et al., 2017). The samples were assayed using a parallel plate geometry setup, where 60 µL of gelMA precursor solution was loaded between the plates with a gap of 50 µm. Paraffin oil was applied at the edges to prevent drying of the gelMA film during measurements. A frequency of 10 Hz and a strain of 10% was applied via the parallel plates ($d = 25$ mm) at

37°C. The parameters were determined to be within the viscoelastic range of gelMA. The temperature was set at 37°C. Each sample was equilibrated for 20 s before the light source was turned on. Storage- (G') and loss moduli (G'') were recorded in second intervals.

2.5 | Photo-encapsulation of human articular chondrocytes

Human articular chondrocytes from three human donors were encapsulated at P3 and P5 in 7.5% and 10% (w/w) gelMA in the presence of 0.6 mM Li-TPO via UV-crosslinking. The cells were harvested, counted and suspended in different pre-warmed gelMA (i.e., 37°C) precursor solutions. A cell density of 0.2×10^6 cells per 30 μ L gelMA scaffold was used. The scaffolds were formed using chambered coverglass (Grace Bio-Labs CultureWell™) with 6 mm diameter and 1 mm depth. These silicon masks were put on a glass slide positioned on a heating plate (at 37°C) and the cell-loaded gelMA solution was dispensed to each well. Then the silicon mask was covered with a second glass slide. To achieve a physical crosslinking, the gelMA samples were cooled down on ice for 30 s. Then the gelMA scaffolds were chemically crosslinked using UV-A light at 365 nm with an intensity of 25 mW/cm² for 10 min. The cross-linked samples were transferred to 48-well plates and washed in CM for 30 min. Then, chondrogenic differentiation medium (CDM), containing different amounts of transforming growth factor- β 3 (TGF- β 3; Lonza) was added (0, 1, or 10 ng/mL). Chondrogenic differentiation medium consisted of DMEM-HG supplemented with 100 U/mL penicillin/streptomycin (Sigma), 2 mM L-glutamin, 0.05 mM L-ascorbic acid 2-phosphate, 5 μ g/mL human serum albumin (Sigma), 2.5 μ g/mL linoleic acid (Sigma), 5 mg/mL insulin and transferrin and 5 ng/mL selenous acid provided as ITS premix (Gibco), 100 nM dexamethasone (Sigma) and 0 ng, 1 ng, or 10 ng of TGF- β 3. GelMA scaffolds were cultured in 280 μ L of CDM, which was exchanged twice a week with freshly prepared medium. The scaffolds were cultured for 3 weeks.

In addition to gelMA embedded samples, standard pellet cultures were included as controls. HAC were suspended in CDM with different amounts of TGF- β 3 (0, 1, or 10 ng/mL) and 0.2×10^6 cells in 280 μ L CDM were transferred to 1.5 mL screw-capped polypropylene tubes (Corning). Cells were centrifuged down at 280 x g for 5 min. The screw-caps were subsequently slightly loosened to allow air exchange, and tubes were placed into the incubator. Compact pellets formed overnight and were treated the same way as experimental gelMA samples. After 5 days, the cell pellets were transferred to 96-U-bottom well plates.

2.5.1 | Live dead staining

Prior to performing live-dead staining, gelMA scaffolds were washed 3 times in PBS. The staining solution was applied, containing 0.6 μ M propidium iodide (Life Technologies) and 0.4 mM calcein-AM (Life Technologies) in PBS. These were incubated for 30 min at standard cell culture conditions and then washed again in PBS. Stained samples were transferred to 35 mm imaging dishes with glass bottom

(ibidi) and imaged in PBS. Three dimensional (3D) images were generated from z-stacks taken at excitation/emission sets of 488/530 nm (green fluorescence of live cells) and 530/580 nm (red fluorescence of dead cells) with the laser scanning microscope (LSM700, Zeiss), with scanning a range of 400 μ m.

2.5.2 | RNA isolation and quantitative reverse transcriptase polymerase chain reaction

After 21 days of culture, samples of the differentiation experiment were harvested and RNA was isolated. To ensure a sufficient RNA yield, three cell-loaded gelMA scaffolds were pooled. The cell-loaded gelMA scaffolds were shock frozen in liquid nitrogen and afterward grinded within the microcentrifuge tube using a micropestle. 900 μ L of Quiazol Lysis Reagent (Quiagen) were added to the tube. RNA was isolated using RNeasy Plus Universal Mini Kit (Quiagen) following manufacturer's instructions. For control pellets, three pellets were pooled. Pellets were incubated overnight in Quiazol Lysis Reagent prior to RNA isolation. For all samples, the yield and purity of RNA were evaluated using a NanoDrop 2000c photometer (Thermo Scientific). RNA samples were purified using AccuRT Genomic DNA Removal Kit (abm) and 700 ng per sample were used to synthesize cDNA using 5X All-In-One RT MasterMix (abm).

Quantitative reverse transcriptase polymerase chain reaction (qRT-PCR) was performed in duplicates using SsoAdvanced Universal SYBR® Green Supermix (BioRAD) and primer mixes also obtained from BioRAD. To analyze the status of redifferentiation, the following genes were investigated: collagen type I, α -1 (COL1A1, qHsaCED0043248), collagen type II, α -1 (COL2A1, qHsaCED0001057), aggrecan (ACAN, qHsaCID0008122), versican (VCAN, qHsaCID0023082). β -2-microglobulin (B2M, qHsaCID0015347) was used as housekeeping gene. The qRT-PCR analysis was carried out on a CFX 96 Connect Real-Time System (BioRAD) and the cycling program was set as follows: polymerase activation and initial denaturation (30 s at 95°C) followed by repeated denaturation (15 s at 95°C) and annealing/extension (15 s at 60°C) for a total of 40 cycles. The melt-curve analysis followed by increasing the temperature from 65°C to 95°C (0.5°C increment for 5 s/step).

The $\Delta\Delta$ Ct method was used for analysis and data was processed using CFX Manager Version 3.1 (BioRad). Ct values of samples were normalized to the housekeeping gene and referenced to time point 0, which represents the day of encapsulation (RNA harvested from 2D monolayer cell culture before encapsulation). For calculations of differentiation indices, ratios of COL2/COL1 and ACAN/VCAN were calculated. Therefore, the geometric means of three biological replicates ($2^{-\Delta\Delta$ Ct}) were used.

2.5.3 | Histology

After 21 days in culture, pellets and gelMA scaffolds were washed in PBS and fixed for 24 h in 4% formalin (Roth). Then, samples were

washed in PBS several times for 1 h and dehydrated starting with 50% ethanol following a series of increasing ethanol concentration and final embedding in paraffin using Tissue Tek VIP (Sakura). Samples were cut to obtain sections of 4 μm thickness. Sections were deparaffinized and stained with Alcian blue (0.3% at pH = 2.5) to determine the presence of glycosaminoglycans (GAG) and with collagen type II antibodies (Thermo Fisher Scientific, clone 6B3) for presence of collagen type II. For immuno-staining BLOXALL (Vector Labs) was used as a blocking reagent for endogenous peroxides and alkaline phosphatase, followed by antigen retrieval using pepsin (pH = 2). Subsequently, sections were incubated with a 1:100 dilution of primary antibody for 1 h at room temperature, followed by BrightVision Poly-HRP (VWR) as secondary antibody. For detection NovaRed (Vector Labs) was used. Nuclear counterstaining was performed using Mayer's hematoxylin.

2.6 | Cartilage specimen preparation for sealing tests

Full-depth osteochondral plugs of OA cartilage of 10 mm diameter were harvested from human femoral heads. To obtain a uniform height, the initial plugs were shortened using a table saw, yielding a length of ~ 8 mm. The OA plugs were coated with 10% gelMA containing: (1) hAC-DiO (hAC were labeled green with Vybrant DiO cell-labeling solution [ThermoFisher Scientific] prior encapsulation, according to manufacturer's instructions) (P1), (2) hTERT immortalized human adipose-derived mesenchymal stem cells (MSC) (ASC/TERT1, Evercyte) transduced with green fluorescent protein (GFP) as explained elsewhere (Knezevic et al., 2017), and (3) a co-culture (1:1) of hAC-DiO (green) and mCherry (red fluorescent protein) transduced ASC/TERT1 (red) (Knezevic et al., 2017). Therefore, freshly isolated primary hAC, were used after 5 days of monolayer-culture. ASC/TERT1-GFP and ASC/TERT1-mCherry were expanded in Endothelial Cell Growth Medium-2 (EGM-2, Lonza). Co-cultures were cultured in Hennig's medium containing DMEM-HG supplemented with 100 U/mL penicillin/streptomycin, 2 mM L-glutamine, 5 mg/mL insulin and transferrin and 5 ng/mL selenous acid provided as ITS premix, 0.17 mM ascorbic acid-2-phosphate, 1 mM sodium pyruvate (Gibco), 0.35 mM L-proline (Sigma), 1.25 mg/mL bovine serum albumine (BSA; Sigma) and 0.1 μM dexamethasone (Nürnberg et al., 2019). A cell density of 0.4×10^6 per 30 μL was used.

For coating, the plugs were placed into custom-built silicon molds. The surface was dried with a sterile paper towel and the liquid cell-loaded gelMA precursor solution was applied. A transparent plastic coverslip was put atop, to overcome capillary forces of the mold walls, and the precursor was crosslinked for 10 min with UV light. The plastic coverslip was peeled off afterward and samples were submerged in the respective medium: hAC in CM, ASC/TERT1 in EGM-2, and co-cultured cells in Hennig's medium supplemented with 1 ng/mL TGF- $\beta 3$ and 1 ng/mL human BMP-6 (R&D Systems). After 30 min, medium was exchanged and samples were cultured

overnight. On the next day, cells were stained with ethidium-homodimer-1 (Life Technologies) to visualize dead cells. Plug samples were cut in half, to observe the sealing effect of gelMA and cellular distribution and Z-stack images of cross-sections were taken using confocal microscopy (LSM700, Zeiss).

2.7 | Mechanical stress tests

A mechanical stress test, simulating the mechanics of human gait within the knee joint, was performed using a tribometer (SRV® test rig (tribometer), Optimol Instruments Prüftechnik) (Göçerler et al., 2019). Osteochondral plugs coated with cell-loaded gelMA containing hAC-DiO (0.4×10^6 cells per 30 μL) were used for testing. After coating as described above, the cartilage portion of the 10 mm plugs was cut using an 8 mm biopsy punch, to remove excess tissue/gel and yield sharp edges. Samples were exposed to mechanical stress using the SRV® test rig (see Figure 6e), in which two samples were loaded against each other. Each plug was placed in one sample holder and the liquid cup was filled with DMEM-HG supplemented with 10% NBCS. The upper and lower sample holder were assembled by placing the two specimen on top of each other. To equilibrate the samples, they were pre-loaded within about 1 s with a normal force of 50 N for 30 min at 37°C (external heating of the liquid cup). Following this phase, the normal load was increased to 180 N within about 1 s. The normal load of 180 N corresponds to a nominal contact pressure of ~ 3.5 MPa, which simulated human gait (Patil et al., 2014; Yoon et al., 2018). Thereafter, the samples were linear oscillating against each other for ± 0.5 mm (1 mm peak to peak, respectively 2 mm per cycle, in total 600 mm sliding path) at a constant relative velocity of 1 mm/sec for 10 min. Then the load was decreased within about 2 s to about 1 N (unloading) for 10 min to stimulate reabsorption of fluid into the system, without losing the contact completely. Loading and unloading were repeated for two more repetitions. All measurements were performed at 37°C (external heating of liquid cup) and the tangential force (resistance to the linear oscillating movement) in the contact zone was monitored continuously over time to calculate the coefficient of friction (per definition: tangential force divided by normal load).

To evaluate, if the encapsulated hAC-DiO survived the mechanical stress, samples were stained with ethidium homodimer-1 immediately after the measurement. Samples were afterward fixed with 4% paraformaldehyde overnight, washed with PBS and analyzed via confocal-microscopy as described above.

2.8 | Statistical analysis

Data were analyzed with IBM SPSS Statistics 24. The normal distribution of data was confirmed using the Shapiro-Wilk test and Q-Q-Plots. The Levene test verified the equality of variances in the samples.

To analyze whether the photoinitiator (with or without activation by UV light) had adverse effects on the metabolic activity of hAC, one-way analysis of variance (ANOVA) was performed. For post-hoc comparison a two-sided many-to-one Dunnett-test was used to compare all groups against the control group without UV irradiation (-UV).

Gene expression of *COL2* for passage 3 was analyzed using a mixed model ANOVA: The different culture conditions (10%, 7.5% gelMA and pellet culture) and the different growth factor concentrations (0, 1 or 10 ng/mL TGF- β 3) were considered repeated measures variables and the donor was considered the between group variable. $p < 0.05$ was considered statistically significant.

3 | RESULTS

We investigated the feasibility of a photo-crosslinkable hydrogel gelMA for use in cartilage tissue engineering. Specifically, we evaluated its cytocompatibility, mechanical properties, and feasibility as environment for chondrocyte redifferentiation. Furthermore, we investigated its applicability on cartilage surfaces and performance under mechanical stress *in vitro*.

3.1 | Phototoxicity of Li-TPO

In order to assess the optimal concentration of the photoinitiator for gel crosslinking and cell encapsulation, phototoxicity testing was performed by exposing hAC in 2D culture to different concentrations of Li-TPO (0.3, 0.6, and 1.2 mM) with and without UV irradiation (Figure 1), and assessing cell metabolism, indirectly reflecting cell survival and toxicity. Concentrations of 0.3 and 0.6 mM Li-TPO did not adversely affect cell metabolic activity compared to untreated control samples, independent of UV light exposure. However, the highest tested concentration (1.2 mM) reduced metabolic activity to 88% (without UV) and 72% for hAC exposed to UV ($p < 0.001$). Overall, 0.6 mM Li-TPO was the highest photoinitiator concentration, without adverse effects on cell metabolism activity, while also enabling efficient crosslinking and was therefore used in all further experiments.

3.2 | Photorheology

The crosslinking dynamics and viscoelastic properties of gelMA were analyzed via oscillatory shear rheology measurements during curing of the hydrogel. Storage- (G') and loss-moduli (G'') were measured as the material responds to the irradiation over a curing time of 10 min (Figure 2). Immediately upon UV irradiation, gelMA began to crosslink. The gel point, where G'/G'' equals 1, defining the transformation of a materials liquid to solid state, was reached within 20 s, except for 5 wt% gelMA, which needed 40 s. After 3 min about 70% and after 5 min about 80% of the final G' (measured after 10 min) was attained except for 5%. Formulations containing 5% gelMA developed inferior mechanical

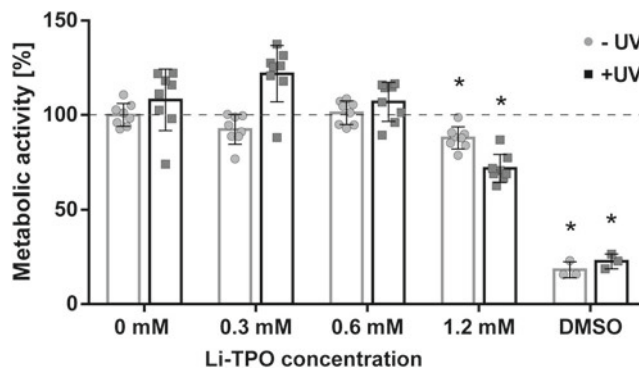


FIGURE 1 Metabolic activity of human articular chondrocytes (P3) exposed to different concentrations of lithium phenyl-2,4,6-trimethyl-benzoylphosphinate (Li-TPO) with and without exposure to UV light. Metabolic activity was measured by resazurin-based Presto Blue staining after 2 h of Li-TPO exposure followed by 24 h of incubation. Presto Blue fluorescence of cells treated with different Li-TPO concentrations is shown as mean percentage \pm standard deviation compared to control (no Li-TPO). $n = 8$ for each group. * highlights significant differences ($p < 0.001$) compared to control -UV. There was no difference between the 0.6 mM Li-TPO and control groups. (Dimethylsulfoxide [DMSO] = negative control, $n = 3$)

properties with only 0.204 kPa ($\pm 9.2 \times 10^{-3}$ kPa) storage modulus at the end of the measurements after 10 min, compared to the other gelMA concentrations (7.5%, 10%, 12.5%). G' for the other gelMA concentrations showed values of 1.7 kPa (± 0.000 kPa) for 7.5% gelMA, 4.5 kPa (± 0.240 kPa) for 10% gelMA and 10.5 kPa ($\pm 0.212 \times 10^{-3}$ kPa) for 12.5% gelMA. As we found that the mechanical stability of 5% gelMA was inferior and that the viscosity of 12.5% gelMA was too high for efficient handling with cells, 7.5% and 10% gelMA were chosen for further encapsulation studies.

3.3 | Encapsulation of human articular chondrocytes

Primary hAC from three different donors were propagated in 2D-culture until P2 or P4 prior to encapsulation in 7.5% (further in the text referred to as soft) or 10% (further in the text referred to as stiff) gelMA, and cultivated (P3 and P5) for another three weeks in medium containing 0, 1 or 10 ng/mL TGF- β 3. Chondrocytes were then analyzed for viability, morphology, gene expression profile, and synthesized matrix (glyco-)proteins. Samples were compared to controls, that is, pellet cultures, which also contained hAC from the three donors.

3.3.1 | Live/dead staining

To assess viability and morphology of hAC within gelMA after three weeks of encapsulation, cells were analyzed using live-dead staining.

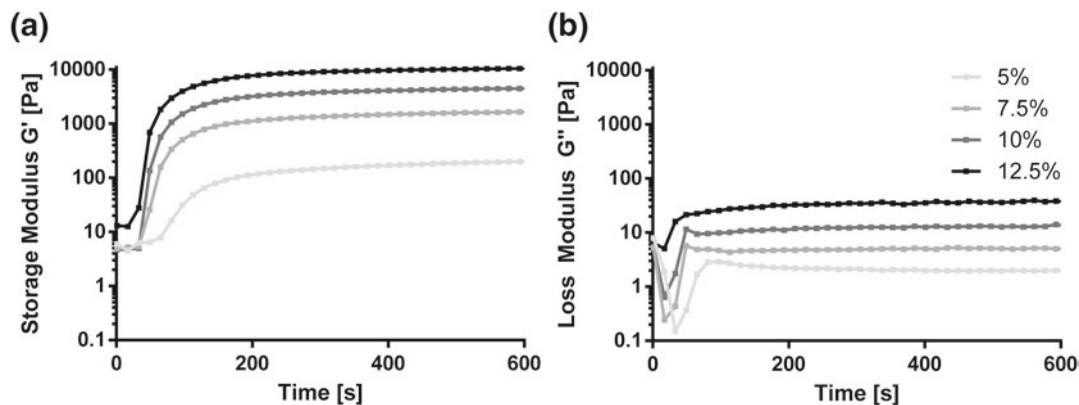


FIGURE 2 Rheological measurements of 5%, 7.5%, 10%, and 12.5% wt% gelatin methacryloyl (gelMA) with 0.6 mM lithium phenyl-2,4,6-trimethyl-benzoylphosphinate. Storage- (G') and loss-moduli (G'') were monitored during oscillatory time sweep over 10 min ($n = 2$) of UV-irradiation using a photorheometer at 37°C. UV irradiation started after 20 s of measurement. G' and G'' are shown as the mean of two measurements. Storage modulus of 12.5% gelMA resulted in highest stiffness (10.5 kPa) followed by 10% (4.5 kPa), 7.5% (1.7 kPa), and 5% (0.204 kPa)

HAC were highly viable in all investigated gelMA formulations and only few dead cells were detected.

HAC cultured in medium containing 10 ng/mL TGF- β 3 were homogeneously distributed and had similar morphology regardless of the gelMA stiffnesses. Cells had either the typical round shape found in native cartilage or were polygonal with small cell processes. However, the stiffness of gelMA did affect the cultivation of hAC in the absence of TGF- β 3 (Figure 3) and 1 ng/mL TGF- β 3 (data not shown). In both growth factor conditions, the spindle-shaped, elongated cell morphology typical for the fibroblast phenotype predominated in the soft (7.5%) gelMA, whereas in the stiff condition a round cell shape was more prevalent.

3.3.2 | qRT-PCR

Gene expression of chondrogenic differentiation markers (*COL1*, *COL2*, *ACAN*, *VCAN*) obtained from P3 and P5 hAC encapsulated within gelMA revealed a redifferentiation pattern similar to pellet cultures, which served as a control. For analysis of the overall effect of hydrogel stiffness/culture system and TGF- β 3 concentrations, a mixed model ANOVA was performed using two different donors (1 and 3, the two most different donors chosen due to model complexity) as a random factor.

In general, when comparing gelMA scaffolds to pellet cultures a comparable state of differentiation could be achieved. When analyzing *COL2* gene expression on the overall level, a significant TGF- β 3 dose dependent upregulation ($p = 0.003$), which was similar in all pellet culture and both gelMA stiffnesses (especially when using 10 ng/mL TGF- β 3), could be observed. This behavior was present in both donors and was consistent until P5, however the total amount of upregulation varied between donors. At lower growth factor concentrations differences between systems (gelMA vs. pellet culture) became more apparent. Medium without TGF- β 3 (0 ng/mL) yielded low *COL2* expression. While in most pellet culture samples a

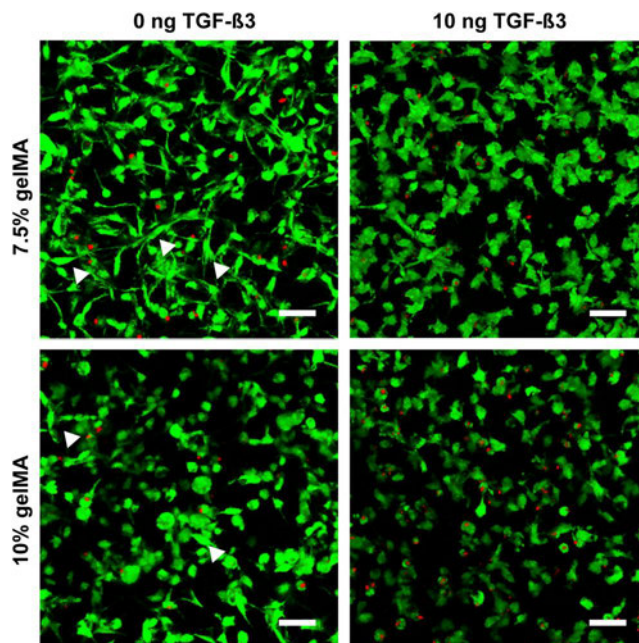


FIGURE 3 Cell morphology of human articular chondrocytes P3 after 3 weeks of encapsulation in soft (7.5%) and stiff (10%) gelatin methacryloyl (gelMA) with and without TGF- β 3. Without TGF- β 3, cell morphology was highly heterogenous in both soft as well as stiff gelMA. Although spindle-shaped (arrow heads) and round cells were found in both stiffnesses, the round cell morphology (chondrocyte like) was favored in the stiffer gelMA, whereas the spindle-like morphology (fibroblast like) was dominant in the softer gelMA. In the 10 ng TGF- β 3 group both stiffnesses contained a rather homogenous cell population of roundish or polygonal cells with little cell processes. Scale bar: 50 μ m

slightly increased differentiation could be observed (in comparison to gelMA), in some cases equal or lower expression (Donor 1 P3, 7.5% gelMA; Donor 1 P5, 10% gelMA; Donor 3 P5, 10% gelMA vs. pellet culture) was found. The most significant differences between gelMA

and pellet culture were observed when using 1 ng/mL TGF- β 3. Except for Donor 1 (where the expression was similar) pellet culture was showing stronger COL2 expression than both gelMA concentrations. The differences described here were not significant when only looking at hydrogel stiffness/culture ($p = 0.058$), but showed significant differences when allowing for factor interaction between gel stiffness/culture system (gelMA, pellet culture), growth factor and donor ($p = 0.007$) in a mixed model ANOVA.

As Donor 3 (P3) responded the strongest to differentiation stimuli this donor's data is presented as an example of gene expression changes after re-differentiation, compared to the hAC de-differentiated state at the time-point of encapsulation (Table 1 and Figure 4; data from other donors is available in Section 1.2 in Supporting Information S1). Changes in gene expression were similar between gelMA and pellet culture, especially when 10 ng/mL TGF- β 3 was added, resulting in a strong upregulation of COL2 (7.5%: 1.9×10^5 , 10%: 2.1×10^5 and pellet culture: 0.9×10^5) and to a lesser extent also COL1 (7.5%: 20.5, 10%: 39.0 and pellet culture: 34.5), ACAN (7.5%: 64.1, 10%: 128.8 and pellet culture: 53.2) and VCAN (7.5%: 3.1, 10%: 4.2 and pellet culture: 3.0). Interestingly, at 1 ng/mL TGF- β 3 pellet culture (P3) not only showed stronger gene expression in all analyzed genes compared to gelMA, but also stronger expression of COL2 and ACAN than using 10 ng/mL TGF- β 3 (pellet culture). Cultures without additional growth factors showed only minimal upregulation of COL2 in gelMA (7.5%: 2.4 fold and 10%: 1.3 fold) and slightly higher upregulation in pellet culture of P3 (131.5). COL1, ACAN and VCAN were slightly downregulated in most cases. When no growth factor was added, differentiation indices followed this trend with low but positive differentiation (COL2/COL1: 7.5%: 3.5, 10%: 2.4 and pellet culture: 426.1; ACAN/VCAN: 7.5%: 0.6, 10%: 0.8 and pellet culture: 2.6), and increasing differentiation with 1 ng/mL (COL2/COL1: 7.5%: 225.9, 10%: 212.1 and pellet culture: 6.3×10^3 ; ACAN/VCAN: 7.5%: 3.9, 10%: 6.8 and pellet culture: 34.0)

and 10 ng/mL (COL2/COL1: 7.5%: 11.4×10^3 , 10%: 5.5×10^3 and pellet culture: 2.3×10^3 ; ACAN/VCAN: 7.5%: 19.3, 10%: 31.3 and pellet culture: 17.1) TGF- β 3 concentrations, with the exception of 1 ng/mL TGF- β 3 in pellet culture showing the strongest differentiation of all conditions.

Weakly responding donors (presented in Section 1.2 in Supporting Information S1) generally followed the same differentiation trend of TGF- β 3 dose-dependent increase (mentioned above), but showed significantly lower expression levels for all analyzed genes. This observation was especially true for ACAN and VCAN where (in low growth factor) media a reduced expression (compared to day 0 levels) was visible.

3.3.3 | Histology

Gelatin methacryloyl encapsulated hAC and pellet culture were histologically analyzed after 21 days in culture and sections were stained with Alcian blue to verify the presence of GAG and antibodies against collagen type II.

Histological stainings reflected the results obtained in qRT-PCR showing mostly no differences between hydrogel stiffnesses. In one donor (Donor 2), however, the stiff hydrogel stained slightly stronger (Sections 1.3.5 and 1.3.6 in Supporting Information S1). Nevertheless, changes in TGF- β 3 concentration showed far stronger effects. Cultures exposed to 0 ng/mL TGF- β 3 were negative for both GAG and collagen type II irrespective of culture type. Using 1 ng/mL, TGF- β 3 both pellet culture and gelMA cultures showed increased GAG deposition, but no collagen type II deposition in most cases. Only hAC from Donor 3 exhibited some collagen type II in pellet culture (Sections 1.3.1 and 1.3.2 in Supporting Information S1) and in individual cells embedded in gelMA. However, in P5 this effect was weaker in pellet culture and wholly absent in gelMA. When 10 ng/mL TGF- β 3

TABLE 1 Relative changes in gene expression (fold) after 3 weeks of hAC encapsulated in gelMA or pellet culture compared to day 0 (= time point of encapsulation) for the chosen Donor 3 P3

gelMA concentration /culture model	TGF- β 3 concentration	COL2	COL1	Differentiation index (COL2/COI1)	ACAN	VCAN	Differentiation index (ACAN/VCAN)
7.5%	0 ng/mL	2.4	0.8	3.5	0.7	0.7	0.6
	1 ng/mL	1.9×10^3	10.9	225.9	2.9	0.7	3.9
	10 ng/mL	1.9×10^5	20.5	11.4×10^3	64.1	3.1	19.3
10%	0 ng/mL	1.3	0.5	2.4	0.4	0.6	0.8
	1 ng/mL	2.8×10^3	14.1	212.1	8.1	1.2	6.8
	10 ng/mL	2.1×10^5	39.0	5.5×10^3	128.8	4.2	31.3
Pellet culture	0 ng/mL	131.5	0.3	426.1	1.3	0.5	2.6
	1 ng/mL	1.9×10^5	32.8	6.3×10^3	63.2	2.0	34.0
	10 ng/mL	0.9×10^5	34.5	2.3×10^3	53.2	3.0	17.1

Abbreviations: ACAN, aggrecan; COL1, collagen type I; COL2, collagen type II; gelMA, Gelatin methacryloyl; hAC, human articular chondrocytes; VCAN, versican.

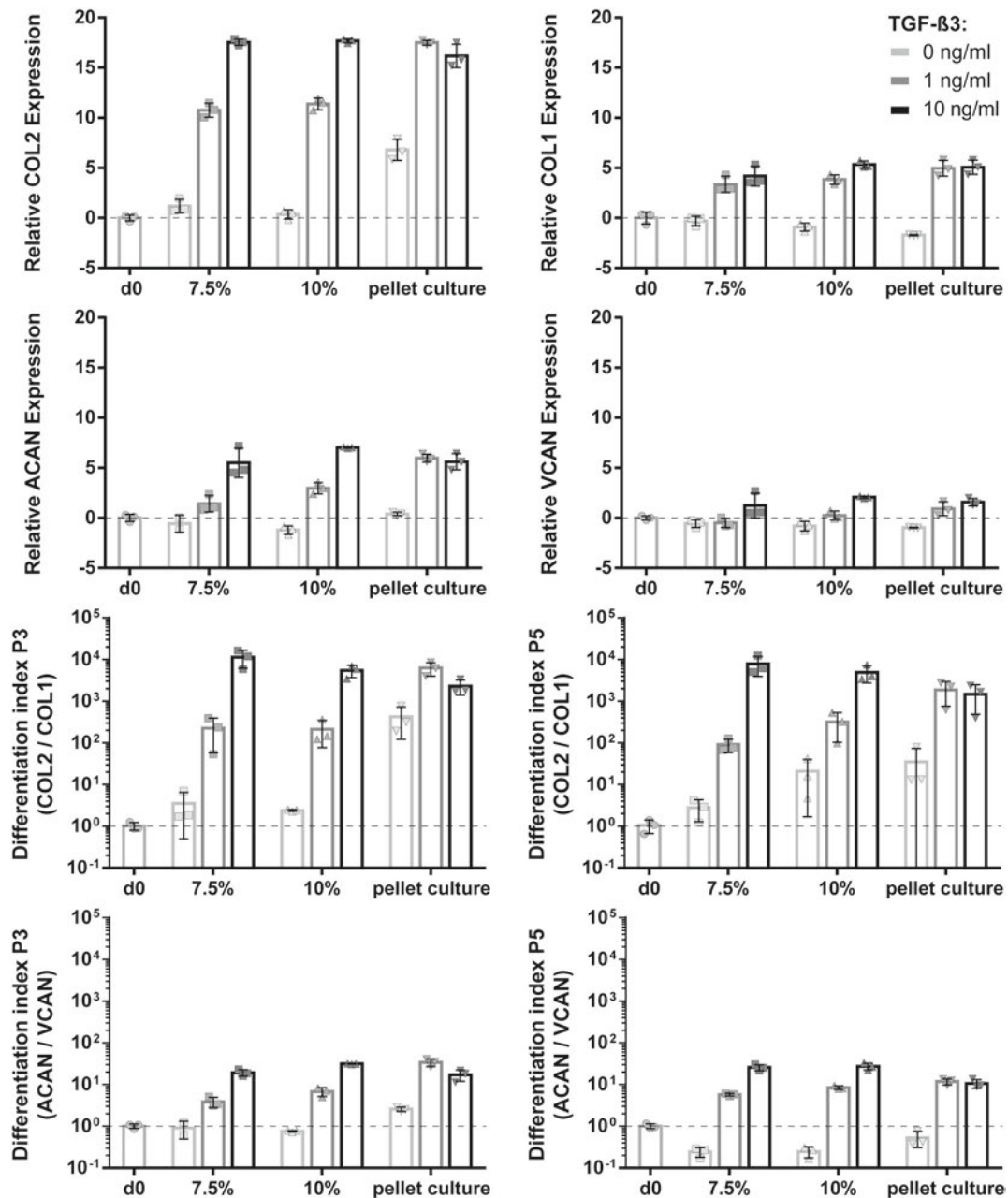


FIGURE 4 Gene expression of chondrogenic markers expressed by human articular chondrocytes (hAC) (Donor 3) encapsulated in gelatin methacryloyl (gelMA) and cultivated under different conditions for 21 days. Cells encapsulated in P3 or P5 in either soft (7.5%) or stiff (10%) gelMA and cultivated in 0, 1 or 10 ng/mL TGF- β 3. As a control, hAC were cultured in pellet culture. Differentiation indices calculated from *COL2/COL1* and aggrecan (*ACAN*)/versican (*VCAN*) are shown. Culture in 10 ng/mL TGF- β 3 showed upregulation of all genes. Cells cultured within gelMA with 10 ng/mL TGF- β 3 showed similar differentiation indices when compared to control (pellet culture). Culture within lower concentrations yielded in lower gene expression of gelMA in comparison to pellet culture. In P5 a similar potential to re-differentiate chondrocytes was found as in P3

was used to stimulate differentiation, all donors exhibited enhanced GAG and collagen type II expression, though the intensity was highly donor dependant. Interestingly, while in qRT-PCR the pellet culture of Donor 3 showed similar expression of *COL2* as other donors, and was the only donor to show collagen type II expression at 1 ng/mL in histological sections, in pellet culture it showed reduced collagen type II protein expression. In contrast, histological analysis of gelMA

cultures showed the highest collagen type II and GAG expression in Donor 3 hAC. This is consistent with qRT-PCR data where Donor 3 showed much higher *COL2* expression in gelMA cultures than other donors.

While both, gelMA and pellet cultures (in all three donors), showed similar response patterns to different TGF- β 3 concentrations (regarding staining intensity) the structure and distribution of cells

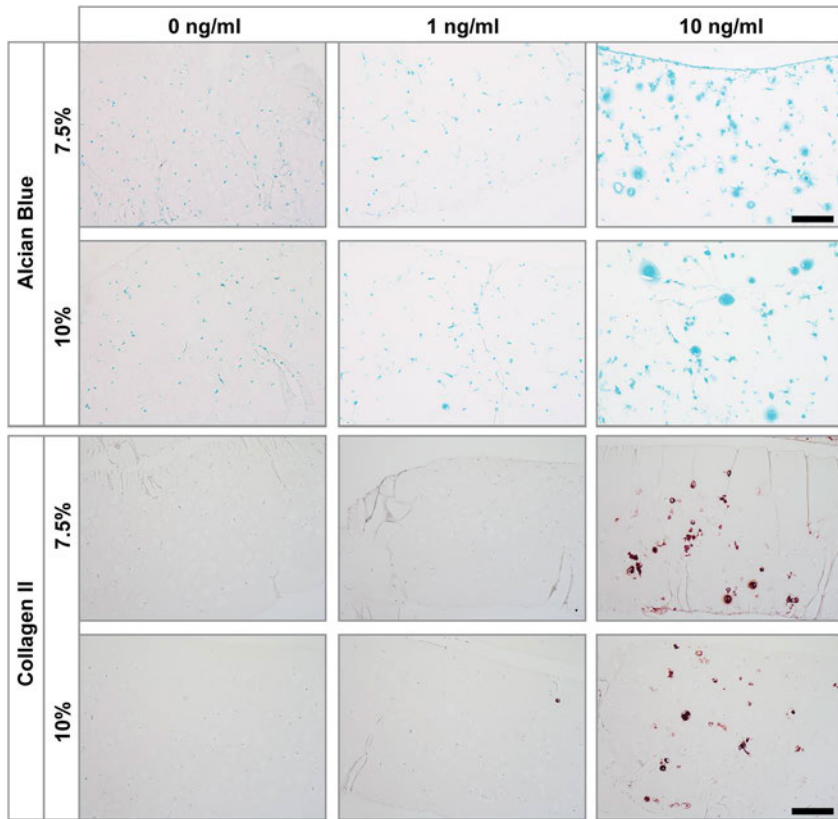


FIGURE 5 Alcian blue and collagen type II stainings of human articular chondrocytes (hAC) (P3, Donor 3) encapsulated in soft (7.5%) and stiff (10%) gelatin methacryloyl (gelMA) after 21 days in culture containing different concentrations of TGF- β 3 (0, 1 and 10 ng/mL). Culture with 0 ng/mL and 1 ng/mL TGF- β 3 displayed a lack of collagen type II staining. Glycosaminoglycans staining was absent in 0 ng/mL TGF- β 3 cultures but showed slight staining at 1 ng/mL TGF- β 3. HAC cultures within 10 ng/mL TGF- β 3 both stainings clearly showed positive cells. The staining was located in close proximity to the cells and within the gelMA matrix. Scale bar: 100 μ m

and matrix differed strongly. In pellet culture the differentiation could be observed in smaller patches and cells were packed together rather densely, only slightly separated by the secreted extracellular matrix. In contrast, in gelMA single cells or small clusters (2–4 cells) were separated by the hydrogel, resembling the structure found in native cartilage, and exhibited staining surrounding the cells. In case of strongly differentiating cells (Donor 3, Figure 5; 10 ng/mL TGF- β 3) GAG and collagen type II were not only found in the immediate cell surroundings, but were deposited into the initial hydrogel.

3.4 | Sealing of OA osteochondral plugs

In order to test the performance of gelMA as a sealant for OA cartilage, osteochondral plugs of OA cartilage with superficial damage and tissue loss were used as a model. The surface of plugs was coated with a cell-loaded gelMA (10%) to fill ridges and furrows, replacing the lost tissue and recover its smooth surface. GelMA was loaded with hAC (DiO-labeled) and ASC/TERT1-GFP, which were used as a more easily available model for primary ASC (which present a suitable alternative cell source for cartilage regeneration (Bielli et al., 2016; Erickson et al., 2002)). It was possible to create a layer of gelMA, infiltrating the superficial irregularities of the cartilage matrix, thereby replacing the degraded tissue (Figure 6). GelMA adhered well to the cartilage matrix and formed a stable layer containing cells with spherical morphology. To analyze cell viability, mono-cultures of hAC and ASC/TERT1 were stained with ethidium homodimer-1, visualizing the nucleus of dead cells in red (Figure 6a,b). In both cell types, few dead cells could be

observed, demonstrating that encapsulation and application procedures are cytocompatible. DiO labeled hAC and ASC/TERT1 were applied to the osteochondral plugs (Figure 6c,d) to validate the possibility of embedded cultures. Cross-sectional imaging showed a homogeneous distribution of both cell-types within the coating layer.

3.5 | Mechanical stress tests

To test the behavior of cell-loaded gelMA under mechanical stress, we used a tribometer to simulate the sliding movement in a tribological loaded contact during human gait by rubbing OA-osteochondral plugs coated with cell-laden gelMA against each other (Figure 6e) (Göçerler et al., 2019). We found that, after mechanical simulation of human gait with 3.5 MPa and 1 mm/sec, the gelMA layers of both samples (upper and lower part) stayed intact (Figure 6f,g). To see if gelMA protected the cells from the applied mechanical stress, samples were stained for viability (Figure 6h).

The normal load and tangential force (to calculate the coefficient of friction) was monitored every second over the course of the measurement. After initial decrease from 0.016 to 0.006 during the first load-and-movement cycle, the coefficient of friction settled at a value of 0.006 with a standard deviation of $\pm 6.5 \times 10^{-4}$ (mean value of all monitored values in the second and third repetition of loading). Due to the contact geometry and the elasticity of the samples, it has to be pointed out that the measured tangential force is a combination of friction force and a force to overcome the elastic material deformation, especially during the running-in after the first loading.

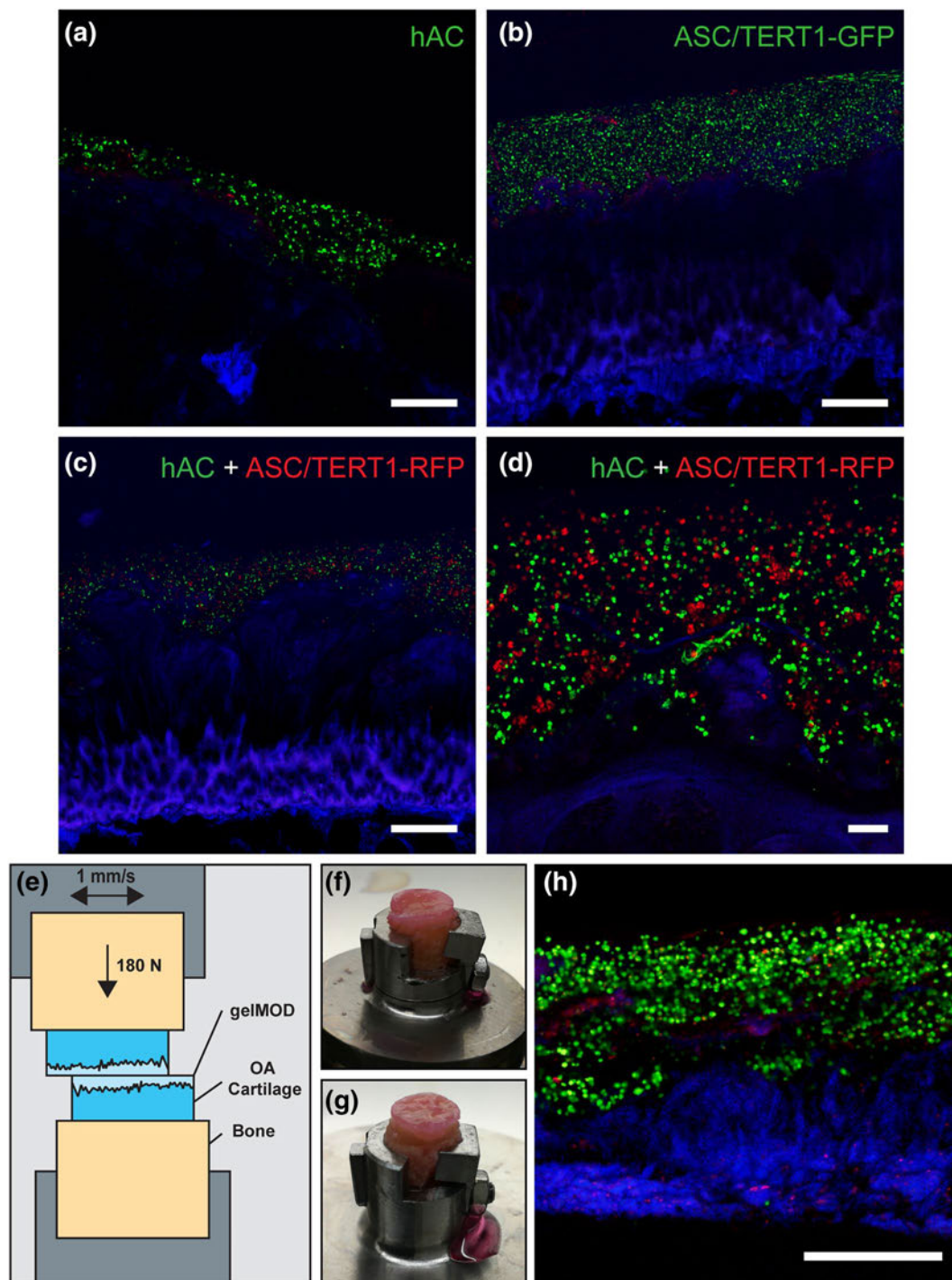


FIGURE 6 Superficially damaged osteoarthritis (OA) cartilage coated with cell-loaded gelatin methacryloyl (gelMA) (10%) after 1 day of cultivation and after simulation of human gait. (a) gelMA loaded with human articular chondrocytes (hAC) (DiO, green) and stained for dead cells (ethidium homodimer 1; red) on cartilage (autofluorescence; blue). (b) gelMA loaded with ASC/TERT1-GFP (GFP-transduced; green) and stained for dead cells (ethidium homodimer 1; red) (c) Overview and (d) detail of co-culture of hAC (green) and ASC/TERT1-mCherry (red). Scale bar: (a–c) 500 μ m and (d) 100 μ m. (e) Schematic of the experimental setup for the mechanical simulation of human gait. Osteoarthritic specimens were coated with cell loaded (hAC-DiO) gelMA (10%) and exposed to mechanical stress to simulate human gait. The gelMA layer stayed intact in both specimens: (f) lower specimen of the measurement, (g) upper specimen. (h) Live/Dead staining of a cross-section of the lower specimen showing living cells (green), dead cells (red) and cartilage (blue). Scale bar: 500 μ m

4 | DISCUSSION

Cartilage is a tissue with a low intrinsic regeneration potential. So far the most frequently used treatment modalities are unsuitable for superficial cartilage defects, as present, for example, in OA. The main problem is the fixation of the cells and/or scaffolds in shallow defects. This is especially hard for sponge-like or fibrous materials (Alves da Silva et al., 2010), as the material ideally needs to adhere to the defect and fill small crevasses. Other materials, using physical crosslinking (e.g., acid-soluble collagen) produce hydrogels, which are able to fill such defects (Chen et al., 2013), but need high protein concentrations to reach comparable stiffnesses, and need cooling to prevent premature gelation. Therefore, innovative solutions are needed to overcome these problems. There are many different materials currently in development for the treatment of cartilage defects, with only a fraction fulfilling the necessary characteristics for the treatment of superficial cartilage defects (Wei et al., 2021). Here we investigate the potential use of a photo-polymerizable gelMA hydrogel as a bio-compatible, biodegradable and injectable hydrogel for cartilage regeneration appearing especially promising for this application. Due to its characteristics such as a short gelation time (2–10 min) and adhesiveness to damaged tissue (Assmann et al., 2017), it allows for easy and accurate administration of therapeutic cells. Due to the covalent bonds created by photo-crosslinking, gelMA exhibits superior stability and mechanical properties compared to physically crosslinked (e.g., by ions or hydrophobicity) hydrogels (Liu et al., 2017). Furthermore, while being biodegradable, its stability is higher than many other covalently crosslinked hydrogels frequently used in clinics (e.g., fibrin), which often degrade within a few weeks (Wolbank et al., 2015). Even though functionalized fibrins have improved material characteristics for cartilage repair (Almeida et al., 2016), degradation behavior is still not ideal without additional crosslinking. The stability of gelMA allows for more extended protection of delivered cells from harmful external influences. Additionally, it is an important factor for cartilage regeneration, as hydrogels should initially support tissue formation and differentiation and later degrade at an appropriate rate so that the cells can simultaneously produce their own matrix and re-establish normal function. This balance is not possible for hydrogels such as alginate, which is not degradable in its unmodified form and therefore unsuitable for this kind of use. Modification of these materials (Park & Lee, 2014) and use of biodegradable synthetic materials reduce some of these issues, however concerns about degradation products remain when thinking about clinical application.

Within this study we investigated the differentiation capacity of hAC (P3 and P5), which was slightly reduced in P5 when embedded in both formulations of gelMA (soft: 7.5% and stiff: 10%) as well as in the biomaterial-free culture form of pellet culture (i.e., a standard way of culturing for redifferentiation assays). Generally, differentiation of hAC in gelMA and pellet culture was determined by the growth factor concentration and little influenced by the culture system. Without addition of growth factors almost no redifferentiation could be achieved, with slightly better performance of pellet culture and stiff gelMA in comparison to soft gelMA hydrogels

in some of the donor cells and passages. Even though sufficiently stiff gels have previously shown to also induce differentiation without the addition of growth factors (Allen et al., 2012), these results were achieved with non-human cells, which have a higher redifferentiation potential due to species or age. Nevertheless, even under these conditions significantly higher differentiation was achieved in synergy with TGF- β (Allen et al., 2012). As we used cells from older human donors (51–66 years old) the effect of gel stiffness was likely not sufficient to induce re-differentiation by itself. However, what we did observe is that without additional growth factors stiff gelMA was able to induce a rounded cell morphology, which is closer to the physiological morphology of differentiated chondrocytes, which has previously been shown for other types hydrogels (Li et al., 2016).

When adding growth factors to the medium, the differentiation of hAC in gelMA and pellet culture was significantly enhanced. A concentration of 10 ng/mL TGF- β 3 was used as a stimulus to analyze the maximal differentiation potential of donor cells. With this high dose, gelMA embedded cells showed similar or even upregulated gene expression of chondrogenic markers (COL2, ACAN) than pellet culture, while histological stainings revealed the deposition of matrix into the hydrogel (Donor 3). Due to the material density it was mainly located in the circumference of chondrocytes, which leads to a chondron-like appearance. The pericellular deposition exhibited in gelMA was similar to what has been previously described for dense fibrin and alginate (Almqvist, 2001; Bachmann et al., 2020). Due to the lower degradation rate of gelMA compared to fibrin, in the long run, cells would have more time to replace the scaffold while it is degraded which might be favorable for defect regeneration. However, higher cell numbers might be necessary if deposition zones cannot grow large enough to fully overlap. As TGF- β 3 is a potent stimulus for chondrogenic differentiation, it might mask possible positive differentiation effects of the embedding hydrogel. Therefore, a concentration of 1 ng/mL TGF- β 3 was tested in order to give cells growth factor stimulus without masking other effects, a problem which has been previously described, for example, for the influence of mechanical stimulation (Li et al., 2010). Indeed, within this group the donor variability was observable with gelMA embedded donor cells performing similar (Donor 1 P3) or slightly better (Donor 1 P5) than pellet culture or significantly worse (Donors 2 and 3). The differentiation effect of the two hydrogel stiffnesses was comparable.

Generally, in comparison to the gelMA groups, the pellet culture promoted increased chondrogenic differentiation, which might be related to the closer proximity of cells, influencing each other by paracrine (Grassel et al., 2010; Li et al., 2010; Takigawa et al., 1997) and cell-cell contact (Tsuchiya et al., 2004) stimulation, which have both been previously shown to stimulate differentiation. Despite that, donor variability was high and especially observable with the addition of low growth factor concentration. Differences were mainly found in the total increase in gene expression, but did not show differences between cultivation systems (gelMA vs. pellet culture). Passage number (P3 vs. P5) only marginally influenced the behavior of the chondrocytes within gelMA and pellet culture for both, low and high doses of growth factors. Chondrogenic differentiation was consistent

between P3 and P5, showing that also after expansion over the critical passage number of 5 (Kang et al., 2007) chondrocyte re-differentiation was possible, both in gelMA and in pellet culture. However, in the clinical setting, the appropriate growth factor condition might not be present, especially in inflammatory conditions such as OA. For such conditions co-embedding of growth factors or anti-inflammatory therapeutics, which has been previously achieved (Gnavi et al., 2014; Moshaverinia et al., 2015; Yamamoto et al., 1999), might be a successful strategy when using a gelMA hydrogel as a delivery system.

Another clinically relevant option for cartilage damage repair is the use of autologous MSC alone or in co-culture as they have a chondrogenic potential and can be more easily obtained, for example, from fat tissue. Likewise the amount of hAC needed for clinical interventions may be reduced, also enabling 1-step procedures, thereby alleviating the need for a second surgery. This aspect, in combination with an overall reduction in amount of cells (due to a direct application to the site of interest and alleviation of cell-loss of non-adhering cells when applied to the joint cavity in suspension), could greatly improve the treatment of diseases such as OA. Furthermore, as MSC are known to have immuno-modulatory effects, they might counteract inflammation, and therefore positively influence cartilage regeneration, in OA defects (van Buul et al., 2012). Additionally some studies suggest a positive effect on differentiation capacity in co-cultures between hAC and MSC (Dahlin et al., 2014; Hildner et al., 2009; Tsuchiya et al., 2004).

In OA non-cell based treatments such as hyaluronic acid (Bowman et al., 2018) or cell-based therapies (Burdick et al., 2016) are frequently applied by an intraarticular injection. This application has resulted in varying degrees of success which is likely caused by low amounts or transient availability of non-cellular therapeutics and/or cells reaching the region of defect, or being maintained there. It has been shown that for cell based therapy in many cases less than 5% of initially applied cells are retained at the site of injection (Burdick et al., 2016). The use of gelMA might alleviate these problems by keeping cells at the defect site, while protecting the cells and smoothing the joint surface, while still being applicable endoscopically, thereby preventing further damage. In this study this was tested using an osteochondral plug model (obtained from OA patients) and simulation of the strain during normal human gait using a tribometer. The results show that the hydrogel was stable on the underlying cartilage when mimicking the conditions within a healthy joint (coefficient of friction of 0.005 – 0.023) (Charnley, 1960), the cells were evenly distributed (mixture of hAC and ASC/TERT1) and remained viable under the applied mechanical stress.

5 | CONCLUSIONS

In conclusion, gelMA is a promising hydrogel for cartilage regeneration as it combines easy application of cells into defect areas and protection against harmful influences, while allowing for efficient (re-)differentiation of hAC. Due to its characteristics, it is possible to fill surface roughness or replace larger superficial tissue loss, for

example, in OA defects, thereby making it a promising tool for the clinical treatment of OA.

5.1 | Limitations of the study

This study is limited by the high donor variability of primary human chondrocytes, which on the other hand is also advantageous, as it reflects the real clinical situation. The limited number of samples was due to limited donor availability and long cultivation time necessary to generate high passage chondrocytes (especially from older donors). Additionally, due to the low reproducibility of the measurements obtained with the available setup for mechanical testing, samples were therefore mainly analyzed for cell viability and intactness/attachment of the hydrogel.

ACKNOWLEDGMENTS

The authors acknowledge the financial support of the European Research Council (Starting Grant-307701, AO) and the project COMET XTribology (Grant 849109). We also acknowledge the professional competence and support of the AC2T research GmbH which helped with scientific knowledge and performance of mechanical stress tests.

The ASC/TERT1 cell line was kindly provided by Evercyte (Vienna, Austria) and Phoenix-Ampho cells were a gift from Regina Grillari (University of Natural Resources and Life Sciences, Vienna, Austria). Transduction of ASC/TERT1 with GFP and mCherry was kindly performed by Severin Mühleder and Wolfgang Holthöner (LBI Trauma, Vienna).

CONFLICT OF INTEREST

The authors declare that there is no conflict of interest.

AUTHOR CONTRIBUTIONS

Writing the manuscript: Katja Hölzl, Marian Fürsatz. Isolation/culture of cells and tissue: Katja Hölzl, Marian Fürsatz, Sara Žigon-Branc, Marica Markovic. Cytotoxicity assays: Katja Hölzl, Rheology: Katja Hölzl, Stefan Baudis, Confocal Imaging: Katja Hölzl, Marian Fürsatz, qRT-PCR: Katja Hölzl, Histology: Barbara Schädli. Synthesis of gelMA: Jasper Van Hoorick, Sandra Van Vlierberghe. Mechanical testing: Hakan Göcerler, Andreas Pauschitz, Katja Hölzl. Statistical analysis: Claudia Gahleitner, Study design: Katja Hölzl, Aleksandr Ovsianikov, Heinz Redl, Sylvia Nürnberger. Data analysis and interpretation: Katja Hölzl, Marian Fürsatz, Hakan Göcerler, Sylvia Nürnberger. Critically reviewing the manuscript: all

DATA AVAILABILITY STATEMENT

The data that support the findings of this study are available from the corresponding author upon reasonable request.

ORCID

Marian Fürsatz  <https://orcid.org/0000-0003-4990-3326>

REFERENCES

- Akkiraju, H., & Nohe, A. (2015). Role of chondrocytes in cartilage formation, progression of osteoarthritis and cartilage regeneration. *Journal of Developmental Biology*, 3(4), 177–192. <https://doi.org/10.3390/jdb3040177>
- Allen, J. L., Cooke, M. E., & Alliston, T. (2012). ECM stiffness primes the TGF β pathway to promote chondrocyte differentiation. *Molecular Biology of the Cell*, 23(18), 3731–3742. <https://doi.org/10.1091/mbc.e12-03-0172>
- Almeida, H. V., Eswaramoorthy, R., Cunniffe, G. M., Buckley, C. T., O'Brien, F. J., & Kelly, D. J. (2016). Fibrin hydrogels functionalized with cartilage extracellular matrix and incorporating freshly isolated stromal cells as an injectable for cartilage regeneration. *Acta Biomaterialia*, 36, 55–62. <https://doi.org/10.1016/j.actbio.2016.03.008>
- Almqvist, K. F. (2001). Culture of chondrocytes in alginate surrounded by fibrin gel: Characteristics of the cells over a period of eight weeks. *Annals of the Rheumatic Diseases*, 60(8), 781–790. <https://doi.org/10.1136/ard.60.8.781>
- Alves da Silva, M. L., Crawford, A., Mundy, J. M., Correló, V. M., Sol, P., Bhattacharya, M., Hatton, P. V., Reis, R. L., & Neves, N. M. (2010). Chitosan/polyester-based scaffolds for cartilage tissue engineering: Assessment of extracellular matrix formation. *Acta Biomaterialia*, 6(3), 1149–1157. <https://doi.org/10.1016/j.actbio.2009.09.006>
- Assmann, A., Vegh, A., Ghasemi-Rad, M., Bagherifard, S., Cheng, G., Sani, E. S., Ruiz-Esparza, G. U., Noshadi, I., Lassaletta, A. D., Gangadharan, S., Tamayol, A., Khademhosseini, A., & Annabi, N. (2017). A highly adhesive and naturally derived sealant. *Biomaterials*, 140, 115–127. <https://doi.org/10.1016/j.biomaterials.2017.06.004>
- Bachmann, B., Spitz, S., Schädli, B., Teuschl, A. H., Redl, H., Nürnberger, S., & Ertl, P. (2020). Stiffness matters: Fine-tuned hydrogel elasticity alters chondrogenic redifferentiation. *Frontiers in Bioengineering and Biotechnology*, 8, 373. <https://doi.org/10.3389/fbioe.2020.00373>
- Bhosale, A. M., & Richardson, J. B. (2008). Articular cartilage: Structure, injuries and review of management. *British Medical Bulletin*, 87, 77–95. <https://doi.org/10.1093/bmb/ldn025>
- Bielli, A., Sciofi, M. G., Gentile, P., Cervelli, V., & Orlandi, A. (2016). Adipose-derived stem cells in cartilage regeneration: Current perspectives. *Regenerative Medicine*, 11(7), 693–703. <https://doi.org/10.2217/rme-2016-0077>
- Boere, K. W. M., Visser, J., Seyednejad, H., Rahimian, S., Gawlitta, D., van Steenbergen, M. J., Dhert, W. J. A., Hennink, W. E., Vermonden, T., & Malda, J. (2014). Covalent attachment of a three-dimensionally printed thermoplast to a gelatin hydrogel for mechanically enhanced cartilage constructs. *Acta Biomaterialia*, 10(6), 2602–2611. <https://doi.org/10.1016/j.actbio.2014.02.041>
- Bowman, S., Awad, M. E., Hamrick, M. W., Hunter, M., & Fulzele, S. (2018). Recent advances in hyaluronic acid based therapy for osteoarthritis. *Clinical and Translational Medicine*, 7(1), 6. <https://doi.org/10.1186/s40169-017-0180-3>
- Brittberg, M., Lindahl, A., Nilsson, A., Ohlsson, C., Isaksson, O., & Peterson, L. (1994). Treatment of deep cartilage defects in the knee with autologous chondrocyte transplantation. *New England Journal of Medicine*, 331(14), 889–895. <https://doi.org/10.1056/NEJM199410063311401>
- Brown, G. C. J., Lim, K. S., Farrugia, B. L., Hooper, G. J., & Woodfield, T. B. F. (2017). Covalent incorporation of heparin improves chondrogenesis in photocurable gelatin-methacryloyl hydrogels. *Macromolecular Bioscience*, 17(12), 1700158. <https://doi.org/10.1002/mabi.201700158>
- Burdick, J. A., Mauck, R. L., & Gerecht, S. (2016). To serve and protect: Hydrogels to improve stem cell-based therapies. *Cell Stem Cell*, 18(1), 13–15. <https://doi.org/10.1016/j.stem.2015.12.004>
- Charnley, J. (1960). The lubrication of animal joints in relation to surgical reconstruction by arthroplasty. *Annals of the Rheumatic Diseases*, 19(1), 10–19. <https://doi.org/10.1136/ard.19.1.10>
- Chen, X., Zhang, F., He, X., Xu, Y., Yang, Z., Chen, L., Zhou, S., Yang, Y., Zhou, Z., Sheng, W., & Zeng, Y. (2013). Chondrogenic differentiation of umbilical cord-derived mesenchymal stem cells in type I collagen-hydrogel for cartilage engineering. *Injury*, 44(4), 540–549. <https://doi.org/10.1016/j.injury.2012.09.024>
- Dahlin, R. L., Ni, M., Meretoja, V. V., Kasper, F. K., & Mikos, A. G. (2014). TGF- β 3-induced chondrogenesis in co-cultures of chondrocytes and mesenchymal stem cells on biodegradable scaffolds. *Biomaterials*, 35(1), 123–132. <https://doi.org/10.1016/j.biomaterials.2013.09.086>
- Enea, D., Ceconi, S., Busilacchi, A., Manzotti, S., Gesuita, R., & Gigante, A. (2012). Matrix-induced autologous chondrocyte implantation (MACI) in the knee. *Knee Surgery, Sports Traumatology, Arthroscopy*, 20(5), 862–869. <https://doi.org/10.1007/s00167-011-1639-1>
- Erickson, G. R., Gimble, J. M., Franklin, D. M., Rice, H. E., Awad, H., & Guilak, F. (2002). Chondrogenic potential of adipose tissue-derived stromal cells in vitro and in vivo. *Biochemical and Biophysical Research Communications*, 290(2), 763–769. <https://doi.org/10.1006/bbrc.2001.6270>
- Fürsatz, M., Gerges, P., Wolbank, S., & Nürnberger, S. (2021). Autonomous spheroid formation by culture plate compartmentation. *Biofabrication*, 13(3), 035018. <https://doi.org/10.1088/1758-5090/abe186>
- Garza, J. R., Campbell, R. E., Tjoumakaris, F. P., Freedman, K. B., Miller, L. S., Santa Maria, D., & Tucker, B. S. (2020). Clinical efficacy of intra-articular mesenchymal stromal cells for the treatment of knee osteoarthritis: A double-blinded prospective randomized controlled clinical trial. *The American Journal of Sports Medicine*, 48(3), 588–598. <https://doi.org/10.1177/0363546519899923>
- Gnavi, S., di Blasio, L., Tonda-Turo, C., Mancardi, A., Primo, L., Ciardelli, G., Gambarotta, G., Geuna, S., & Perroteau, I. (2014). Gelatin-based hydrogel for vascular endothelial growth factor release in peripheral nerve tissue engineering: VEGF-releasing hydrogel. *Journal of Tissue Engineering and Regenerative Medicine*, 11(2), 459–470. <https://doi.org/10.1002/term.1936>
- Gorsche, C., Harikrishna, R., Baudis, S., Knaack, P., Husar, B., Laeuger, J., Hoffmann, H., & Liska, R. (2017). Real time-NIR/MIR-photorheology: A versatile tool for the *in situ* characterization of photopolymerization reactions. *Analytical Chemistry*, 89(9), 4958–4968. <https://doi.org/10.1021/acs.analchem.7b00272>
- Göçerler, H., Pfeil, B., Franek, F., Bauer, C., Niculescu-Morza, E., & Nehrer, S. (2019). The dominance of water on lubrication properties of articular joints. *Industrial Lubrication & Tribology*, 72(1), 31–37. <https://doi.org/10.1108/ILT-02-2019-0064>
- Grassel, S., Rickert, M., Opolka, A., Bosserhoff, A., Angele, P., Grifka, J., & Anders, S. (2010). Coculture between periosteal explants and articular chondrocytes induces expression of TGF-1 and collagen I. *Rheumatology*, 49(2), 218–230. <https://doi.org/10.1093/rheumatology/kep326>
- Gu, L., Li, T., Song, X., Yang, X., Li, S., Chen, L., Liu, P., Gong, X., Chen, C., & Sun, L. (2020). Preparation and characterization of methacrylated gelatin/bacterial cellulose composite hydrogels for cartilage tissue engineering. *Regenerative Biomaterials*, 7(2), 195–202. <https://doi.org/10.1093/rb/rbz050>
- Han, L., Xu, J., Lu, X., Gan, D., Wang, Z., Wang, K., Zhang, H., Yuan, H., & Weng, J. (2017). Biohybrid methacrylated gelatin/polyacrylamide hydrogels for cartilage repair. *Journal of Materials Chemistry B*, 5(4), 731–741. <https://doi.org/10.1039/C6TB02348G>
- Han, M.-E., Kang, B. J., Kim, S.-H., Kim, H. D., & Hwang, N. S. (2017). Gelatin-based extracellular matrix cryogels for cartilage tissue engineering. *Journal of Industrial and Engineering Chemistry*, 45, 421–429. <https://doi.org/10.1016/j.jiec.2016.10.011>
- Häuselmann, H. J., Masuda, K., Hunziker, E. B., Neidhart, M., Mok, S. S., Michel, B. A., & Thonar, E. J. (1996). Adult human chondrocytes cultured in alginate form a matrix similar to native human articular cartilage. *American Journal of Physiology*, 271(3 Pt 1), C742–C752. <https://doi.org/10.1152/ajpcell.1996.271.3.C742>

- Hildner, F., Concaro, S., Peterbauer, A., Wolbank, S., Danzer, M., Lindahl, A., Gatenholm, P., Redl, H., & van Griensven, M. (2009). Human adipose-derived stem cells contribute to chondrogenesis in coculture with human articular chondrocytes. *Tissue Engineering Part A*, 15(12), 3961–3969. <https://doi.org/10.1089/ten.tea.2009.0002>
- Hunziker, E. B., Lippuner, K., Keel, M. J. B., & Shintani, N. (2015). An educational review of cartilage repair: Precepts & practice--myths & misconceptions--progress & prospects. *Osteoarthritis and Cartilage*, 23(3), 334–350. <https://doi.org/10.1016/j.joca.2014.12.011>
- Kang, S.-W., Yoo, S. P., & Kim, B.-S. (2007). Effect of chondrocyte passage number on histological aspects of tissue-engineered cartilage. *Bio-Medical Materials and Engineering*, 17(5), 269–276.
- Knezevic, L., Schupper, M., Mühleder, S., Schimek, K., Hasenberg, T., Marx, U., Priglinger, E., Redl, H., & Holthöner, W. (2017). Engineering blood and lymphatic microvascular networks in fibrin matrices. *Frontiers in Bioengineering and Biotechnology*, 5. <https://doi.org/10.3389/fbioe.2017.00025>
- Koh, R. H., Jin, Y., Kim, J., & Hwang, N. S. (2020). Inflammation-modulating hydrogels for osteoarthritis cartilage tissue engineering. *Cells*, 9(2), 419. <https://doi.org/10.3390/cells9020419>
- Lee, D. A., Reisler, T., & Bader, D. L. (2003). Expansion of chondrocytes for tissue engineering in alginate beads enhances chondrocytic phenotype compared to conventional monolayer techniques. *Acta Orthopaedica Scandinavica*, 74(1), 6–15. <https://doi.org/10.1080/00016470310013581>
- Li, X., Chen, S., Li, J., Wang, X., Zhang, J., Kawazoe, N., & Chen, G. (2016). 3D culture of chondrocytes in gelatin hydrogels with different stiffness. *Polymers*, 8(8), 269. <https://doi.org/10.3390/polym8080269>
- Li, Z., Kupcsik, L., Yao, S.-J., Alini, M., & Stoddart, M. J. (2010). Mechanical load modulates chondrogenesis of human mesenchymal stem cells through the TGF- β pathway. *Journal of Cellular and Molecular Medicine*, 14(6a), 1338–1346. <https://doi.org/10.1111/j.1582-4934.2009.00780.x>
- Liu, M., Zeng, X., Ma, C., Yi, H., Ali, Z., Mou, X., Li, S., Deng, Y., & He, N. (2017). Injectable hydrogels for cartilage and bone tissue engineering. *Bone Research*, 5, 17014. <https://doi.org/10.1038/boneres.2017.14>
- Majima, T., Schnabel, W., & Weber, W. (1991). Phenyl-2,4,6-trimethylbenzoylphosphinates as water-soluble photoinitiators. Generation and reactivity of O=b(C6Hs)(O-) radical anions. *Makromolekulare Chemie*, 192(10), 2307–2315. <https://doi.org/10.1002/macp.1991.021921010>
- Markovic, M., Van Hoorick, J., Hölzl, K., Tromayer, M., Gruber, P., Nürnberger, S., Dubrue, P., Van Vlierberghe, S., Liska, R., & Ovsianikov, A. (2015). Hybrid tissue engineering scaffolds by combination of three-dimensional printing and cell photoencapsulation. *Journal of Nanotechnology in Engineering and Medicine*, 6(2), 021001. <https://doi.org/10.1115/1.4031466>
- Migliorini, F., Rath, B., Colarossi, G., Driessen, A., Tingart, M., Niewiera, M., & Eschweiler, J. (2020). Improved outcomes after mesenchymal stem cells injections for knee osteoarthritis: Results at 12-months follow-up: A systematic review of the literature. *Archives of Orthopaedic and Trauma Surgery*, 140(7), 853–868. <https://doi.org/10.1007/s00402-019-03267-8>
- Moshaverinia, A., Chen, C., Xu, X., Ansari, S., Zadeh, H. H., Schrickler, S. R., Paine, M. L., Moradian-Oldak, J., Khademhosseini, A., Snead, M. L., & Shi, S. (2015). Regulation of the stem cell-host immune system interplay using hydrogel coencapsulation system with an anti-inflammatory drug. *Advanced Functional Materials*, 25(15), 2296–2307. <https://doi.org/10.1002/adfm.201500055>
- Mouser, V. (2018). Ex vivo model unravelling cell distribution effect in hydrogels for cartilage repair. *ALTEX*, 35(1), 65–76. <https://doi.org/10.14573/altex.1704171>
- Muñoz-Criado, I., Meseguer-Ripolles, J., Mellado-López, M., Alastrue-Agudo, A., Griffeth, R. J., Forteza-Vila, J., Cugat, R., García, M., & Moreno-Manzano, V. (2017). Human suprapatellar fat pad-derived mesenchymal stem cells induce chondrogenesis and cartilage repair in a model of severe osteoarthritis. *Stem Cells International*, 2017, 1–12. <https://doi.org/10.1155/2017/4758930>
- Nürnberger, S., Schneider, C., van Osch, G. V. M., Keibl, C., Rieder, B., Monforte, X., Teuschl, A. H., Mühleder, S., Holthöner, W., Schädli, B., Gahleitner, C., Redl, H., & Wolbank, S. (2019). Repopulation of an auricular cartilage scaffold, AuriScaff, perforated with an enzyme combination. *Acta Biomaterialia*, 86, 207–222. <https://doi.org/10.1016/j.actbio.2018.12.035>
- Ovsianikov, A., Deiwick, A., Van Vlierberghe, S., Dubrue, P., Möller, L., Dräger, G., & Chichkov, B. (2011). Laser fabrication of three-dimensional CAD scaffolds from photosensitive gelatin for applications in tissue engineering. *Biomacromolecules*, 12(4), 851–858. <https://doi.org/10.1021/bm1015305>
- Park, H., & Lee, K. Y. (2014). Cartilage regeneration using biodegradable oxidized alginate/hyaluronate hydrogels: Cartilage regeneration using biodegradable hydrogels. *Journal of Biomedical Materials Research Part A*, 102(12), 4519–4525. <https://doi.org/10.1002/jbm.a.35126>
- Patil, S., Steklov, N., Song, L., Bae, W. C., & D'Lima, D. D. (2014). Comparative biomechanical analysis of human and caprine knee articular cartilage. *The Knee*, 21(1), 119–125. <https://doi.org/10.1016/j.knee.2013.03.009>
- Perka, C., Schultz, O., Lindenhayn, K., Spitzer, R. S., Muschik, M., Sittlinger, M., & Burmester, G. R. (2000). Joint cartilage repair with transplantation of embryonic chondrocytes embedded in collagen-fibrin matrices. *Clinical & Experimental Rheumatology*, 18(1), 13–22.
- Salam, N., Toumpaniari, S., Gentile, P., Marina Ferreira, A., Dalgarno, K., & Partridge, S. (2018). Assessment of migration of human MSCs through fibrin hydrogels as a tool for formulation optimisation. *Materials*, 11(9), 1781. <https://doi.org/10.3390/ma11091781>
- Song, Y., Du, H., Dai, C., Zhang, L., Li, S., Hunter, D. J., Lu, L., & Bao, C. (2018). Human adipose-derived mesenchymal stem cells for osteoarthritis: A pilot study with long-term follow-up and repeated injections. *Regenerative Medicine*, 13(3), 295–307. <https://doi.org/10.2217/rme-2017-0152>
- Sophia Fox, A. J., Bedi, A., & Rodeo, S. A. (2009). The basic science of articular cartilage. *Sport Health*, 1(6), 461–468. <https://doi.org/10.1177/1941738109350438>
- Takigawa, M., Okawa, T., Pan, H.-O., Aoki, C., Takahashi, K., Zue, J.-D., Suzuki, F., & Kinoshita, A. (1997). Insulin-like growth factors I and II are autocrine factors in stimulating proteoglycan synthesis, a marker of differentiated chondrocytes, acting through their respective receptors on a clonal human chondrosarcoma-derived chondrocyte cell line. *Endocrinology*, 138(10), 11.
- Toupet, K., Maumus, M., Peyrafitte, J.-A., Bourin, P., van Lent, P. L. E. M., Ferreira, R., Orsetti, B., Pirot, N., Casteilla, L., Jorgensen, C., & Noël, D. (2013). Long-term detection of human adipose-derived mesenchymal stem cells after intraarticular injection in SCID mice: Biodistribution and long-term detection of human AD-MSCs in SCID mice. *Arthritis & Rheumatism*, 65(7), 1786–1794. <https://doi.org/10.1002/art.37960>
- Tsuchiya, K., Chen, G., Ushida, T., Matsuno, T., & Tateishi, T. (2004). The effect of coculture of chondrocytes with mesenchymal stem cells on their cartilaginous phenotype in vitro. *Materials Science and Engineering: C*, 24(3), 391–396. <https://doi.org/10.1016/j.msec.2003.12.014>
- van Buul, G. M., Villafuertes, E., Bos, P. K., Waarsing, J. H., Kops, N., Narcisi, R., Weinans, H., Verhaar, J. A. N., Bernsen, M. R., & van Osch, G. J. V. M. (2012). Mesenchymal stem cells secrete factors that inhibit inflammatory processes in short-term osteoarthritic synovium and cartilage explant culture. *Osteoarthritis and Cartilage*, 20(10), 1186–1196. <https://doi.org/10.1016/j.joca.2012.06.003>
- Van Den Bulcke, A. I., Bogdanov, B., De Rooze, N., Schacht, E. H., Cornelissen, M., & Berghmans, H. (2000). Structural and rheological

- properties of methacrylamide modified gelatin hydrogels. *Biomacromolecules*, 1(1), 31–38. <https://doi.org/10.1021/bm990017d>
- Van Hoorick, J., Declercq, H., De Muynck, A., Houben, A., Van Hoorebeke, L., Cornelissen, R., Van Erps, J., Thienpont, H., Dubruel, P., & Van Vlierberghe, S. (2015). Indirect additive manufacturing as an elegant tool for the production of self-supporting low density gelatin scaffolds. *Journal of Materials Science: Materials in Medicine*, 26(10), 247. <https://doi.org/10.1007/s10856-015-5566-4>
- Van Hoorick, J., Gruber, P., Markovic, M., Rollot, M., Graulus, G.-J., Vagenende, M., Tromayer, M., Van Erps, J., Thienpont, H., Martins, J. C., Baudis, S., Ovsianikov, A., Dubruel, P., & Van Vlierberghe, S. (2018). Highly reactive thiol-norbornene photo-click hydrogels: Toward improved processability. *Macromolecular Rapid Communications*, 39(14), 1800181. <https://doi.org/10.1002/marc.201800181>
- Van Hoorick, J., Tytgat, L., Dobos, A., Ottevaere, H., Van Erps, J., Thienpont, H., Ovsianikov, A., Dubruel, P., & Van Vlierberghe, S. (2019). (Photo-)crosslinkable gelatin derivatives for biofabrication applications. *Acta Biomaterialia*, 97, 46–73. <https://doi.org/10.1016/j.actbio.2019.07.035>
- Wang, K.-Y., Jin, X.-Y., Ma, Y.-H., Cai, W.-J., Xiao, W.-Y., Li, Z.-W., Qi, X., & Ding, J. (2021). Injectable stress relaxation gelatin-based hydrogels with positive surface charge for adsorption of aggrecan and facile cartilage tissue regeneration. *Journal of Nanobiotechnology*, 19(1), 214. <https://doi.org/10.1186/s12951-021-00950-0>
- Wei, W., Ma, Y., Yao, X., Zhou, W., Wang, X., Li, C., Lin, J., He, Q., Leptihn, S., & Ouyang, H. (2021). Advanced hydrogels for the repair of cartilage defects and regeneration. *Bioactive Materials*, 6(4), 998–1011. <https://doi.org/10.1016/j.bioactmat.2020.09.030>
- Wolbank, S., Pichler, V., Ferguson, J. C., Meinel, A., van Griensven, M., Goppelt, A., & Redl, H. (2015). Non-invasive *in vivo* tracking of fibrin degradation by fluorescence imaging: *In vivo* imaging of fibrin degradation. *Journal of Tissue Engineering and Regenerative Medicine*, 9(8), 973–976. <https://doi.org/10.1002/term.1941>
- Yamamoto, M., Tabata, Y., & Ikada, Y. (1999). Growth factor release from gelatin hydrogel for tissue engineering. *Journal of Bioactive and Compatible Polymers*, 14(6), 474–489. <https://doi.org/10.1177/088391159901400603>
- Yoon, J., Ha, S., Lee, S., & Chae, S.-W. (2018). Analysis of contact pressure at knee cartilage during gait with respect to foot progression angle. *International Journal of Precision Engineering and Manufacturing*, 19(5), 761–766. <https://doi.org/10.1007/s12541-018-0091-2>
- Yue, K., Li, X., Schrobback, K., Sheikhi, A., Annabi, N., Leijten, J., Zhang, W., Zhang, Y. S., Huttmacher, D. W., Klein, T. J., & Khademhosseini, A. (2017). Structural analysis of photocrosslinkable methacryloyl-modified protein derivatives. *Biomaterials*, 139, 163–171. <https://doi.org/10.1016/j.biomaterials.2017.04.050>
- Zhang, L., Hu, J., & Athanasiou, K. A. (2009). The role of tissue engineering in articular cartilage repair and regeneration. *Critical Reviews in Biomedical Engineering*, 37(1–2), 1–57.
- Zhou, F., Hong, Y., Zhang, X., Yang, L., Li, J., Jiang, D., Bunpetch, V., Hu, Y., Ouyang, H., & Zhang, S. (2018). Tough hydrogel with enhanced tissue integration and *in situ* forming capability for osteochondral defect repair. *Applied Materials Today*, 13, 32–44. <https://doi.org/10.1016/j.apmt.2018.08.005>
- Žigon-Branc, S., Markovic, M., Van Hoorick, J., Van Vlierberghe, S., Dubruel, P., Zerobin, E., Baudis, S., & Ovsianikov, A. (2019). Impact of hydrogel stiffness on differentiation of human adipose-derived stem cell microspheroids. *Tissue Engineering Part A*, 25(19–20), 1369–1380. <https://doi.org/10.1089/ten.tea.2018.0237>

SUPPORTING INFORMATION

Additional supporting information may be found in the online version of the article at the publisher's website.

How to cite this article: Hölzl, K., Fürsatz, M., Göcerler, H., Schädli, B., Žigon-Branc, S., Markovic, M., Gahleitner, C., Hoorick, J. V., Van Vlierberghe, S., Kleiner, A., Baudis, S., Pauschitz, A., Redl, H., Ovsianikov, A., & Nürnberger, S. (2021). Gelatin methacryloyl as environment for chondrocytes and cell delivery to superficial cartilage defects. *Journal of Tissue Engineering and Regenerative Medicine*, 1–16. <https://doi.org/10.1002/term.3273>

1 SUPPLEMENTARY DATA

1.1 qRT-PCR statistical analysis

There was no significant effect found for the cell culture method (soft/stiff hydrogel and pellet culture, p -value=0.058) when the total of all COL2 values of both donors and growth factor concentrations were compared in general. This indicates that overall COL2 expressions were the same in different culture methods.

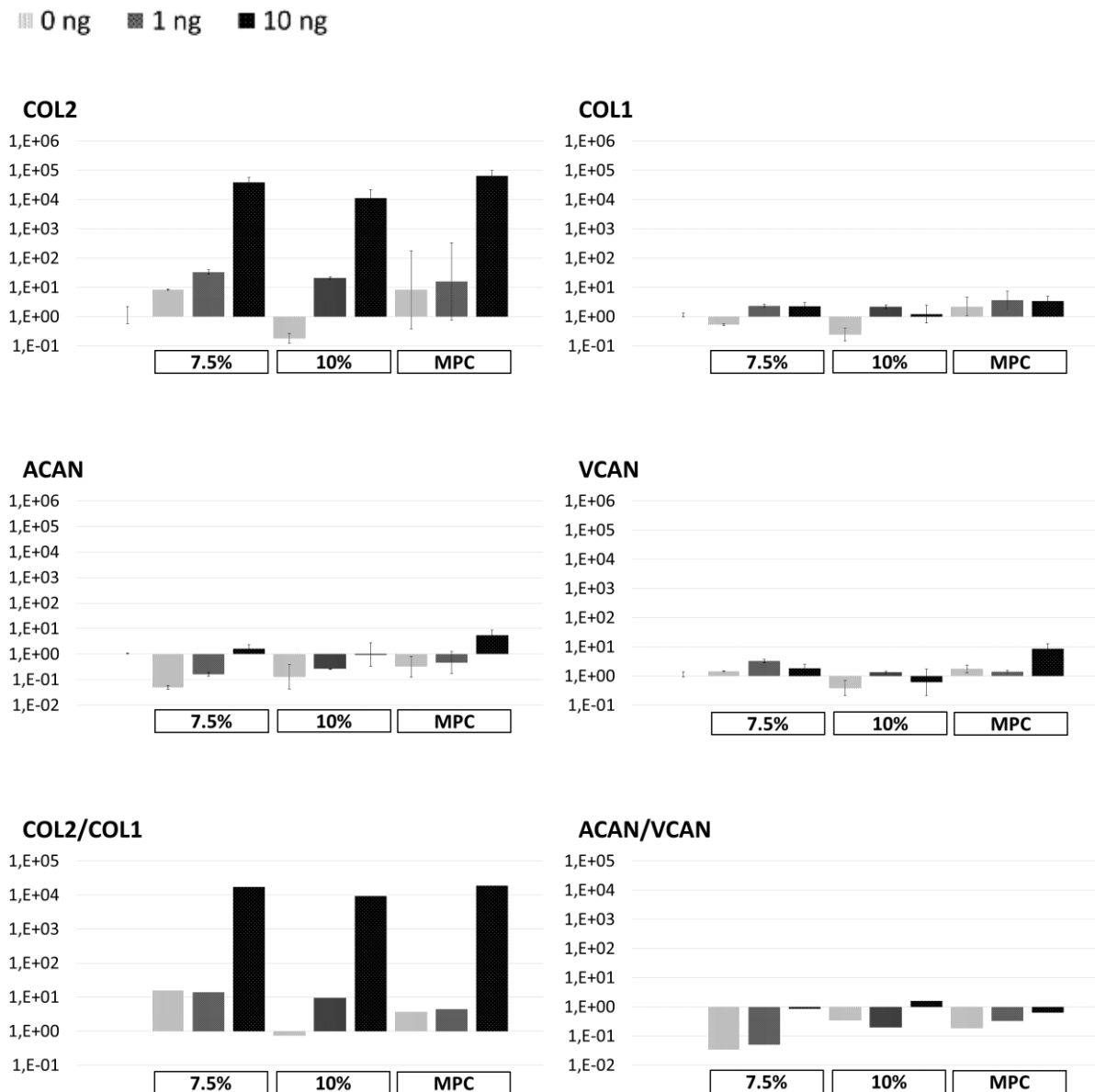
Comparing the different growth factor concentrations used, a significant increase in COL2 from 0 ng to 1 ng ($p < 0.001$) as well as from 1 ng to 10 ng TGF- β 3 ($p = 0.002$) was found in general for both donors. Having a closer look at this general comparison, contrasts were performed comparing each level of growth factor (0 ng -> 1 ng -> 10 ng TGF- β 3) across donor 1 as well as across donor 3 specifically. This revealed a significantly higher increase from 0 ng -> 1 ng ($p < 0.001$) as well as from 1 ng -> 10 ng ($p = 0.031$) for donor 3, when compared to donor 1. Therefore, it was found that donor 1 has a lower increase from 0 ng to 1 ng to 10 ng TGF- β 3 in COL2 than Donor 3. This already shows the strong influence of donor variability in the redifferentiation process.

Comparing the culture methods more closely in relation to the used amounts of growth factors revealed that there is a significant interaction effect between the level of growth factor and the culture method ($p = 0.020$). This indicates that the values of COL2 expression of different levels of growth factor differed according to the culture method. To break down this interaction, contrasts were performed comparing each level of growth factor to each culture method. It was shown that for Donor 1 and Donor 3 no significant differences were found between 10% and 7.5% hydrogel for any amount of TGF- β 3. When pellet culture was compared to 7.5% hydrogel with an amount of growth factor of 10 ng compared to 1 ng, a significant difference occurred ($p = 0.017$). It was shown, that from hydrogel 7.5% to pellet culture there is an increase in COL2 for 1 ng TGF- β 3 and a decrease for COL2 for 10 ng TGF- β 3. In a further comparison it was also found that this difference was attributable to the good performance of donor 3, which showed already great redifferentiation potential at 1 ng TGF- β 3.

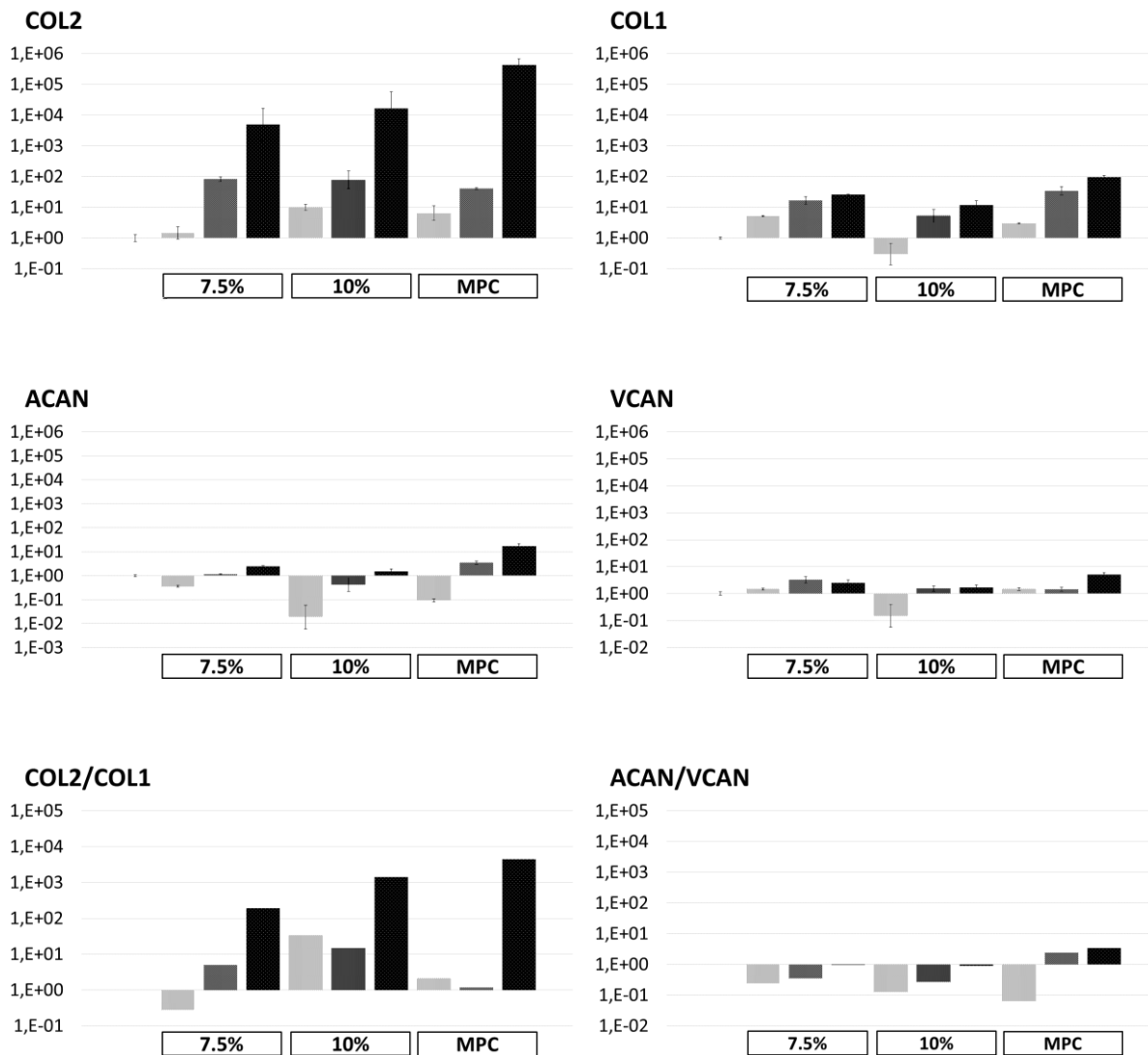
1.2 Gene expression of investigated donors

The following figures show the gene expression of chondrogenic differentiation markers of hydrogel encapsulated hAC of diverse donors (donor 1-3) in different conditions after 21 days in culture. Cells in P3 or P5 encapsulated in either soft (7.5%) or stiff (10%) hydrogel and cultivated in 0, 1 or 10 ng/mL TGF- β 3. As a control hAC were cultured in pellet culture. Differentiation indices calculated from COL2/COL1 and ACAN/VCAN are shown.

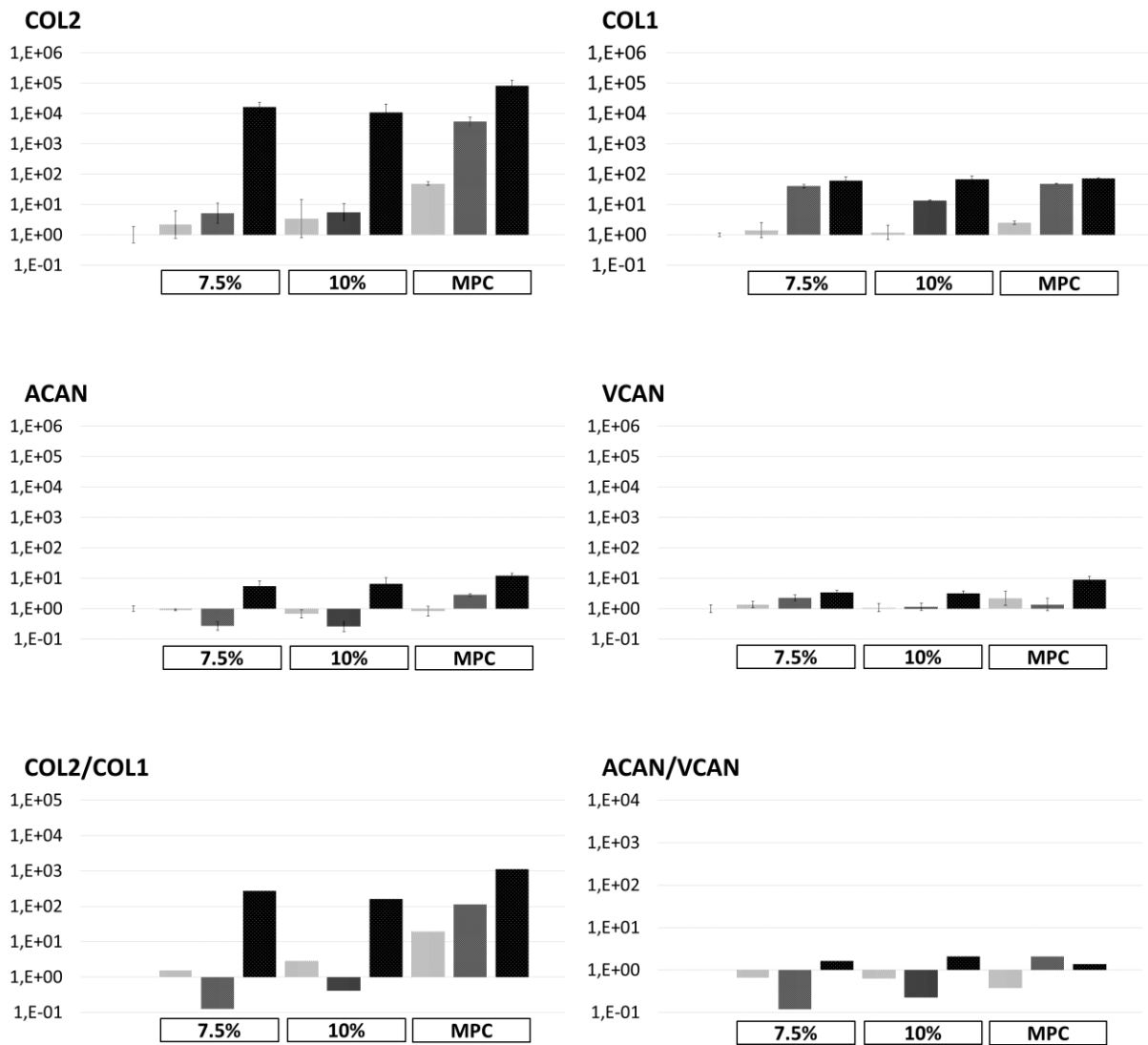
1.2.1 Donor 1, Passage 3



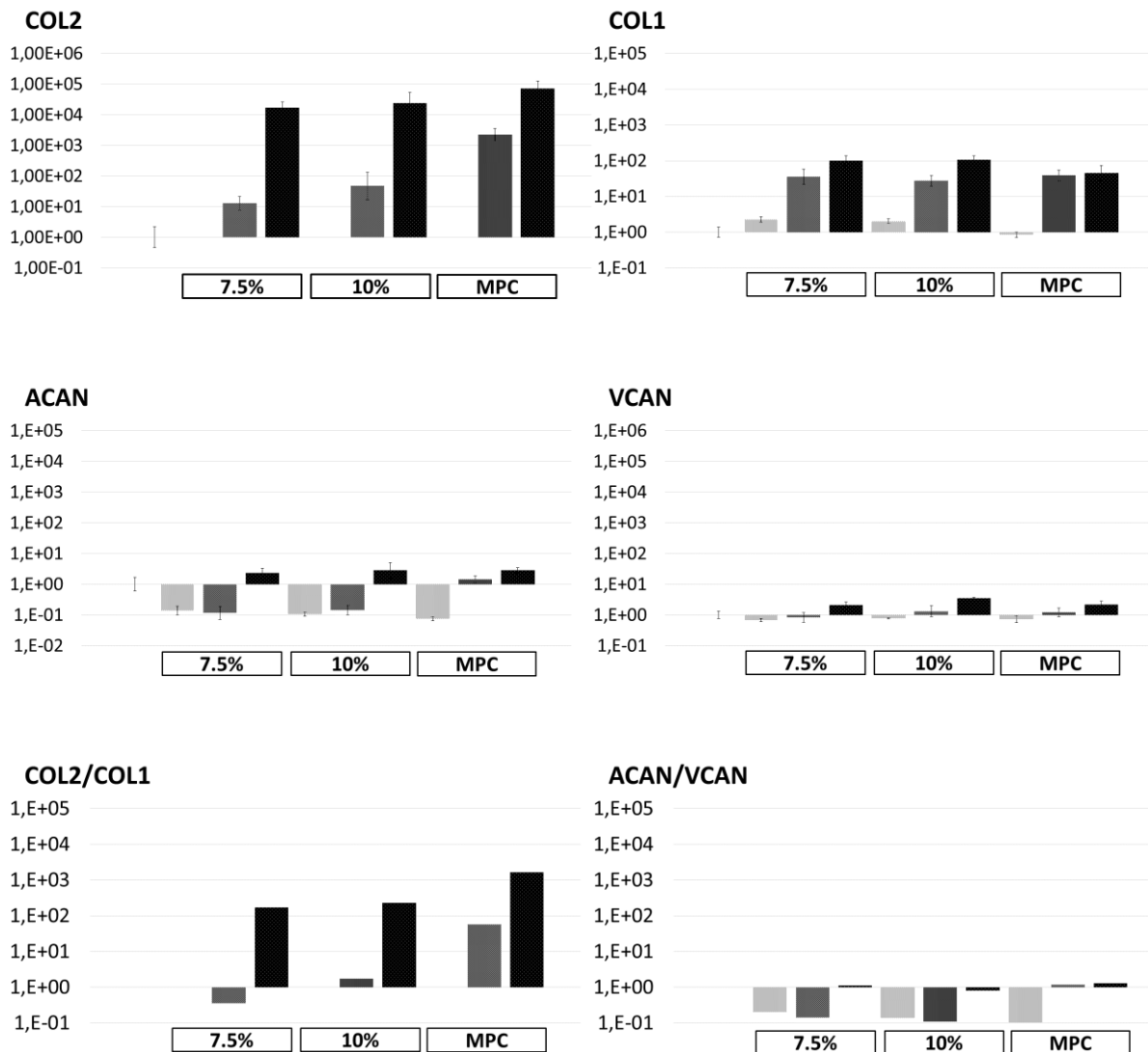
1.2.2 Donor 1, Passage 5



1.2.3 Donor 2, Passage 3

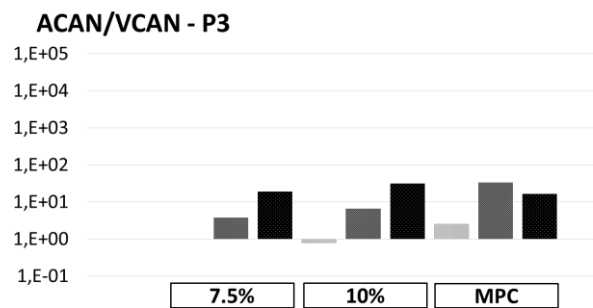
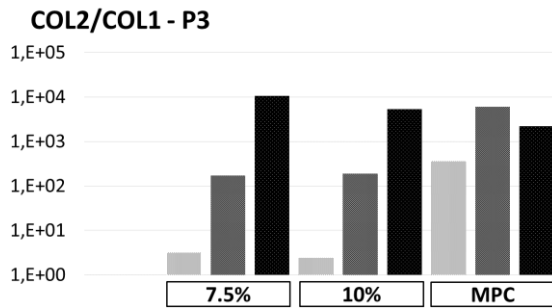
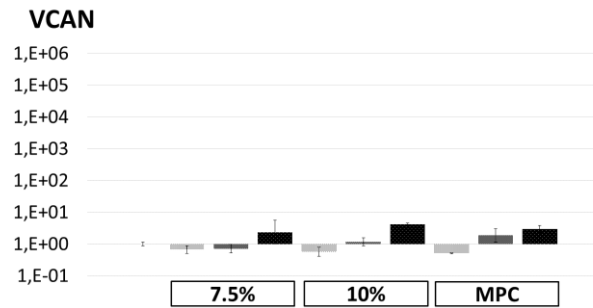
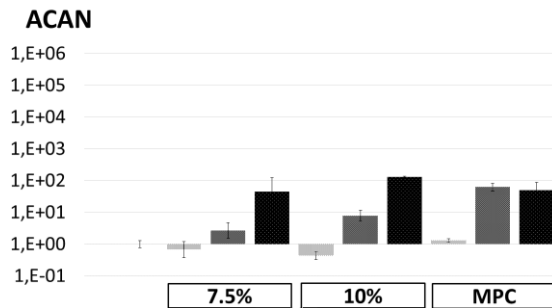
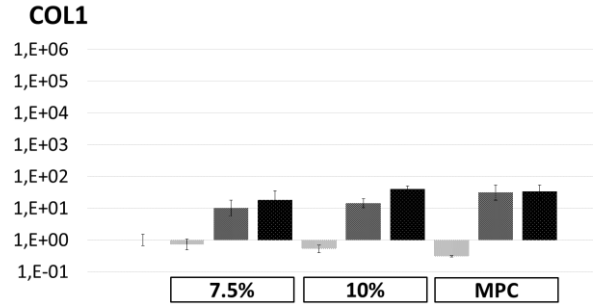
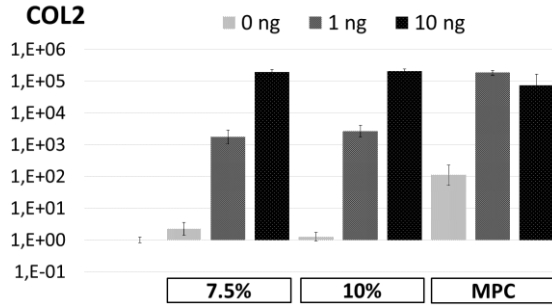


1.2.4 Donor 2, Passage 5

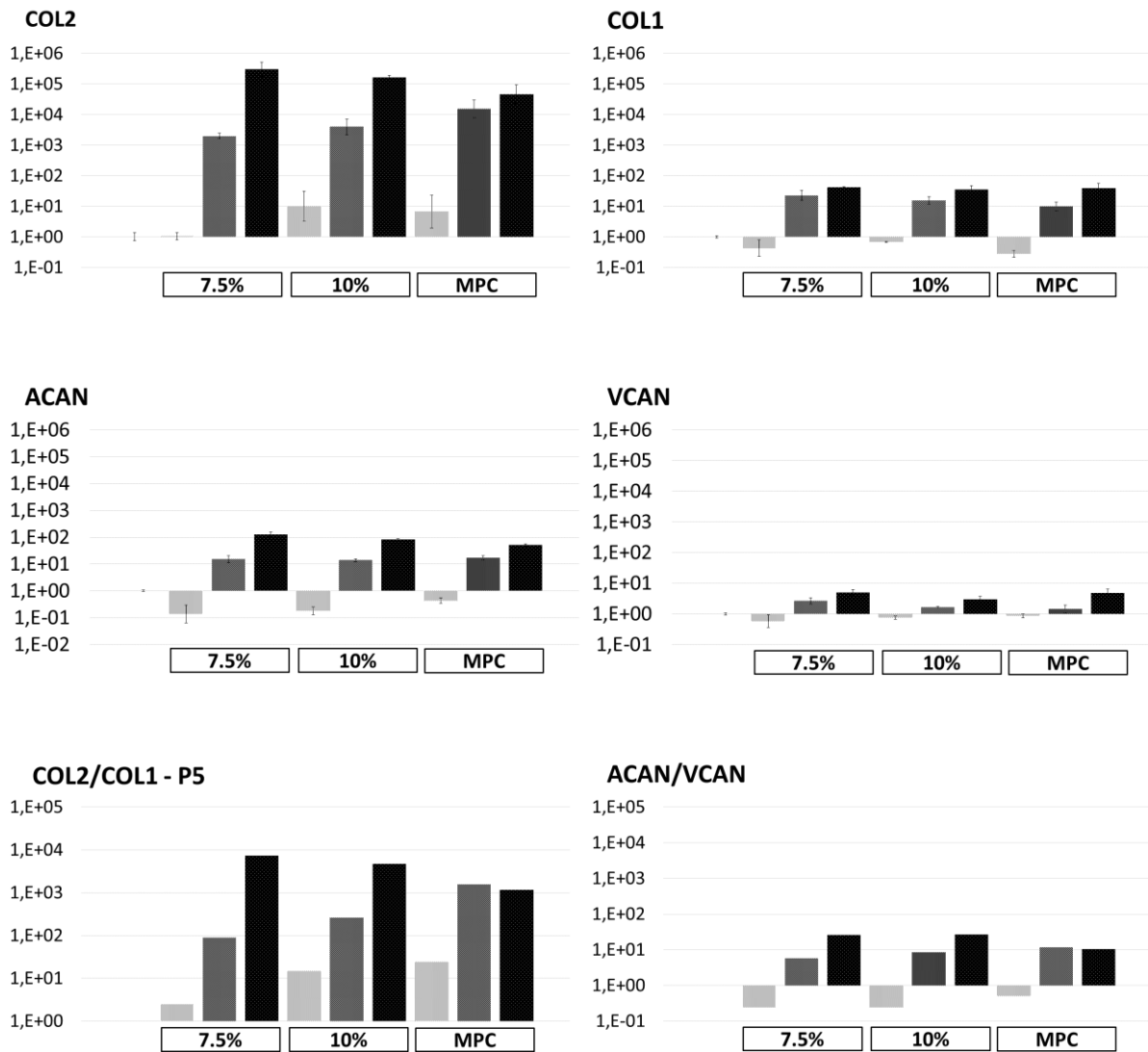


1.2.5 Donor 3, Passage 3

(already shown within the text)

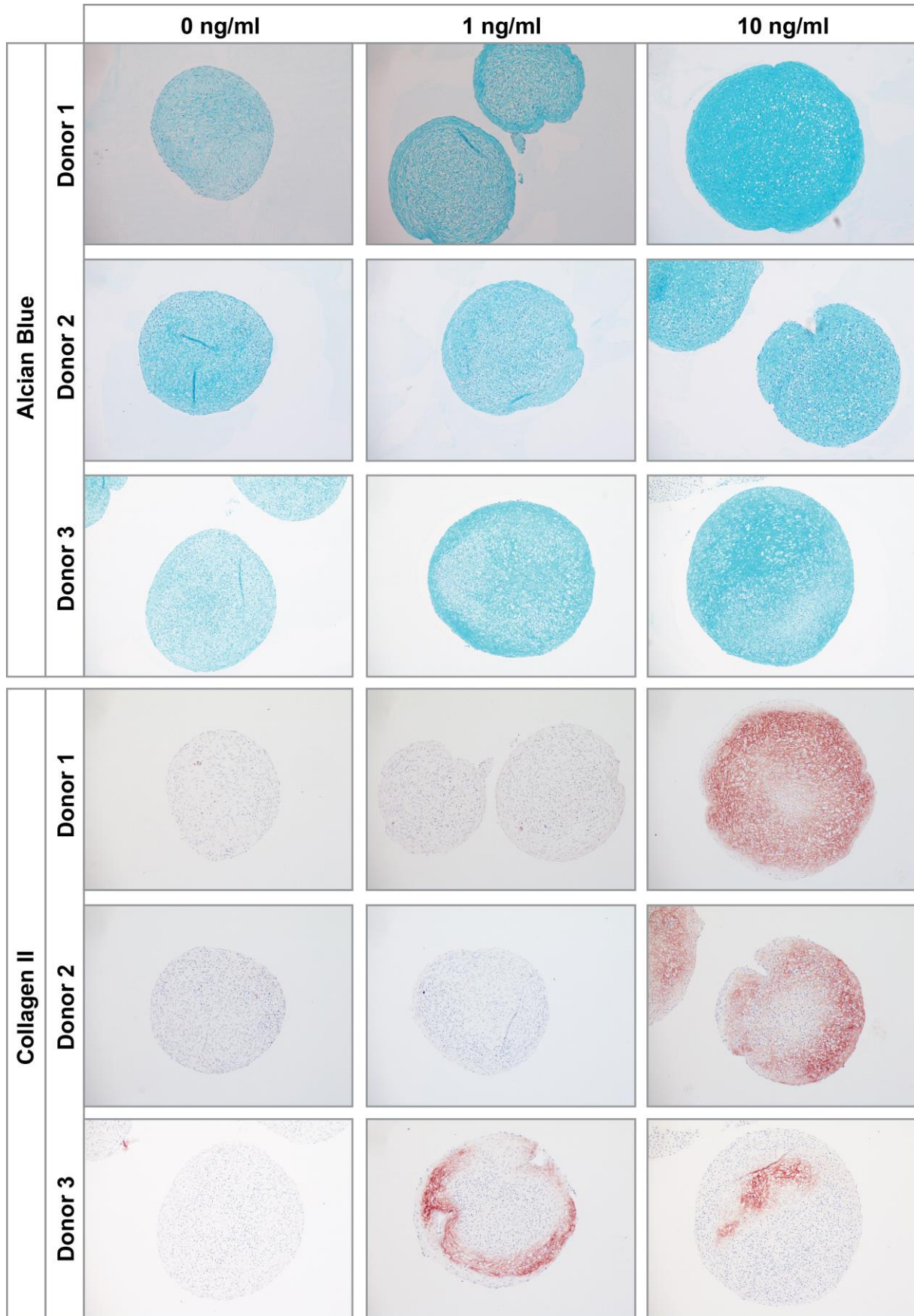


1.2.6 Donor 3, Passage 5

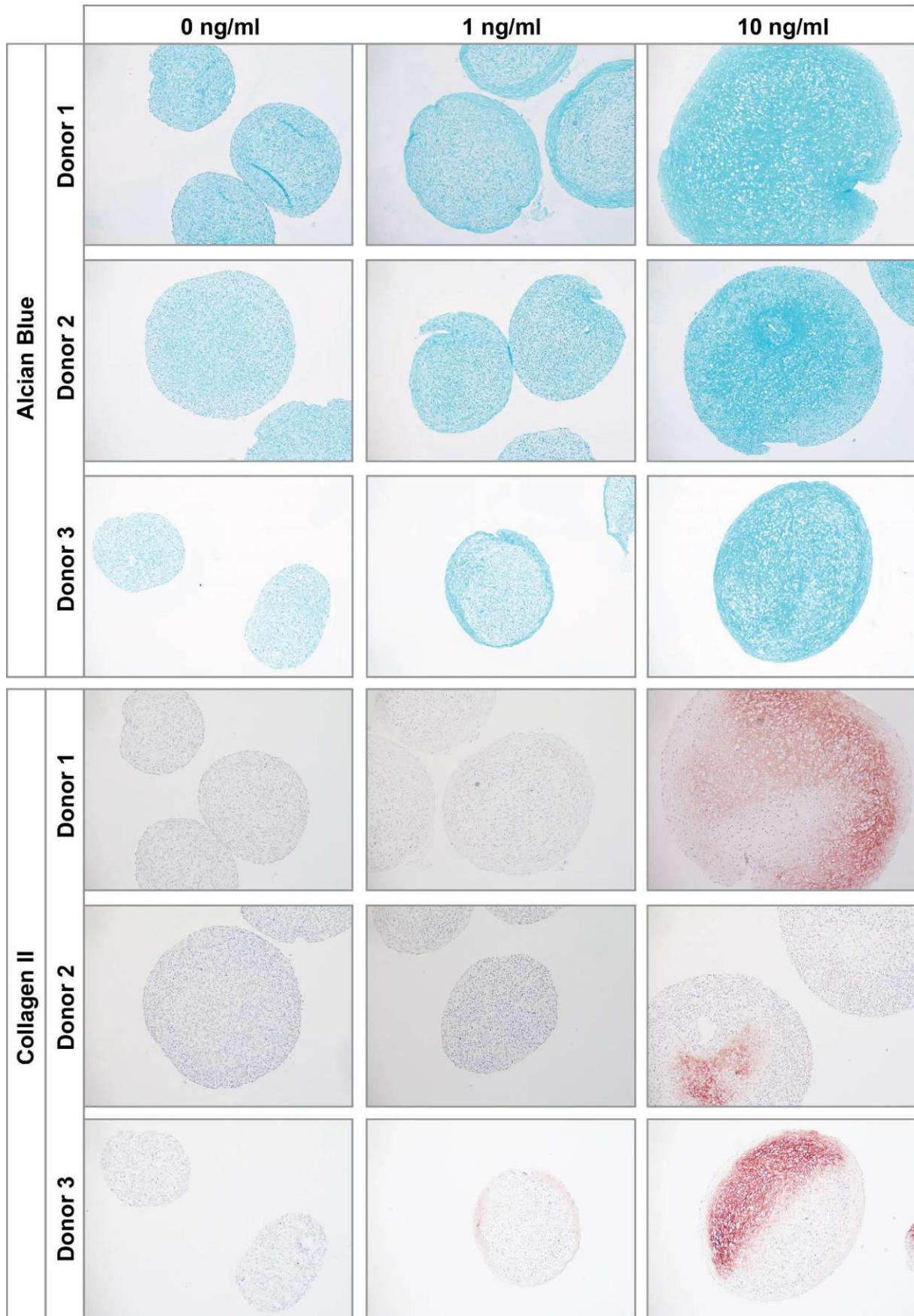


1.3 Histological analysis of investigated donors

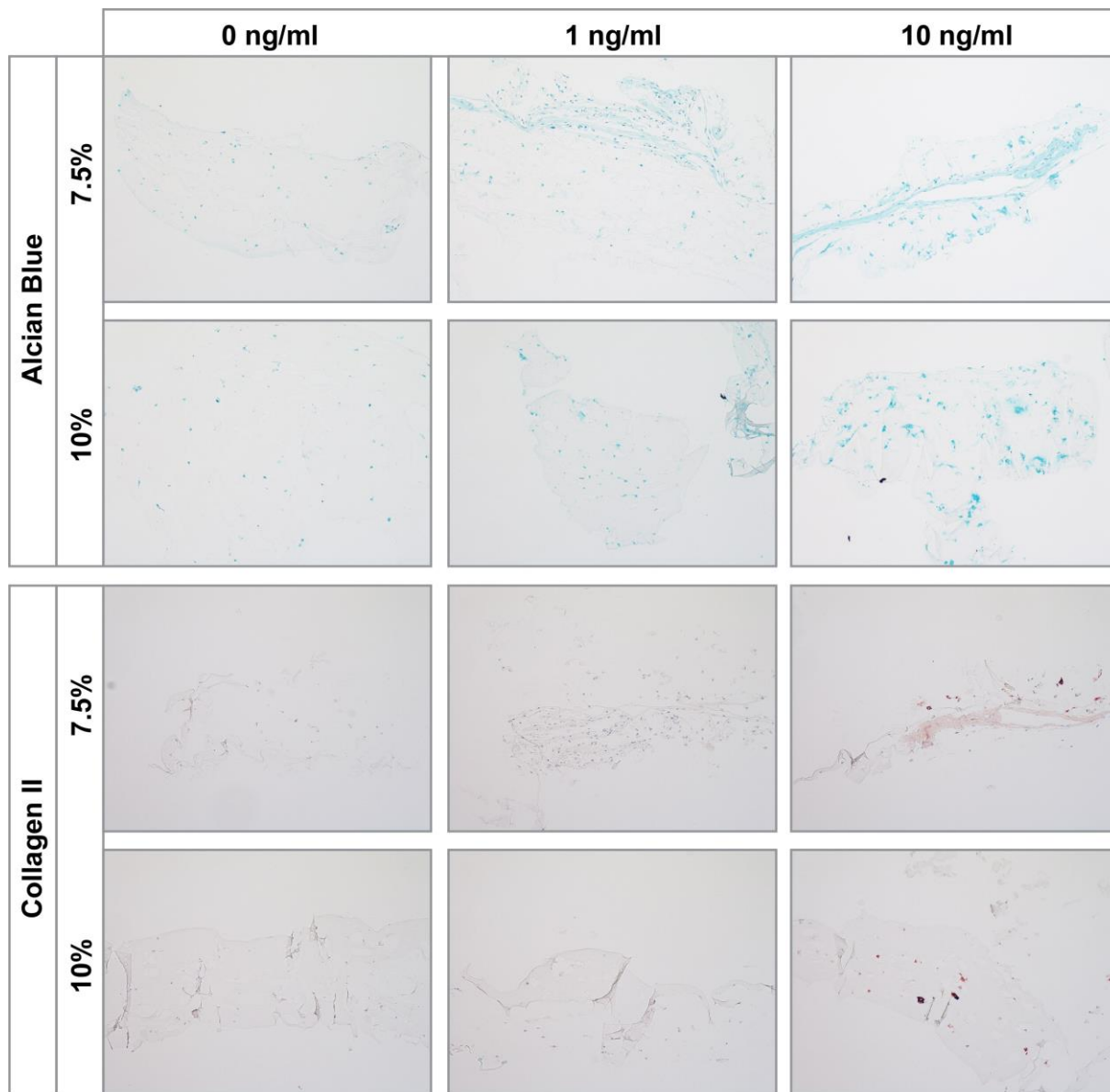
1.3.1 Pellet culture, Passage 3



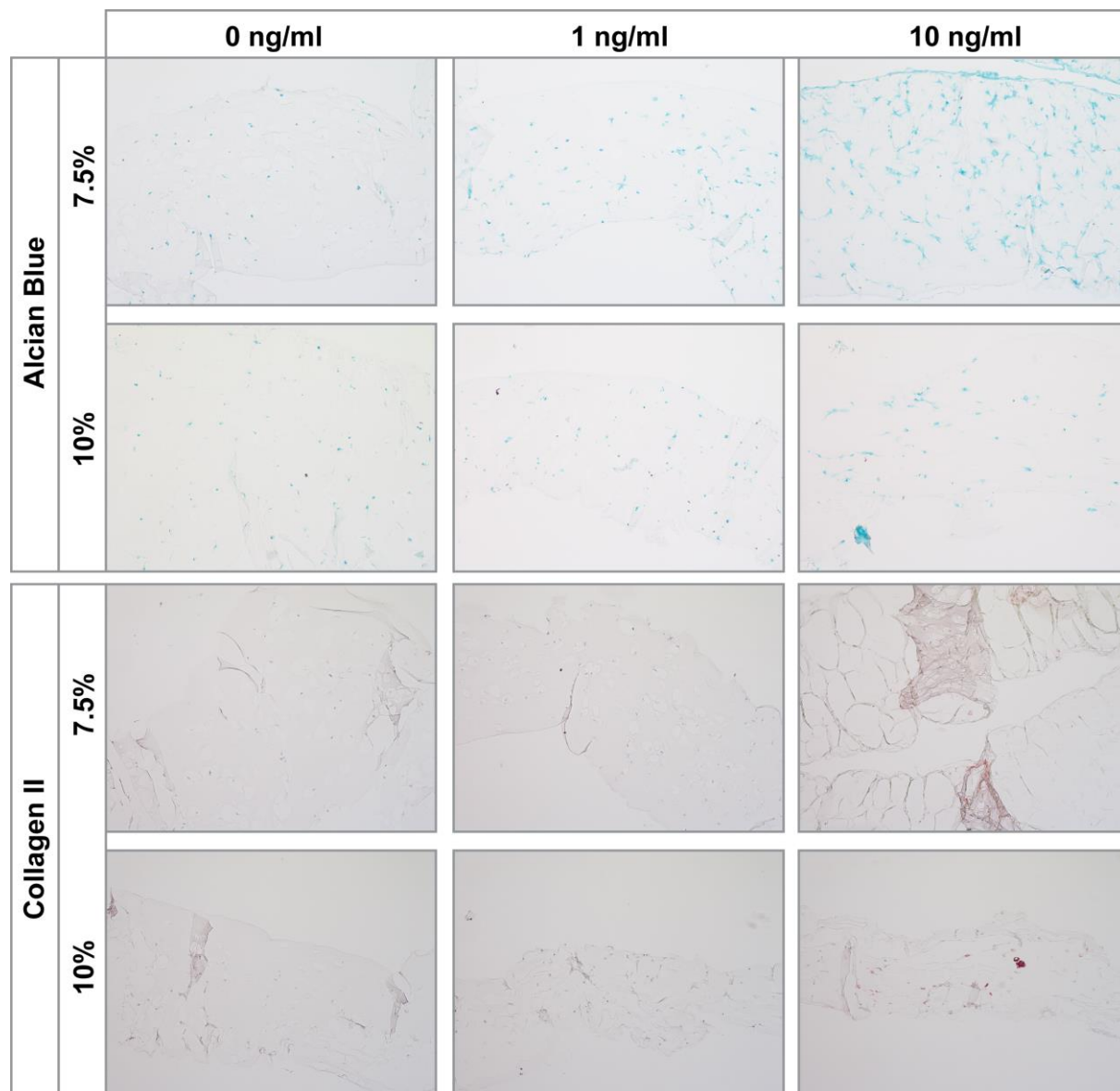
1.3.2 Pellet culture, Passage 5



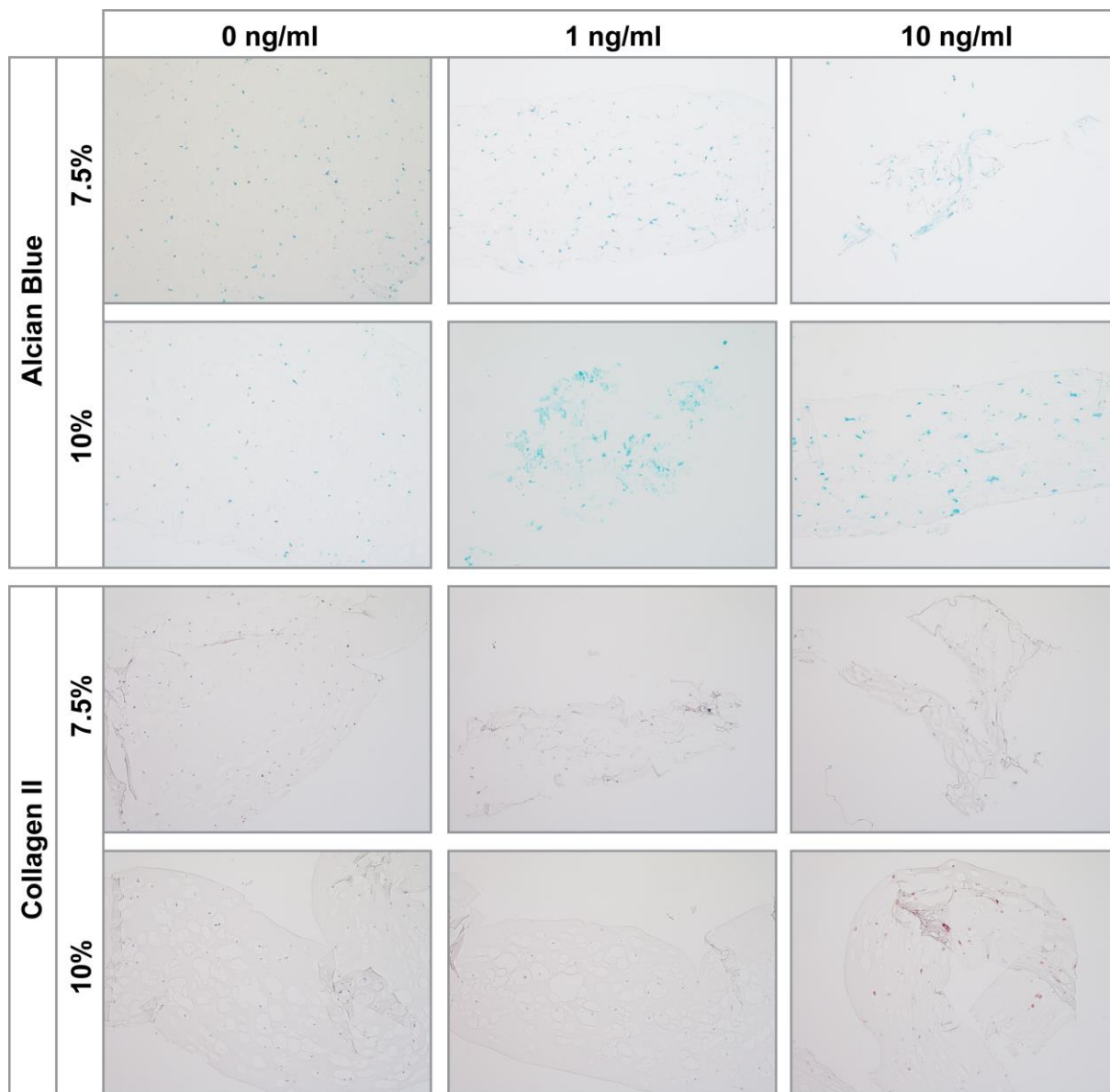
1.3.3 gelMA Donor 1, Passage 3



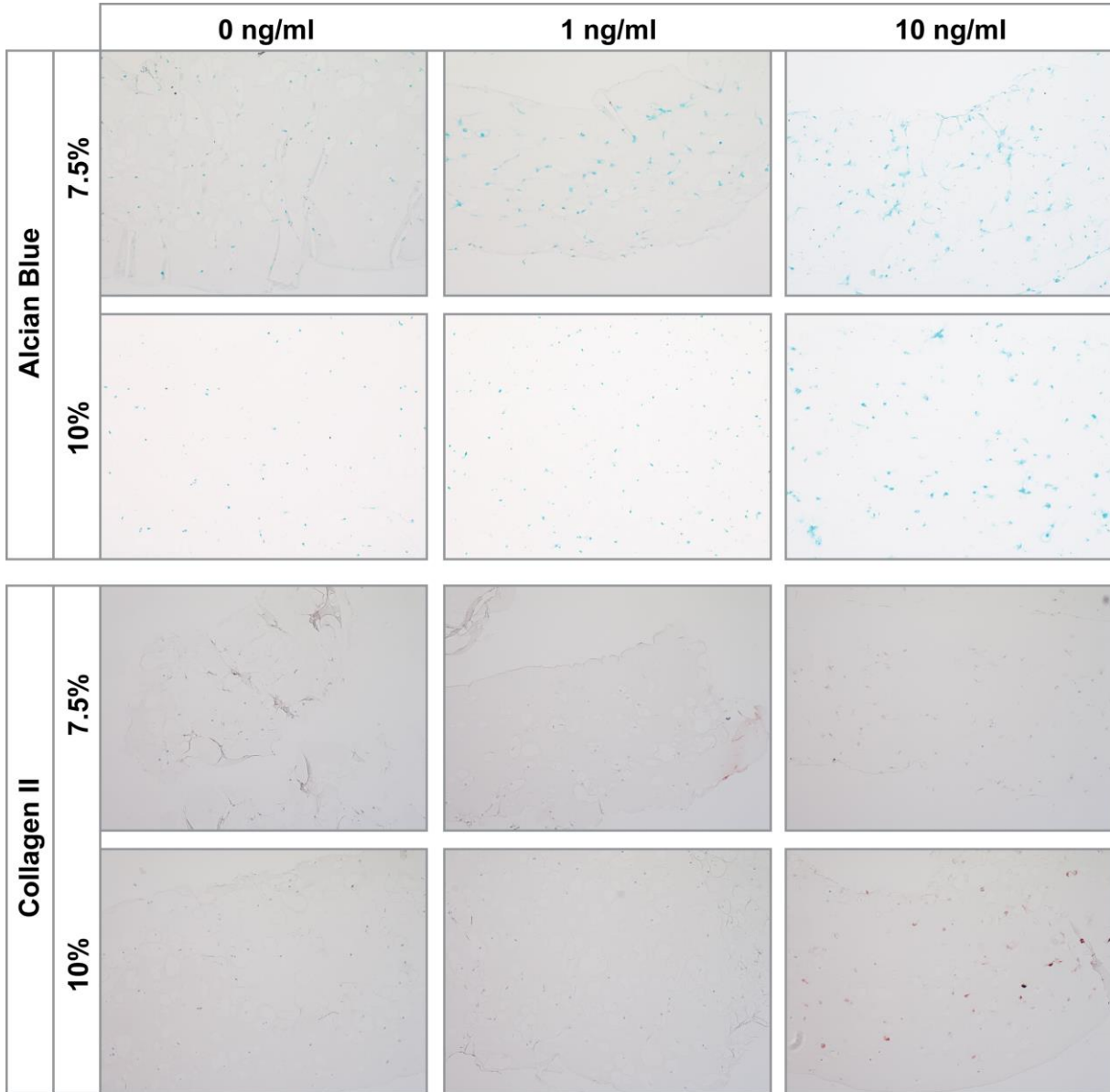
1.3.4 gelMA Donor 1, Passage 5



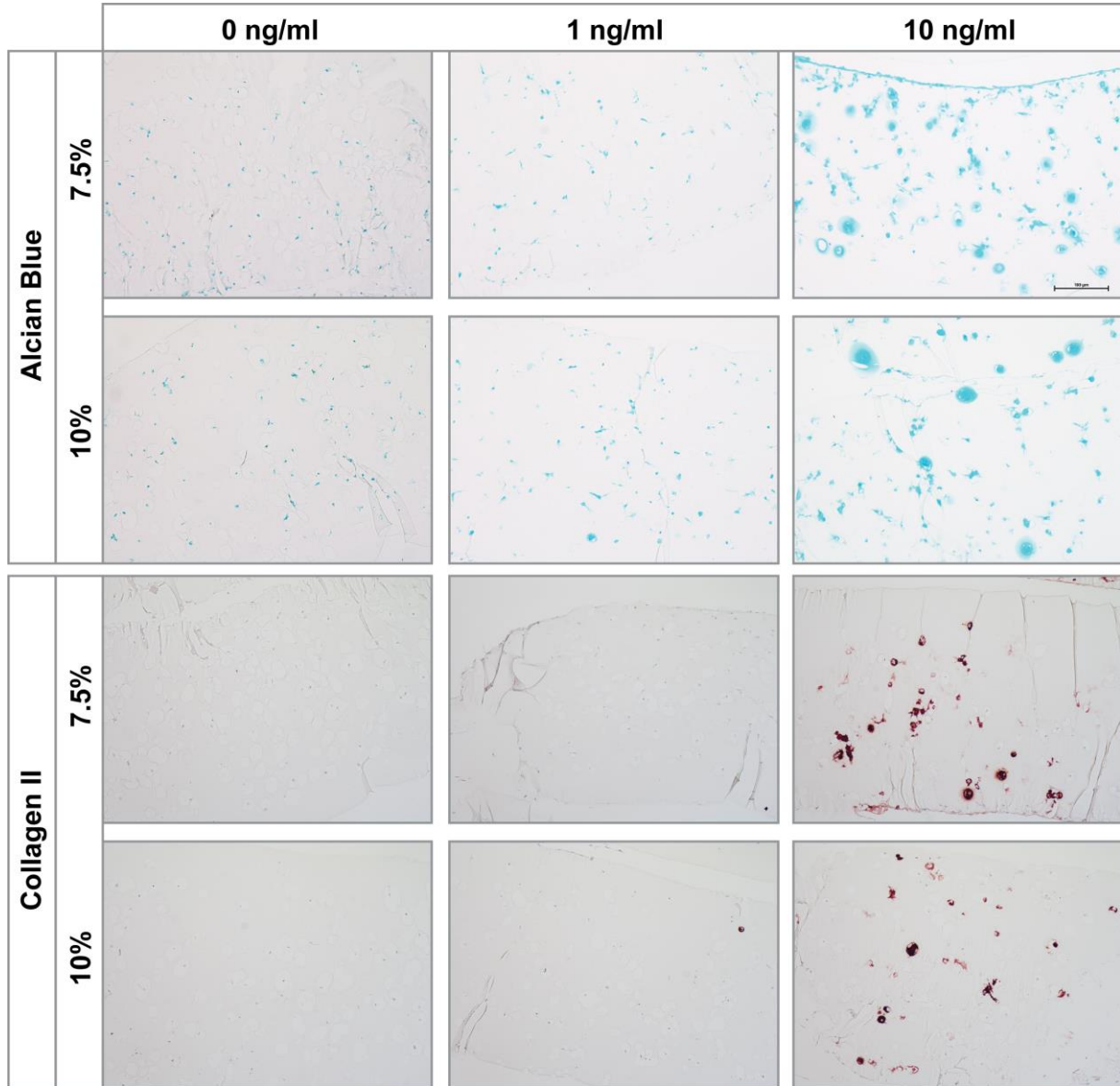
1.3.5 gelMA Donor 2, Passage 3



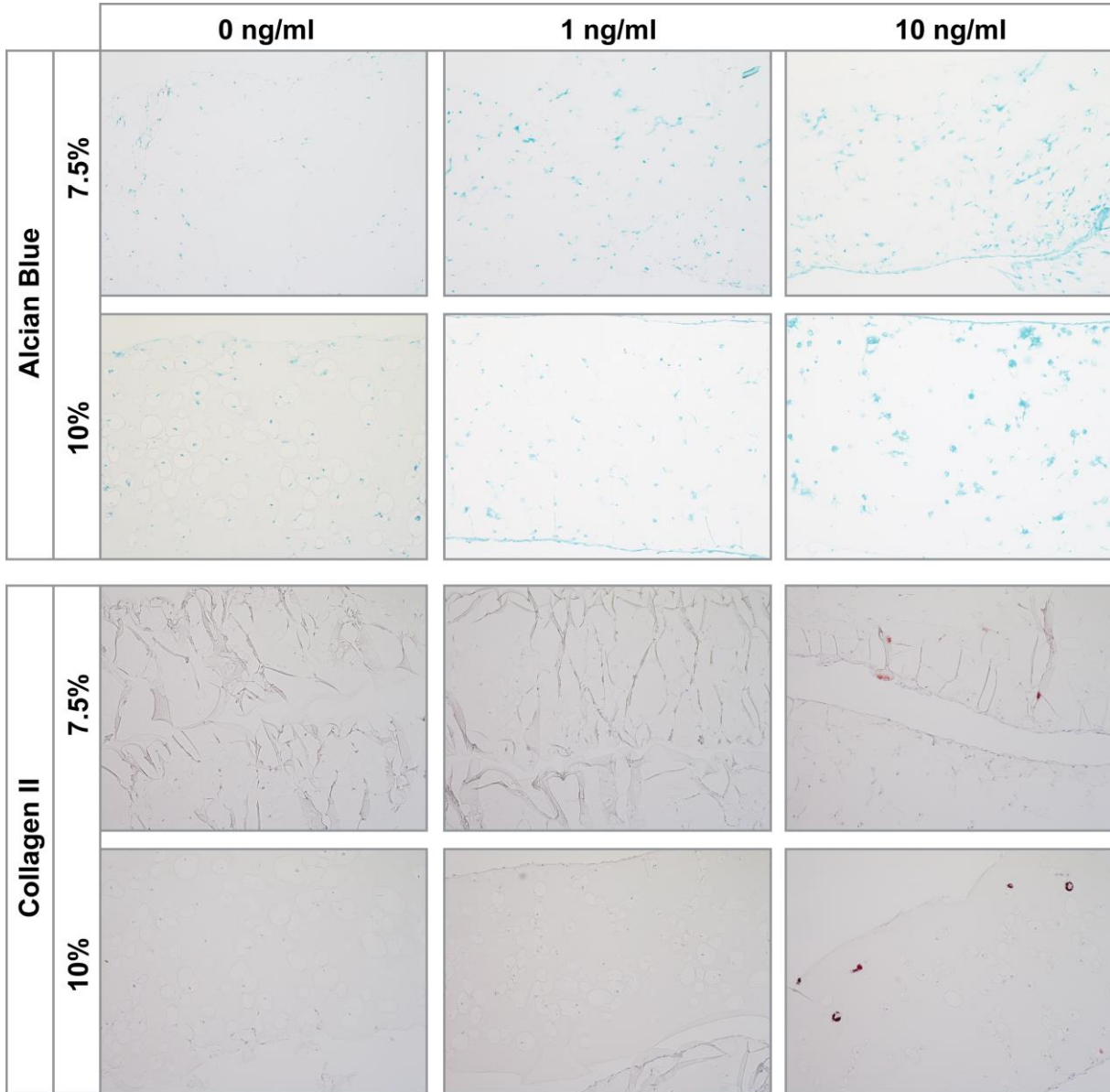
1.3.6 gelMA Donor 2, Passage 5



1.3.7 gelMA Donor 3, Passage 3



1.3.8 gelMA Donor 3, Passage 5



CURRICULUM VITAE

PERSONAL INFORMATION

Katja Hölzl, MSc.

[REDACTED]



[REDACTED]



[REDACTED]



[REDACTED] [REDACTED]



WORK EXPERIENCE

Aug 2019 - Present

Takeda Pharmaceuticals

Supervisor Quality Assurance

Feb 2019 – Jul 2019

Takeda Pharmaceuticals

Teamleader Quality Assurance

Feb 2015 – Feb 2019

TU Wien, Institute of Materials Science and Technology

Project Assistant

Research and development of three-dimensional (3D) cell culture systems for tissue engineering using hydrogels; in collaboration with the *Medical University of Vienna*.

Research on:

- redifferentiation of human primary chondrocytes in 3D hydrogel culture
- the suitability of the hydrogel as a clinical application in arthrotic cartilage/traumatic cartilage defect treatment
- the influence of mechanical stimuli on stem cell differentiation in 3D hydrogel culture

Establishment of:

- RNA isolation procedure and qPCR for cell loaded hydrogel samples
- Stem cell culture in our laboratory

Feb 2014 - Oct 2014

TU Wien, Institute of Materials Science and Technology

Master's Thesis

"Hydrogels as engineered extracellular matrix for three-dimensional cell culture"

honoured with the *Innovation Award* of the University of Applied Sciences Upper Austria (1st place)

Aug 2013

Salzburger Landeskrankenhaus, Universitätsklinik für Kinder- und Jugendheilkunde

Research Project

Establishing western blot analysis for the characterization of mitochondrial respiratory chain complexes of different types of immune cells.

- Nov 2011 - Feb 2013 **OpenLab Wels**
Tutor in the field of molecular biology and chemistry
- April 2012 - Jul 2012 **Institute for Tissue- and Organ Reconstruction IGO®, Wels**
Bachelor's Thesis
“*Decellularization and recellularization of human cartilage*”
- Sept 2011 **LVA GmbH, Vienna**
Internship: Department microbiology
- Oct 2010 - Feb 2011 **University of Applied Sciences Upper Austria, Campus Wels**
Research Project
Functional Food: Optimization of extraction and analysis of health relevant contents
- Jul 2010 **BLT: Biomass Logistics Technology, Francisco Josephinum Wieselburg**
Internship: Laboratory for alternative fuels

EDUCATION AND TRAINING

- Oct 2012–Dec 2014 **Master of Science in Engineering**
University of Applied Sciences Upper Austria, Campus Wels
Master's degree programme: Bio- and Environmental Technology
Passed with distinction
- Oct 2009–Sept 2012 **Bachelor of Science in Engineering**
University of Applied Sciences Upper Austria, Campus Wels
Bachelor's degree programme: Bio- and Environmental Technology
Passed with distinction
- Jun 2009 **Higher School Certificate (Matura)**
BG/BRG Wieselburg
Focus in natural sciences

PERSONAL SKILLS

- Mother tongue German
- Other language(s) English: C1 level
- Communication Skills** **Social Skill Seminars attended in:**
Conflict management, Teambuilding, Cross-cultural communication, Leadership skills
- Digital Competence** Experienced user of computer software (Office software, Mindmaps)
Basic knowledge in engineering software (Catia, AutoCAD)
Basic knowledge in calculating software (SPSS, Mathematica)
- Job-related Skills** Tissue Culture/Stem Cell Culture
Experience in GMP
Western Blot
qPCR
Confocal microscopy
Cytotoxicity testings

PUBLICATIONS

- “*Gelatin methacryloyl as environment for chondrocytes and cell delivery to superficial cartilage defects*”
Journal of Tissue Engineering and Regenerative Medicine 2021; 1-16
- “*Dynamic Coordination Chemistry Enables Free Directional Printing of Biopolymer Hydrogel*”
Chemistry of Material 2017; 29(14)
- “*Bioink properties before, during and after 3D bioprinting*”
Biofabrication 2016; 8(3); **Field Citation Ratio: 106**
- “*Hybrid Tissue Engineering Scaffolds by Combination of Three-Dimensional Printing and Cell Photoencapsulation*”
Journal of Nanotechnology in Engineering and Medicine 2015; 6(2)

REFERENCES

Project Supervisor (MedUni)

Dr. Sylvia Nürnberger

sylvia.nuernberger@meduniwien.ac.at

+43 1 40400 59440

Univ. Prof. Dr. Heinz Redl

heinz.redl@trauma.lbg.ac.at